Global View of the Origin of Tropical Disturbances and Storms

by
William M. Gray

Technical Paper No. 114
Department of Atmospheric Science
Colorado State University
Fort Collins, Colorado

Colorado State University

Department of Atmospheric Science

Paper No. 114

GLOBAL VIEW OF THE ORIGIN OF TROPICAL DISTURBANCES AND STORMS

by
William M. Gray

Department of Atmospheric Science
Colorado State University
Fort Collins, Colorado

October 1967

Atmospheric Science Paper No. 114

TABLE OF CONTENTS

ABSTRACT

A global observational study of atmospheric conditions associated with tropical disturbance and storm development is presented. This study primarily uses upper-air observations which have become available over the tropical oceans in the last decade. Climatological values of vertical stability, low-level wind, tropospheric vertical wind shear and other parameters relative to the location and seasons of tropical disturbance and storm development are discussed. Individual storm data is also presented in summary form for over two hundred development cases (with over one thousand individual observation times) for three genesis areas in the Northern Hemisphere.

Results show that most tropical disturbances and storms form in regions equatorward of 20° latitude on the poleward side of doldrum Equatorial Troughs where the tropospheric vertical shear of horizontal wind (i.e., baroclinicity) is a minimum or zero. Storm development occurring on the poleward side of 20° latitude in the NW Atlantic and NW Pacific takes place under significantly different environmental conditions which are described. These latter developments make up but a small percentage of the global total.

Observations are also presented which indicate that over the tropical oceans where disturbances and storms form, there is a distinct Ekman or frictional veering of the wind in the sub-cloud layer (surface to 600 m) of approximately 10°. This produces or enhances synoptic-scale low-level convergence and cumulus convection in regions of large positive relative vorticity which exist in the cyclonic wind shear areas surrounding doldrum Equatorial Troughs.

Tropical disturbance and later storm development is viewed as primarily a result of large-scale Ekman or frictionally forced surface convergence (with resulting cumulus production and tropospheric heating), and a consequent inhibition of tropospheric ventilation by initially existing small vertical wind shear, and later inhibition of ventilation by cumulus up- and downdrafts acting to prevent increase of vertical shear as baroclinicity increases. The above processes produce the necessary condensation heating and allow for its concentration and containment in selective areas. Development is thus explained from a simple warming, hydrostatic adjustment point of view with the energy source analogous to Charney and Eliassen's (1964b) proposed "conditional instability of the second kind."

1. INTRODUCTION

General agreement on the environmental conditions and the physical mechanisms which bring about tropical disturbance and tropical storm development is lacking. Meteorologists in the various parts of the world emphasize and discuss different onset and development criteria, but the basic physical processes which accompany the development of these warm-core cyclones must be very similar. This lack of general agreement, while partly due to semantical differences, is primarily explained by deficient observational evidence from which early empirically based conclusions could have been established.

Riehl (1948a, 1948b, 1950) has viewed the formation process, in general, as a progressive intensification of a westerly moving disturbance or wave embedded in the trade winds which moves under a favorable upper tropospheric divergent environment. He was the first to point out the association of typical upper and lower tropospheric flow patterns prior to disturbance intensification. In a broad sense, Yanai (1961a) and Fett (1964b, 1966) have agreed with Riehl with regard to wave or disturbance progressive intensification within a trade-wind environment. Yanai looks to deep, broad-scale vorticity convergence as an important initial requirement. From a similar point of view, Dunn (1940) and others earlier observed that intensification in the North Atlantic occurs from westerly moving isallobaric waves within the trade winds.

Sadler (1964, 1965, 1966), Tanabe (1963), Ramage (1959), and Gabites (1963b), all of whom have primarily studied Pacific storms, have advanced other opinions on development. Sadler observes storm intensification as occurring from an initially established surface equatorial trough vortex or from the downward tropospheric intensification of a pre-existing upper tropospheric trough. Ramage looks to an energy dispersion mechanism from a mid-oceanic upper troposphere trough as a favorable initiator of upper divergence over an incipient disturbance. Tanabe observes a strong association of development with the position of the Equatorial Trough. When discussing tropical storm development, Gabites has stated, "In the southwest Pacific it is evident that easterly waves play very little part." Is it likely that development conditions would be different in the various parts of the globe? The author feels there must be a basic similarity of development.

Upper-air information over the tropical oceans was very sparse until the middle 1950's. The addition of new upper-air stations in the tropics and the development of the weather satellites has substantially added to our observational information. With this new data it is now possible to obtain a more unified global view of tropical disturbance and storm development. The purpose of this paper is to present observational information on the environmental conditions surrounding tropical disturbances which later develop into tropical storms in order to obtain a better understanding of the relevant physical processes concerning development. In the author's opinion, there has been too much qualitative and incomplete reasoning concerning the physical processes of development. General conclusions have been drawn from atypical case studies. Theories of development have been advanced without supporting data or plausible physical substantiation. Numerical model experiments have been made where initial assumptions are not realistic. In order to more realistically organize the information on this subject, the author has chosen to take the empirical approach and go directly to the observations.

2. GLOBAL CLIMATOLOGY OF STORM DEVELOPMENT

Location and Frequency of Initially Observed Disturbances and Storms. The small dots of Fig. 1 show where initial disturbances from which tropical storms later develop were first detected. As the number of years of available records for the different areas are not equal, these dots should not be considered to be representative of relative storm frequency.[1] Recent satellite information indicates that the majority of the locations of initial detection in the NW Atlantic (where data has been especially scarce) should be relocated in the Cape Verde Island area or over west central Africa, as discussed by Aspliden, et al., (1966) and Arnold (1966). In other development areas the location of many initial disturbances might be more realistically located slightly to the east of the positions shown.

In this paper, tropical storms will be defined as warm-core cyclonically rotating wind systems in which the maximum sustained winds are 35 knots (i. e., 40 mph) or greater. Hurricanes, typhoons, and cyclones (Southern Hemisphere) are also included in this definition.[2]

Tropical disturbances are defined as distinctly organized cloud and wind patterns in the width range of 100 to 600 km which possess a conservatism in time of at least a day or more. Wind speeds may be very weak. The typical distinctly organized and separate "cloud blob" patterns as viewed from satellite pictures within the trade winds are considered to be tropical disturbances. The isolated "cloud blob" patterns of Fig. 4 portray this type of typical disturbance. The so-called "Equatorial Trough," henceforth abbreviated Eq. T.,

---

[1] Data sources are listed in Appendix.

[2] As defined by the U. S. Weather Bureau a tropical storm has sustained winds of 40 miles per hour (mph) or greater; a hurricane, typhoon, or cyclone (of the Southern Hemisphere) has sustained winds of at least 75 mph. In this paper the term tropical storms as defined refers to both tropical storms and to hurricanes. The physical mechanisms which operate to produce storms of 40 to 75 mph and those which produce storms with winds greater than 75 mph are assumed to be similar.

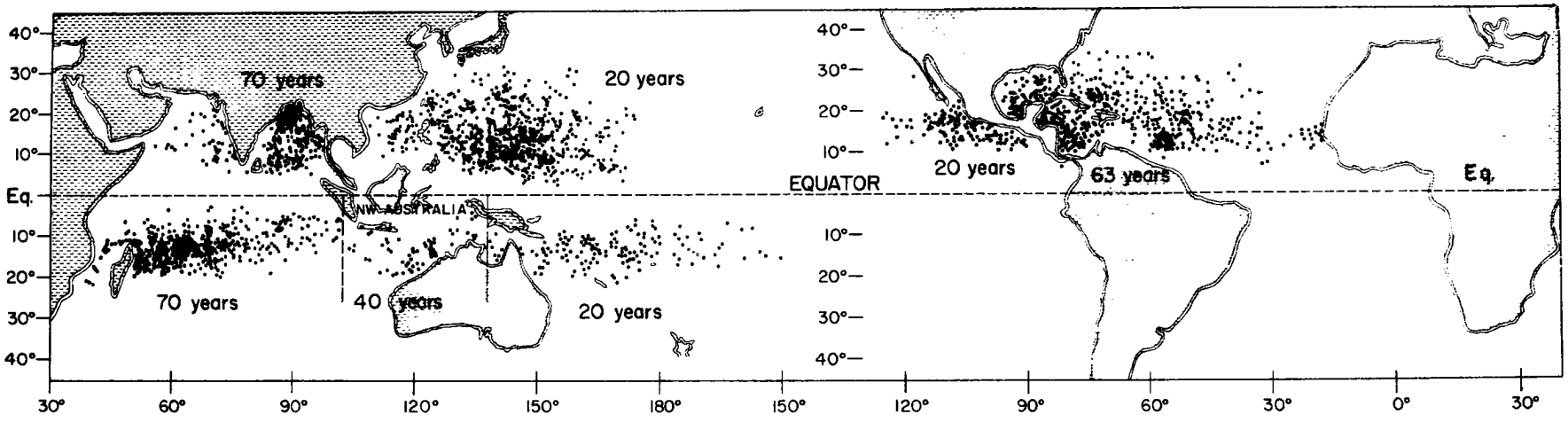

Fig. 1. Location points of first detection of disturbances which later became tropical storms.

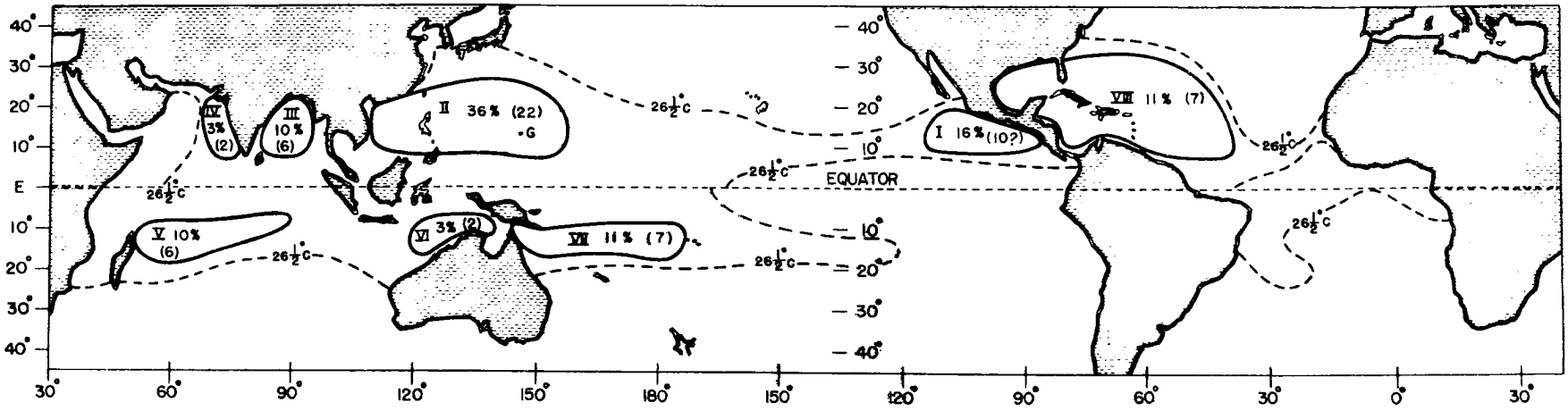

Fig. 2. Designation of various tropical storm development regions and percentage of tropical storms occurring in each region relative to the global total. Numbers in parentheses are those of the average number of tropical storms occurring in each region per year. The 26 1/2°C isotherm for August in the Northern Hemisphere and January in the Southern Hemisphere is also shown.

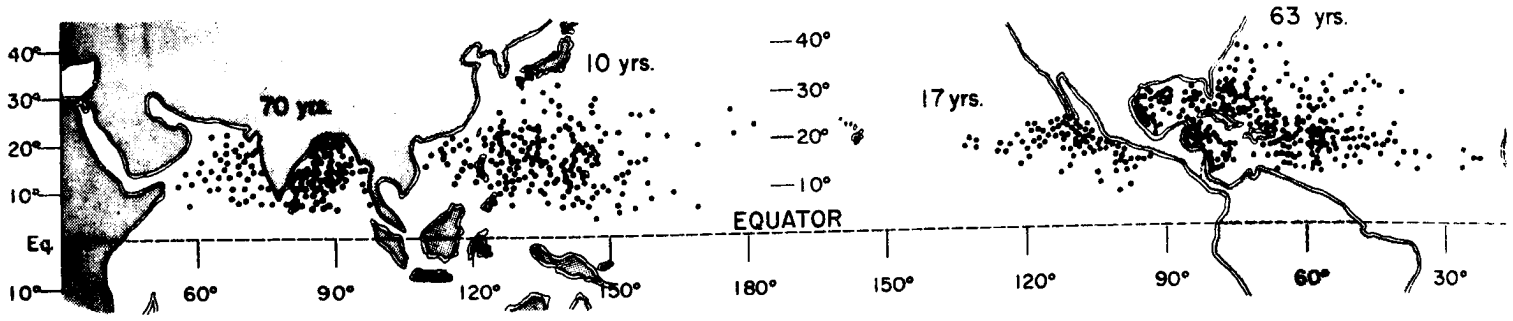

Fig. 3. Location points of storms where hurricane intensity winds were first observed.

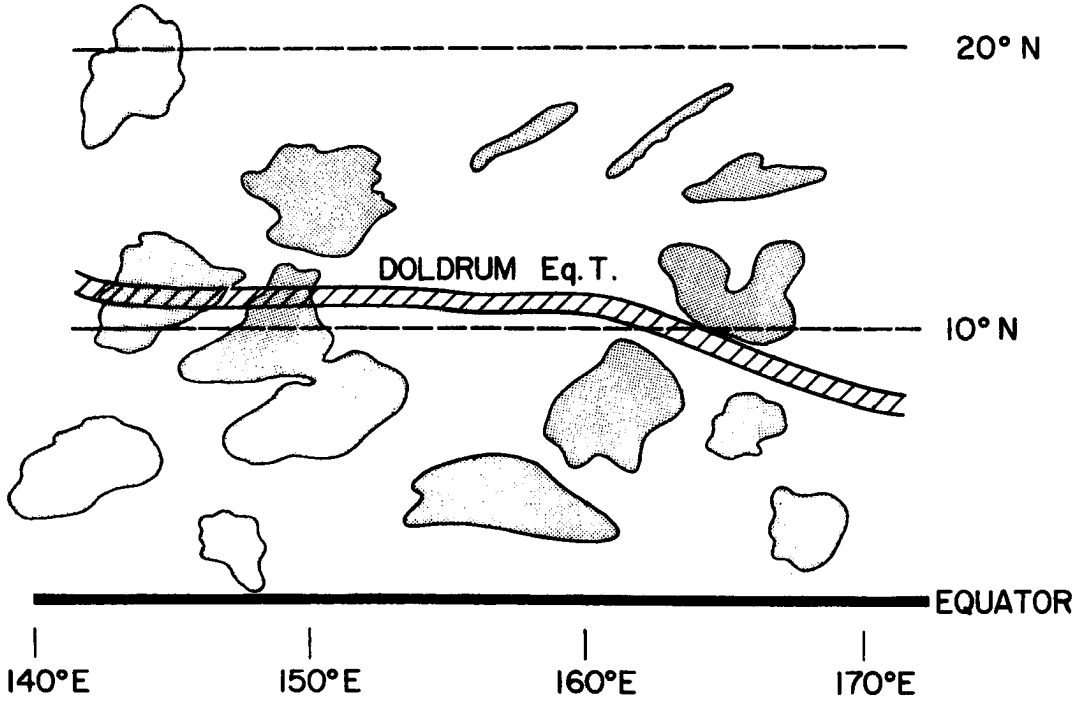

Fig. 4. Typical satellite observed cloud blob patterns relative to a doldrum Equatorial Trough. Tropical storms develop from conservative cloud blob patterns on the poleward side of a doldrum Eq. T.

is shown by the long thin dashed area. "Cloud blob" patterns on the equatorward side of this line exist in larger vertical wind shear, have little or no conservatism in time, and are not considered to be typical disturbances.

The average annual number of tropical storms and the percentage of these to the global total occurring in each of eight development areas are shown in Fig. 2. Table 1 lists these areas by name and gives further description. Fig. 3 shows the points at which tropical storms reached hurricane intensity (~ 75 mph sustained wind) in the Northern Hemisphere. Except for the North Atlantic (excluding the western Caribbean), the points of initial disturbance location and points at which hurricane intensity is reached are not far distant. In the NE Pacific, the average distance from the point of initial location of disturbance to hurricane intensity is approximately 7° latitude; for the NW Pacific, 11° latitude; for the North Indian Ocean, 7° latitude; for the western Caribbean, 8° latitude. In the South Indian Ocean, the average distance between initial observation of disturbance in the trades and point of recurvature into the westerlies is 7° latitude. Thus, except in the North Atlantic, tropical storms usually develop within 10° latitude from the position of initial disturbance detection. This distance can vary from 10° to 70° longitude for initial disturbance formation over or off the west African coast during the middle of the hurricane season.

Fig. 5 portrays the number of tropical disturbances which later developed into tropical storms that originated or were first detected in each 2 1/2° latitude belt of both the Northern and Southern Hemispheres. Approximately 75% of all tropical storms develop in the Northern Hemisphere. Approximately 87% of all storms had their initial disturbance location at latitudes equatorward of 20°. Fig. 6 is similar to Fig. 5 and shows the latitudes of initial disturbances in each 2 1/2° belt for each of the major development regions. Note that all disturbances later developing into tropical storms which are first detected at latitudes poleward of 22 1/2° are located in either the NW Atlantic or NW Pacific. Figs. 7 and 8 show the global distribution of tropical storms in both hemispheres by month relative to the calendar and solar years.

Figs. 9 and 10 portray the information of Figs. 1 and 3 in normalized form. The frequency of tropical disturbances which were initially detected in each 5° latitude-longitude square per 25 years

TABLE 1

AREAS WHERE TROPICAL STORMS DEVELOP[1]

Area No.	Area Location	Average Percentage of Global Total	Average Number of Tropical Storms Per Year
I	NE Pacific	16 (?)	10 (?)
II	NW Pacific	36	22
III	Bay of Bengal	10	6
IV	Arabian Sea	3	2
V	South Indian Ocean	10	6
VI	Off NW Australian Coast	3	2
VII	South Pacific	11	7
VIII	NW Atlantic (including W. Caribbean and Gulf of Mexico)	11	7
	Total	100	62

[1]Tropical storms are defined as a warm-core vortex circulation with sustained maximum winds of at least 40 mph.

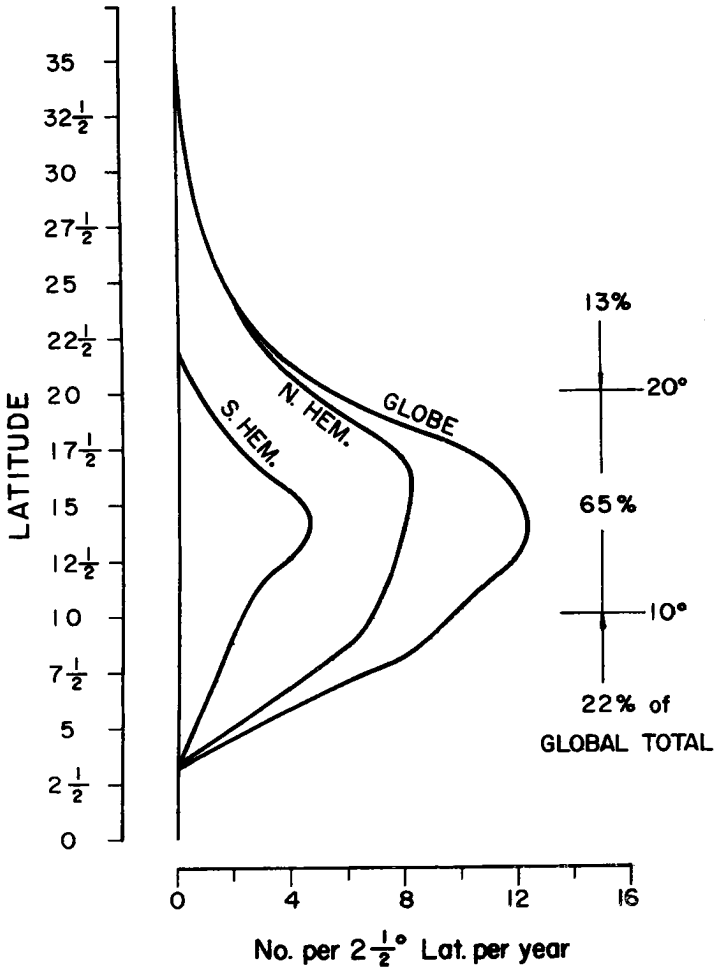

Fig. 5. Latitude at which initial disturbances which later became tropical storms were first detected.

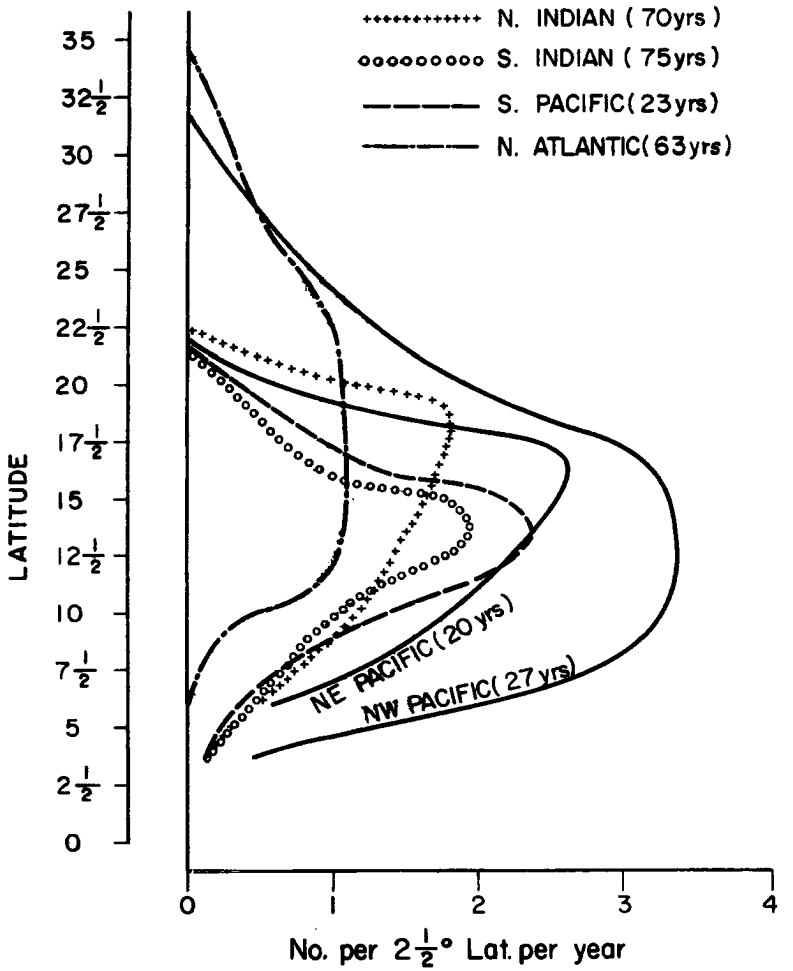

Fig. 6. Latitude at which initial disturbances which later became tropical storms were first detected for the various development regions. Number of years in data average in parentheses.

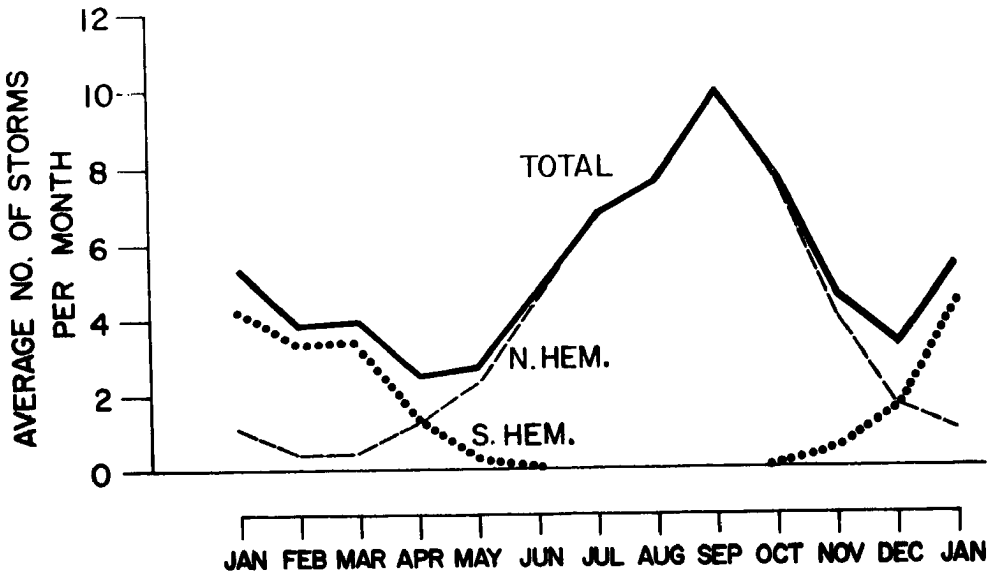

Fig. 7. Global total of tropical storms relative to calendar year.

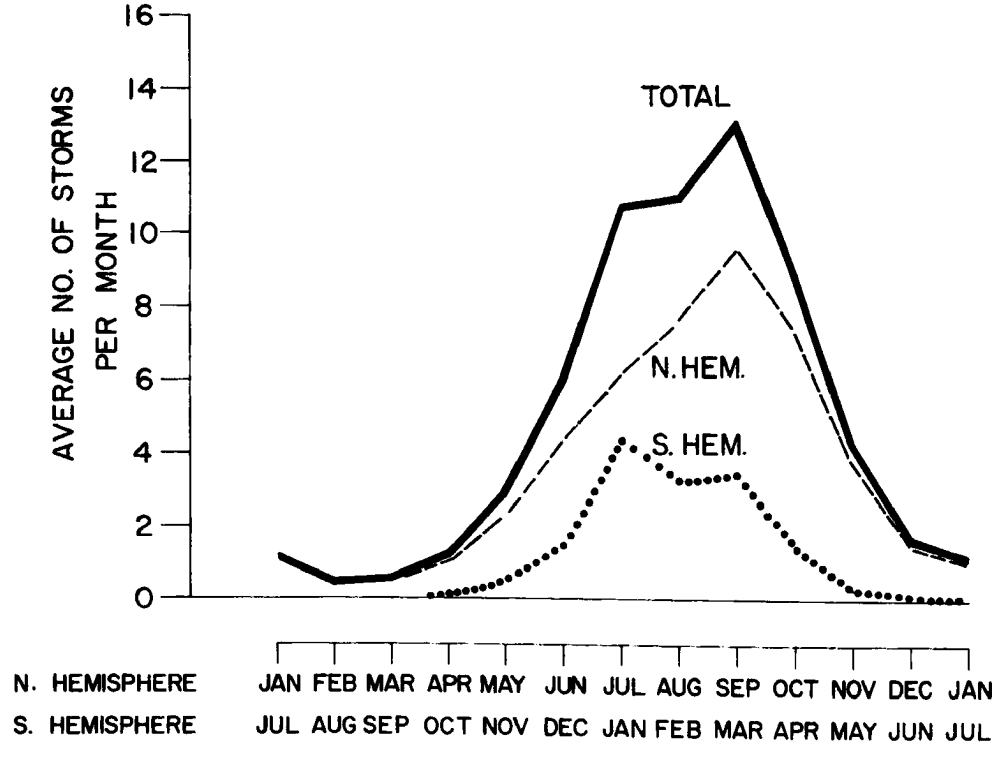

Fig. 8. Global total of tropical storms relative to solar year.

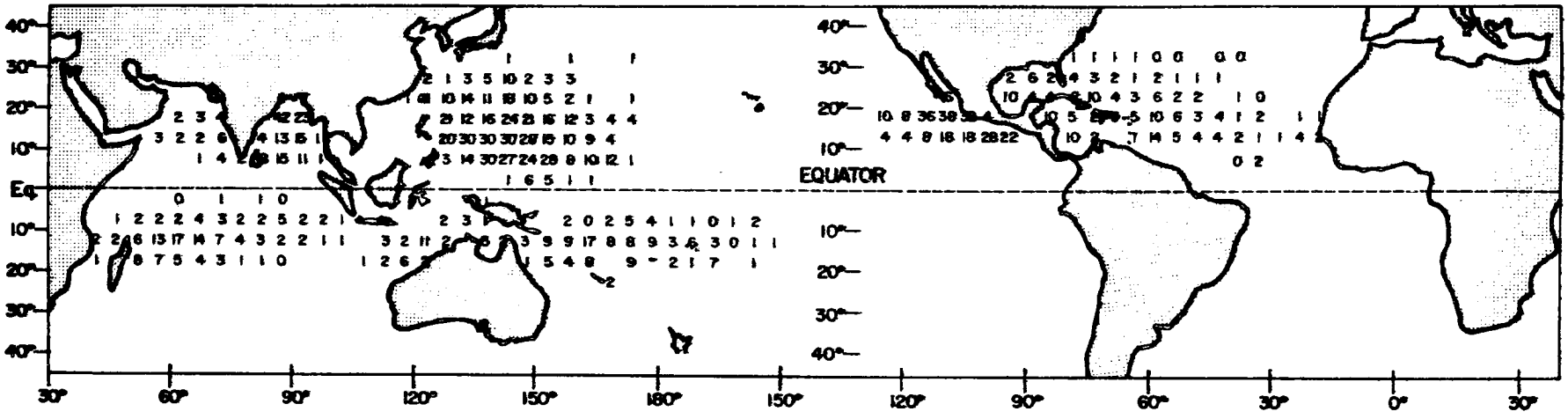

Fig. 9. Frequency of initial location of disturbances which later became tropical storms per 5° lat. - long. area per 25 years. The lack of any initial disturbance genesis in the South China Sea may not be representative.

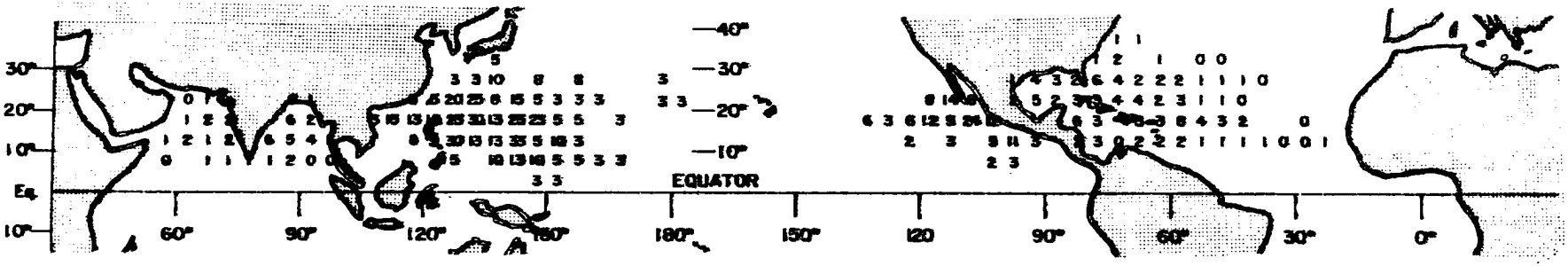

Fig. 10. Frequency of storm location with first observed hurricane intensity winds per 5° lat. - long. area per 25 years.

(and which later obtained sustained wind speeds of 40 mph or greater) is shown by Fig. 9.[1] The frequency of initial hurricane location in similar latitude-longitude squares for the Northern Hemisphere is shown in Fig. 10. Note the strong concentration of initial disturbance detection and initial hurricane position in selected locations. Why should this area concentration exist? To answer this question we must specify and physically interpret the differences in environmental conditions between the development and non-development regions.

Climatology of Equatorial Trough (Eq. T.). Figs. 11 and 12 portray typical surface wind conditions for the months of January and August over tropical regions. The Eq. T. is portrayed by the thick solid line and dashed line which extend east and west closely parallel with the latitude circles. The streamlines of these figures portray idealized climatological surface wind conditions. The solid portion of the Eq. T. line denotes a "doldrum Eq. T.," or an area along which calm surface conditions prevail. Thus, in the NW Pacific in the month of August, weak westerly or southwesterly surface winds are typically present on the equatorward side of this line. Easterly trade winds are present on the poleward side. By defining the doldrum type of Eq. T. with respect to wind, calm surface conditions are required along the Eq. T. in the region of change from westerlies to easterlies. When the Eq. T. is not displaced far from the equator, northeast and southeast trade winds tend to meet along a line of lowest pressure (as occurs in the eastern and central Pacific and central Atlantic). Calm wind conditions are not observed. This type of Equatorial Trough, which is best defined with respect to lowest pressure, will henceforth be designated a "trade-wind Eq. T." Fig. 13 shows idealized flow patterns associated with each of these types of surface wind configurations. The dashed line on the pole-

---

[1] As previously mentioned, values for the Atlantic are not representative. Until satellite coverage, disturbances first located in the center of the Atlantic in the middle of the hurricane season probably had origin just off or on the west African coast. The concentration of initial disturbance position in the central Atlantic should be relocated off the NW African coast. Sixty-three years of data have been used. New information has significantly altered the typical initial detection location (Asplidin, et al.). Initial disturbance locations during the early and late portions of the hurricane season in the western Caribbean and Gulf of Mexico are, however, representative.

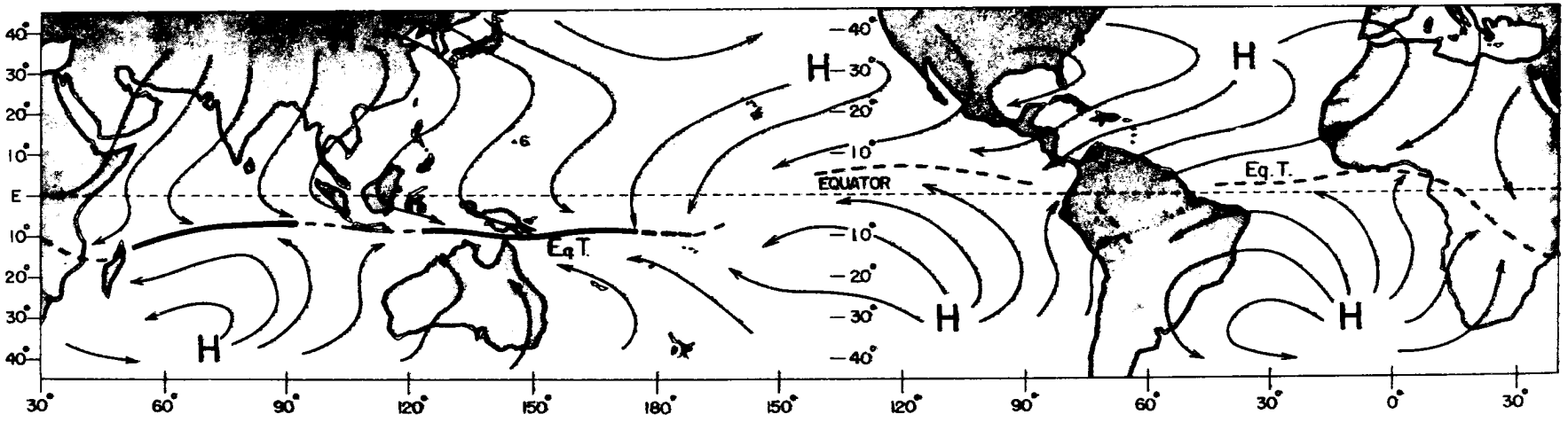

Fig. 11. Idealized monthly mean flow conditions for January. The heavy solid line represents doldrum Equatorial Trough; the heavy dashed line represents trade-wind Equatorial Trough.

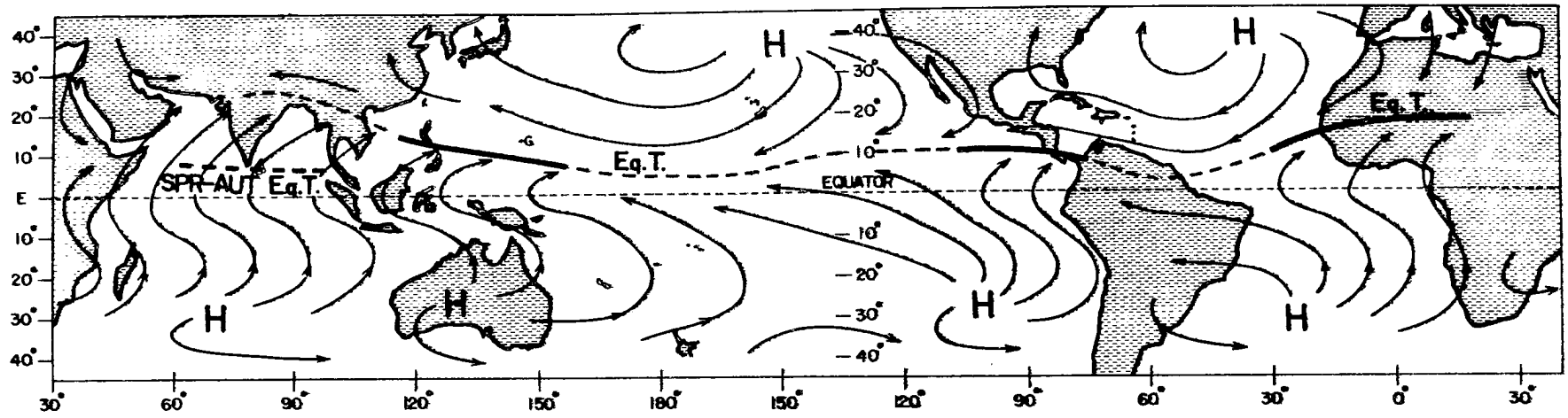

Fig. 12. Idealized surface mean flow conditions for August. The heavy solid lines represent doldrum Equatorial Troughs; the heavy dashed lines represent trade-wind Equatorial Troughs. The very heavy dashed line over the North Indian Ocean represents the average position of the Equatorial Trough in spring and autumn.

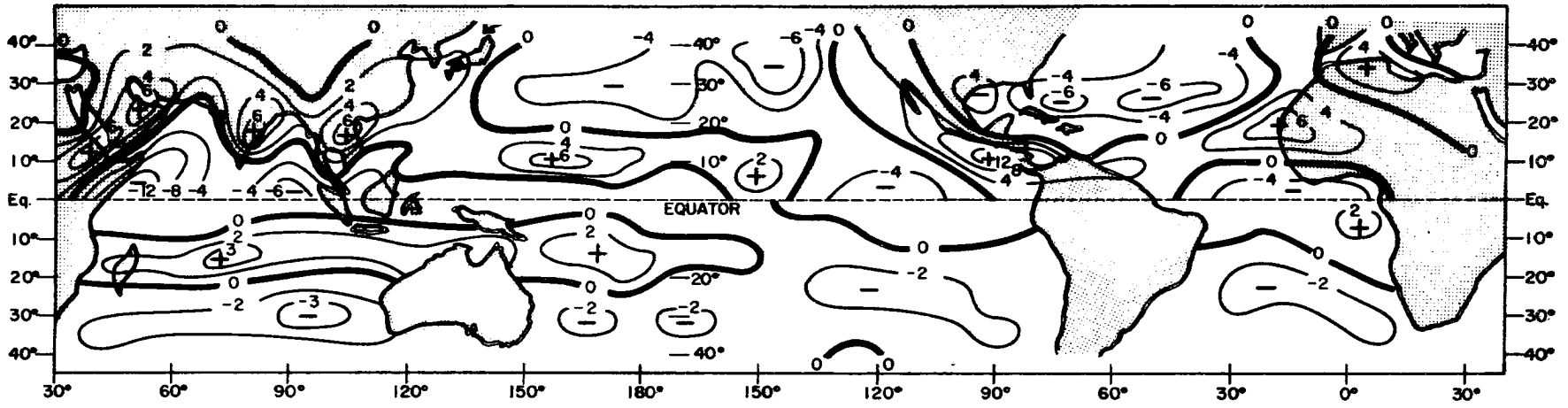

Fig. 14. Monthly averages of surface relative vorticity in units of 10^{-6} sec^{-1} for the Northern Hemisphere in August and the Southern Hemisphere in January. Note high correlation of initial disturbance genesis with maximum centers of surface relative vorticity.

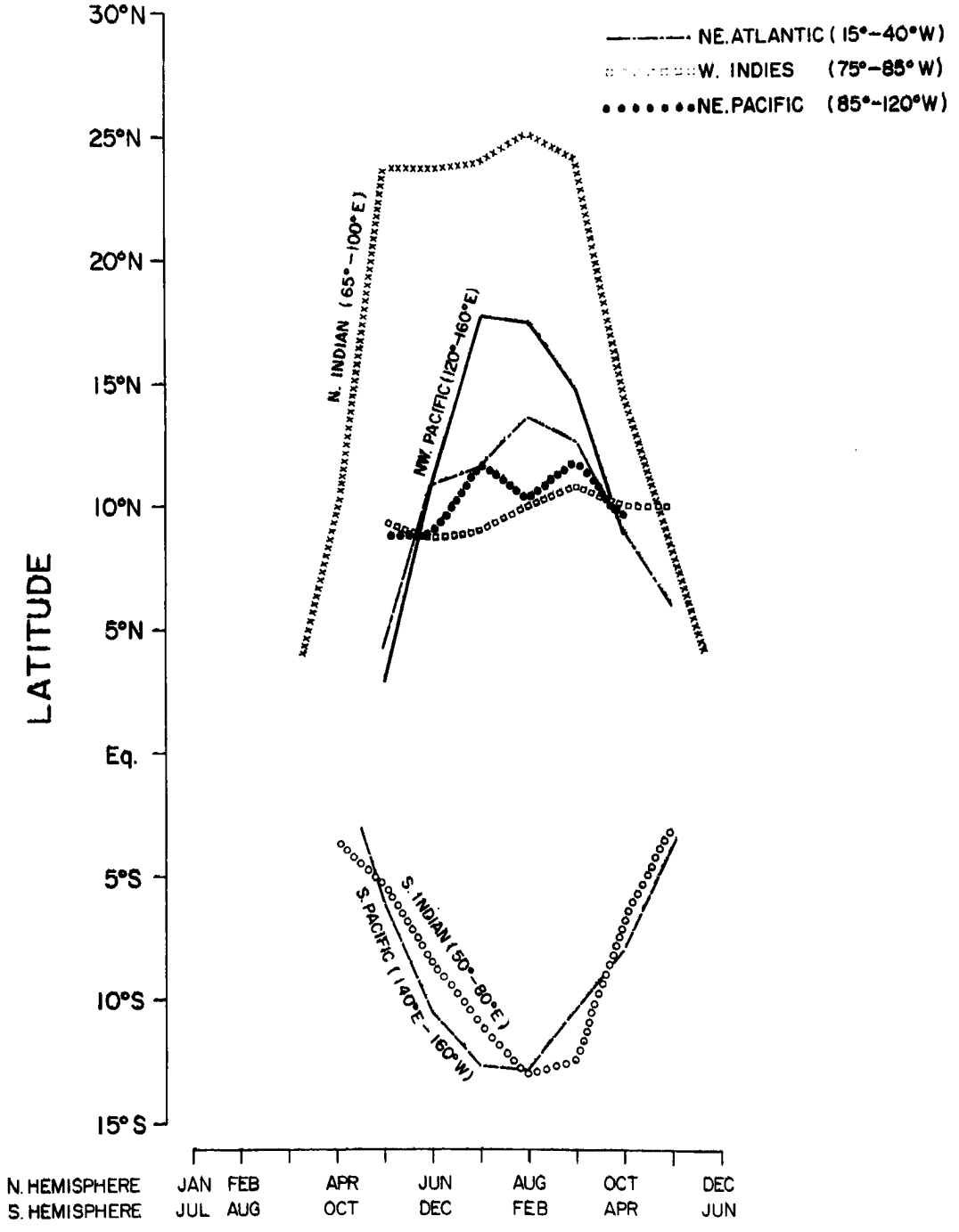

Fig. 15. Seasonal latitude variation of the Equatorial Trough in the various development regions.

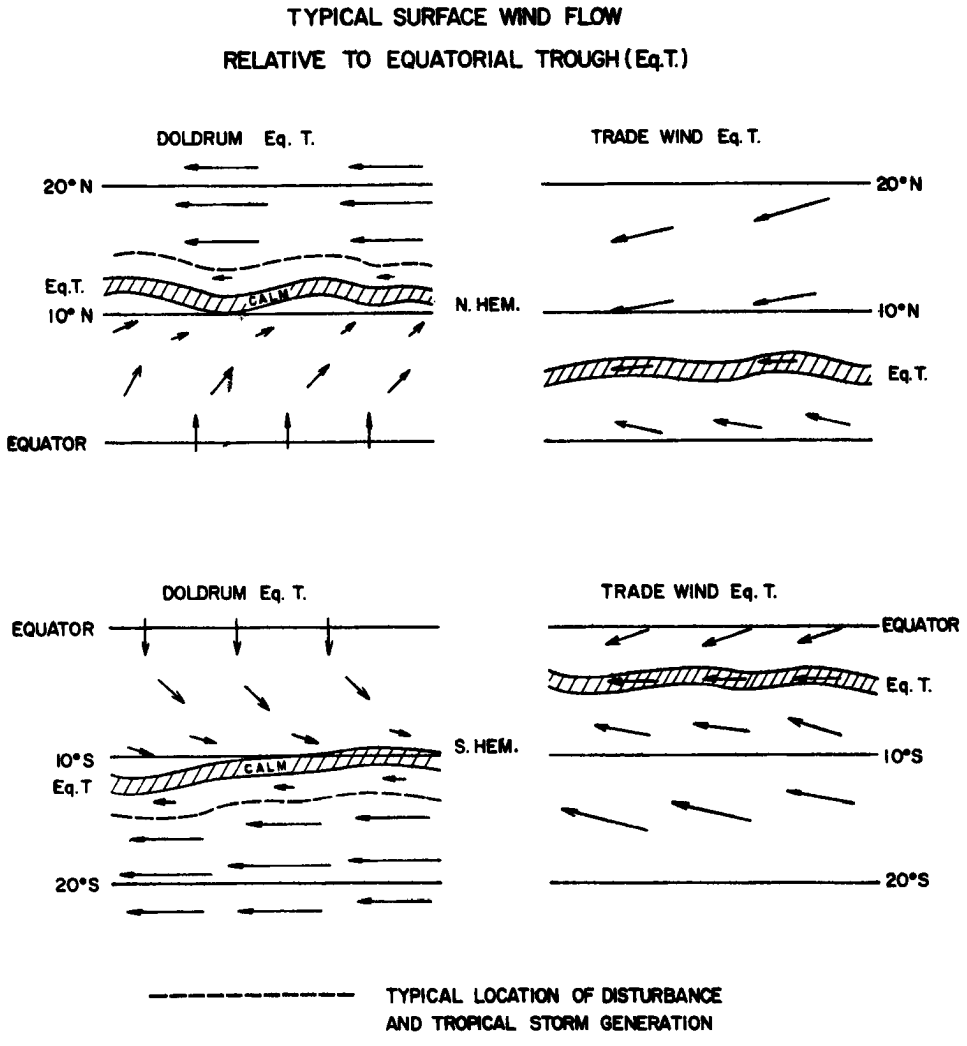

Fig. 13. Portrayal of typical doldrum and trade-wind Equatorial Troughs (Eq. T.) in both the Northern and Southern Hemispheres. Dotted line on poleward side of doldrum Eq. T. represents typical location of initial disturbance genesis.

ward side of the doldrum Eq. T. appears to be the typical location of initial disturbance genesis. The idealized surface climatology of Figs. 11 and 12 is felt to be approximately representative of the flow conditions one might observe on the individual day. Elimination of individual disturbance and developed storm data would not significantly change the climatology in the doldrum Equatorial Trough areas which are displaced more than 8-10° latitude from the equator. When the Eq. T. is close to the equator, individual disturbances may have an influence on altering the monthly climatology.

Association of Equatorial Trough with Initial Disturbance Location. By comparing Fig. 1 with Figs. 11 and 12, it should be noted that (except for development areas in the NW Atlantic and in the NW Pacific poleward of 20° latitude) the initial detection of disturbances from which tropical storms later develop occurs almost exclusively just to the poleward side of doldrum Equatorial Troughs. These regions on the equatorward side of the trade winds (and poleward of the Eq. T.) are areas of large-scale surface cyclonic wind shear (i. e., large-scale relative vorticity). These horizontal shear regions are hypothesized to be necessary in establishing a frictionally forced surface convergence (due to Ekman-type frictional veering) and consequent upward vertical motion at the top of the sub-cloud layer. Broad-scale frictionally induced convergence by itself is enough to develop significant cumulus cloud density to cause slow tropospheric warming.

Fig. 14 portrays surface relative vorticity (calculated on a 5° latitude-longitude grid interval) for the Northern Hemisphere in August and the Southern Hemisphere in January. Except for the NW Atlantic, note the strong correlation between the places of initial disturbance formation and high values of surface relative vorticity. In the NW Atlantic, disturbance genesis occurs further east than the data indicates.

Fig. 15 shows the monthly latitude variation of the doldrum Eq. T. in the various development regions. Fig. 16 gives the regional variations of latitude of first detection of tropical disturbances (except for the NW Atlantic) which later became tropical storms. By comparing Fig. 15 with Fig. 16 one notes the strong climatological correlation between doldrum Eq. T. latitude variation and initial disturbance latitude variation. Fig. 17 is similar to Fig. 16, but for various sub-areas of the NW Atlantic region. In the North Atlantic,

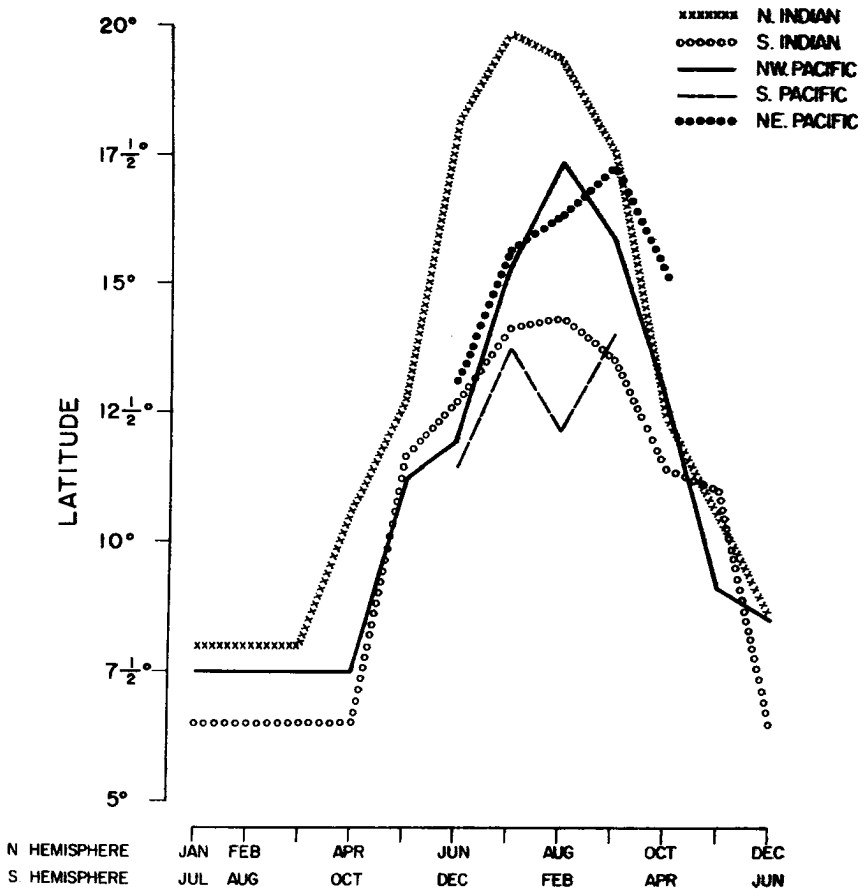

Fig. 16. Seasonal latitude variation of initially located disturbances which later became tropical storms. The North Atlantic is not included.

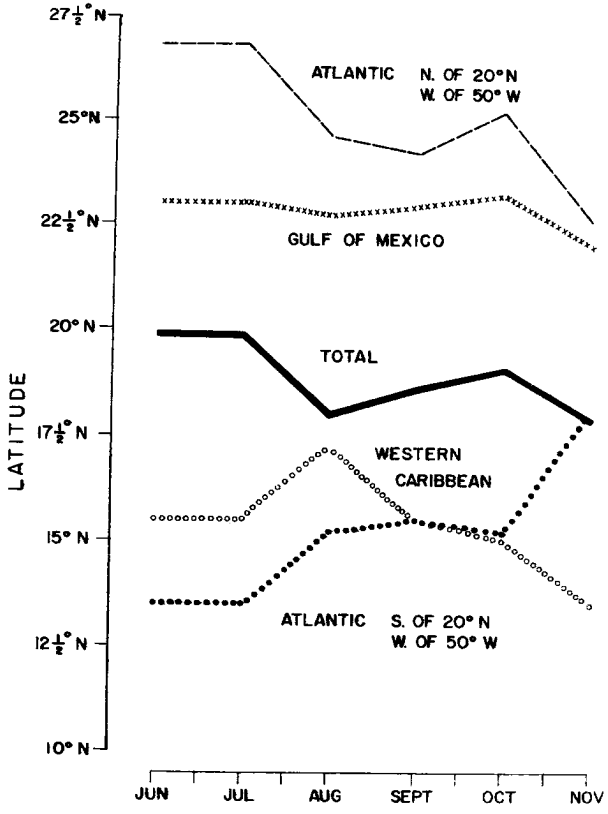

Fig. 17. Seasonal latitude variation of initially located disturbances in the North Atlantic which later developed into tropical storms.

disturbances have no significant seasonal variation in their latitude of formation.

Fig. 18 gives a statistical portrayal of the location of individual initial disturbances which later became tropical storms relative to the climatological monthly positions of the doldrum Eq. T. in the various development regions. Almost all initial disturbance locations are found within 10° latitude of the climatological location of the Eq. T. Except for the western Caribbean, the NW Atlantic region has not been included. Thirty-five percent of the observations indicate a latitude location of initial disturbance on the equatorward side of the climatological Eq. T. This is partly due to inaccuracies of initial disturbance location but it is primarily due to the daily and monthly deviations of the doldrum Eq. T. from its climatological position. As best it can be determined, individual observations never show a disturbance which later becomes a tropical storm to be located within surface westerly winds equatorward of the Eq. T.

At higher latitudes in the NW Atlantic, Gulf of Mexico, and poleward of 20° in the NW Pacific, however, disturbance intensification can occur within environmental conditions which are significantly different than above. Surface westerlies are initially absent for a large distance on the equatorward side of these sub-tropical type of disturbance intensifications. Upper level wind conditions are also different. Due to the much smaller frequency of disturbance genesis at these higher latitudes (~ 15% of global total), however, these latter cases may be considered as atypical.

Fig. 19 portrays the percentage of average yearly storms occurring in each month for each of the global development regions. Note the double maxima (associated with the onset and retreat of monsoon) in the Arabian Sea and Bay of Bengal and the central peaks in late summer in the other regions. In general, frequency of development is largest when the Eq. T. is displaced farthest from the equator. [1]

---

[1] In the single month of August 1950, when the Eq. T. was displaced 5-10° latitude further north of its normal position in the NW Pacific, no less than 16 named tropical storms developed.

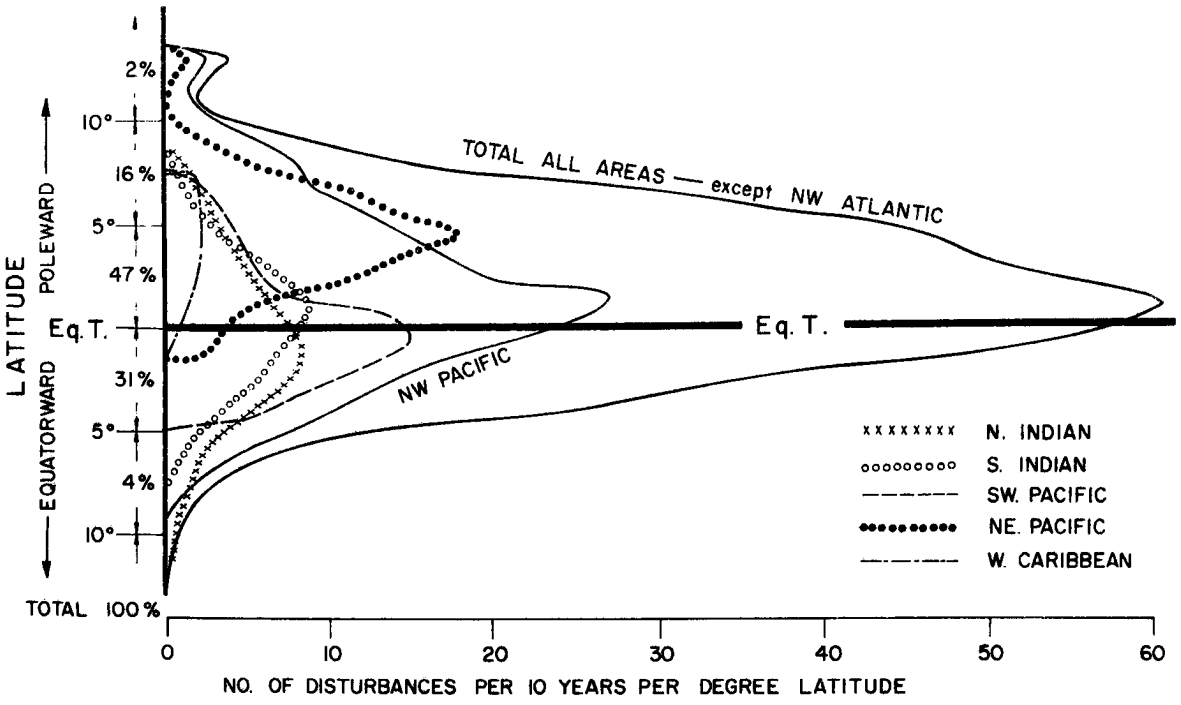

Fig. 18. North-south position location (in degrees Lat.) relative to climatological monthly positions of doldrum Eq. T. of first location of disturbances which later became tropical storms for the various development regions.

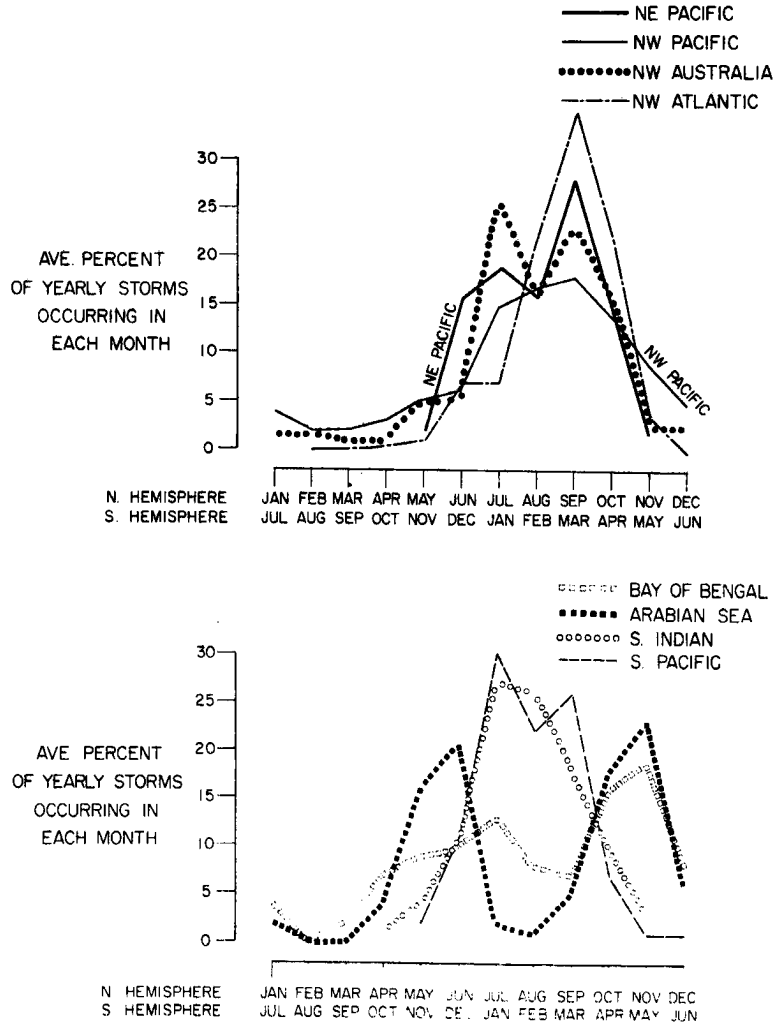

Fig. 19. Seasonal distribution of tropical storms in each of the development regions.

Climatology of Potential Buoyancy in Lower Half of the Troposphere. Fig. 20 gives the latitude distribution of sea surface temperatures (SST) in the regions where disturbances and storms develop. It will be seen that only in the NW Atlantic, Gulf of Mexico, and the NW Pacific does the 26 1/2°C isotherm (mentioned by Palmén, 1948, 1956, as necessary for development) extend poleward of 20°. The SST has a strong influence on the potential buoyancy of the cumulus clouds. Because of the primary importance of cumulonimbus in warming the middle and upper troposphere to develop the tropical disturbance and later storm, it is important to know the magnitude of the cumulus potential buoyancy in the lower half of the tropical troposphere. The maps of Figs. 21 and 22 show isopleths of average potential buoyancy over the tropical oceans in summer and winter respectively. Potential buoyancy has been defined as the difference of equivalent potential temperature (θ_e) from the surface to 500 mb. Figs. 23 and 24 portray potential buoyancy over the North Indian Ocean for the months of May and November. Note that potential buoyancy is large over all the tropical oceans. In summer it varies little with longitudes. Observe also that the difference in potential buoyancy from summer to winter months is small in tropical latitudes equatorward of 15°. Although individual-level summer to winter temperature-moisture changes may be significant, the average vertical gradient of these differences through the lower half of the troposphere does not show substantial seasonal variation. One observes that in summer the potential buoyancy drops off sharply on the poleward side of 20° latitude except in the NW Atlantic and NW Pacific. Except in the latter regions, development does not occur poleward of 20°.

Figs. 25 and 26 show the average tropospheric vertical distribution of equivalent potential temperature (θ_e) in the various developmental regions during the year's two warmest and two coolest months. Note that there is very little regional difference in the vertical distribution of this parameter.

Figs. 27 and 28 portray the differences in the vertical distribution of θ_e between winter and summer for the NW Pacific and West Indies area. Although there is significant decrease of surface θ_e between summer and winter, middle-level decrease of θ_e also occurs. Thus, the vertical gradients of θ_e in the lower half of the troposphere do not show large variation from summer to winter. The potential of the cumulus for initially warming the lower and middle tropospheric levels is just as great in winter as in summer. In the upper troposphere, however, the potential for warming is much less due to the lower cross-over point (350 mb vs. 200 mb) with surface values. The primary effect of differences in potential buoyancy between summer and winter is in reduction of winter cumulonimbus intensity.

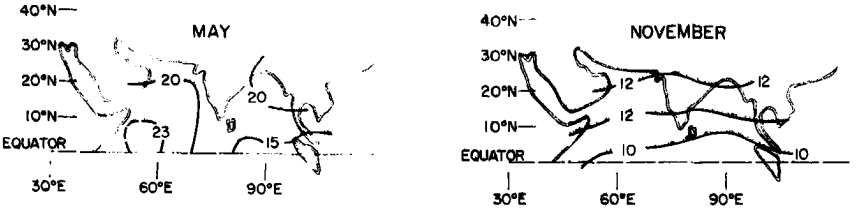

Figs. 23 and 24. Surface minus 500 mb equivalent potential temperature difference for May and November in the North Indian Ocean.

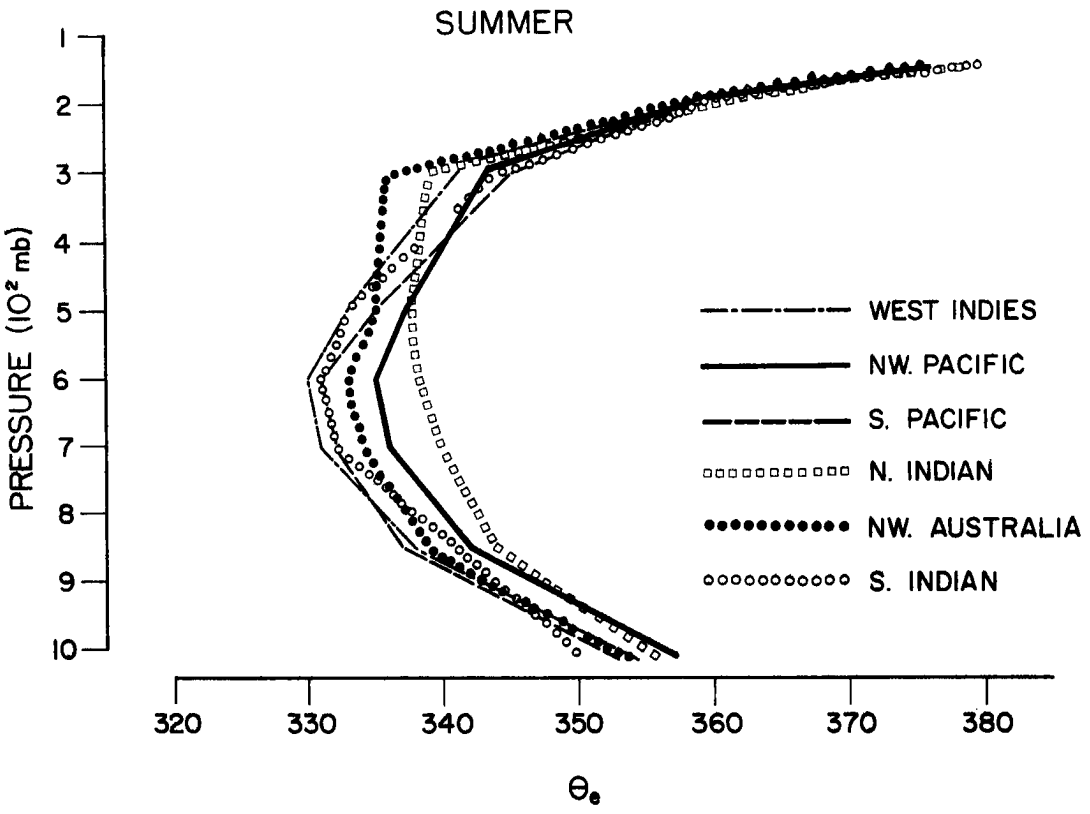

Fig. 25. Average vertical distribution of equivalent potential temperature (θ_e) during the two warmest summer months in the various development regions.

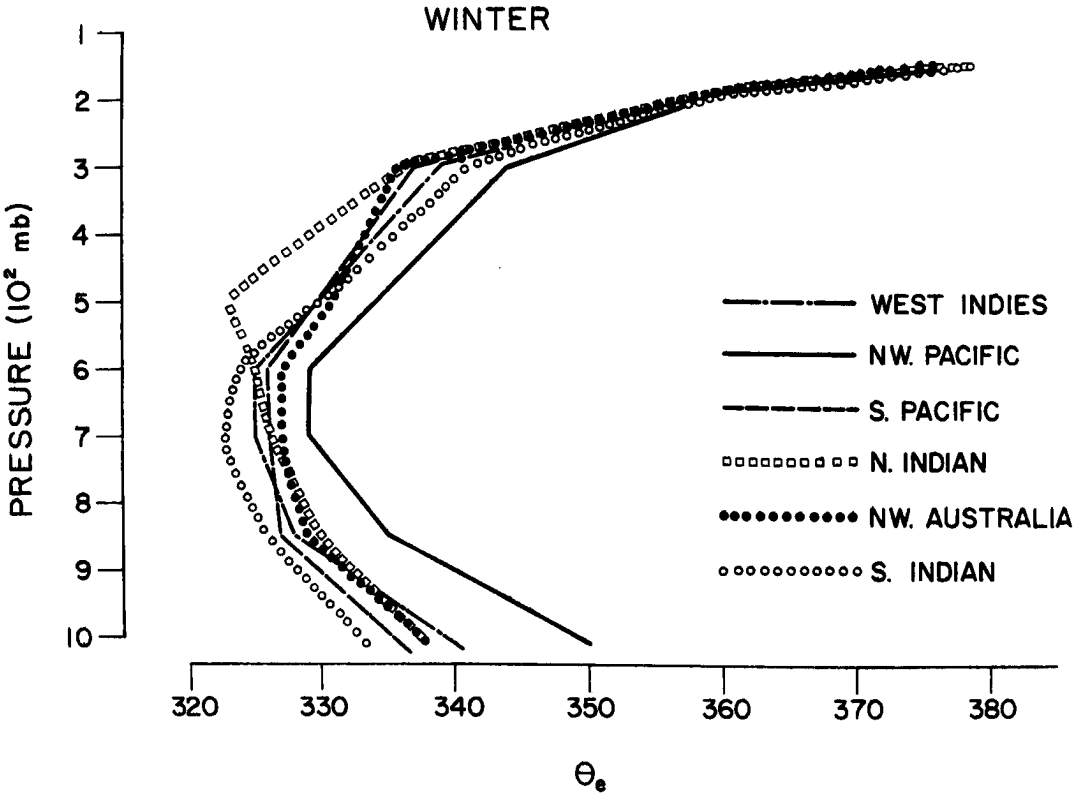

Fig. 26. Average vertical distribution of equivalent potential temperature (θ_e) during the two coldest winter months in the various development regions.

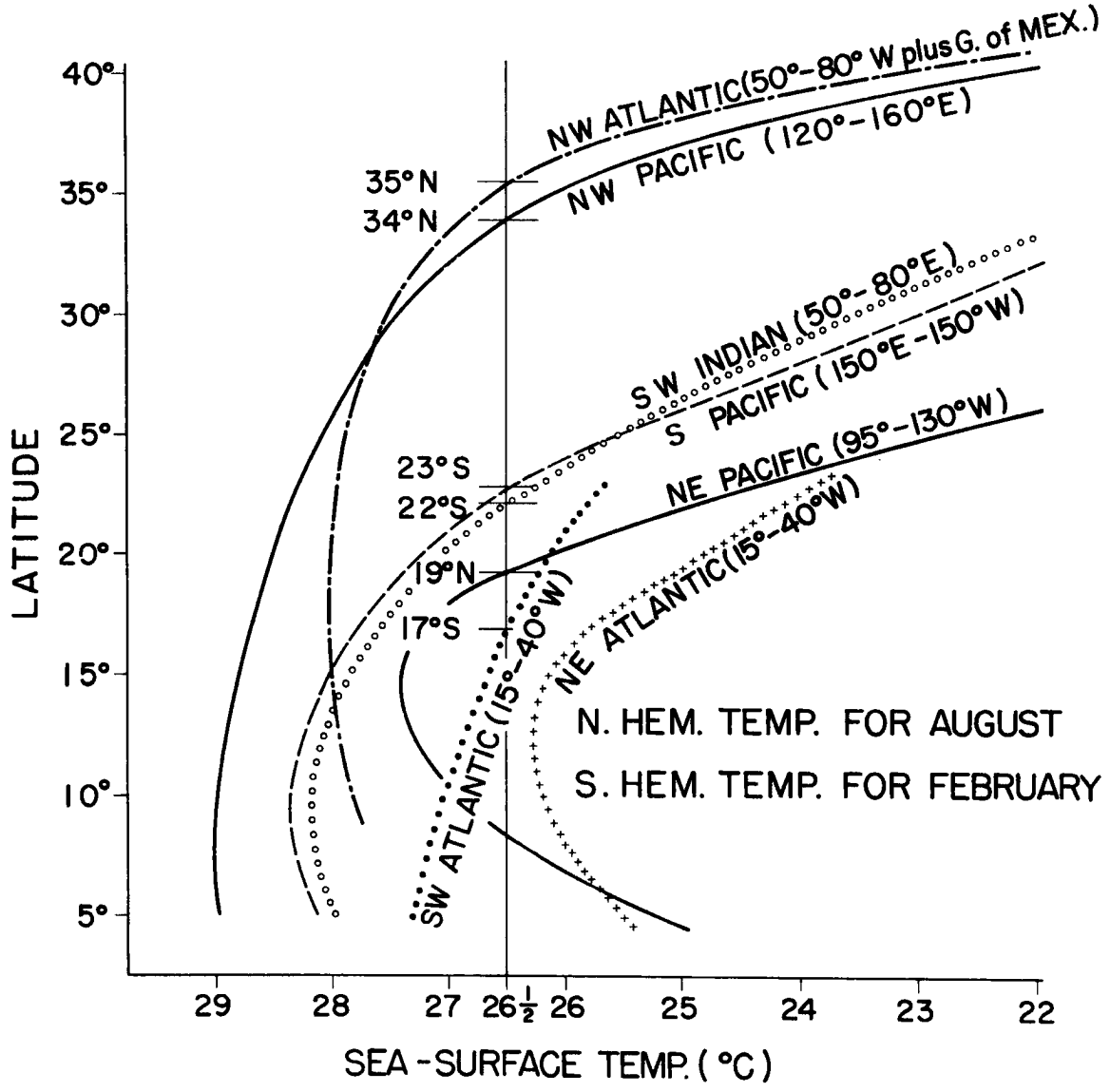

Fig. 20. Latitude variations of sea surface temperatures (SST) in the various development regions during the warmest summer month.

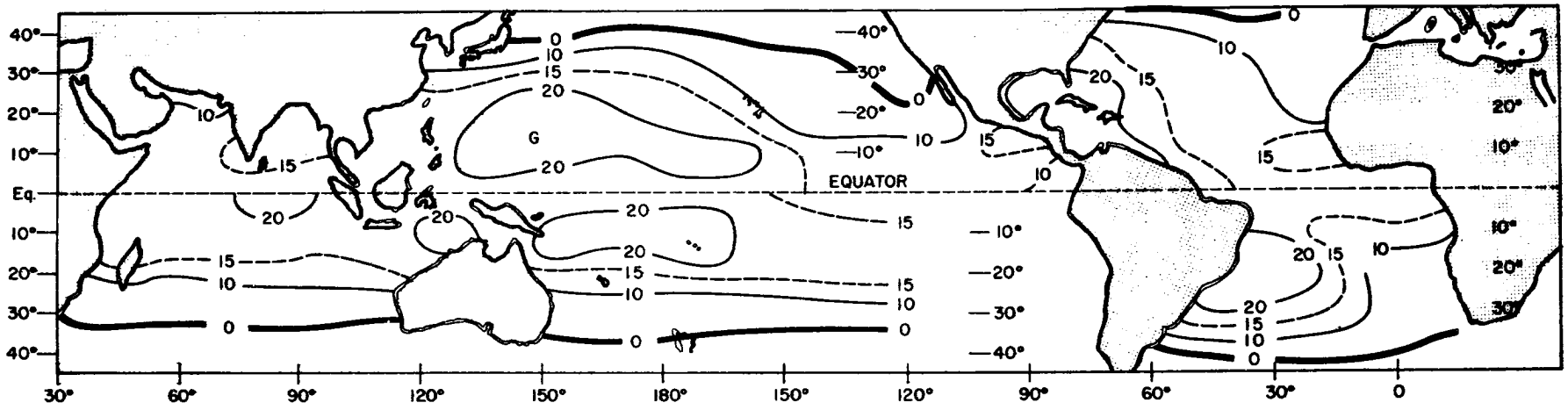

Fig. 21. Potential buoyancy of cumulus. Summer climatology of surface minus 500 mb level equivalent potential temperature difference. Northern Hemisphere is for an August-September average; Southern Hemisphere is for a January-February average.

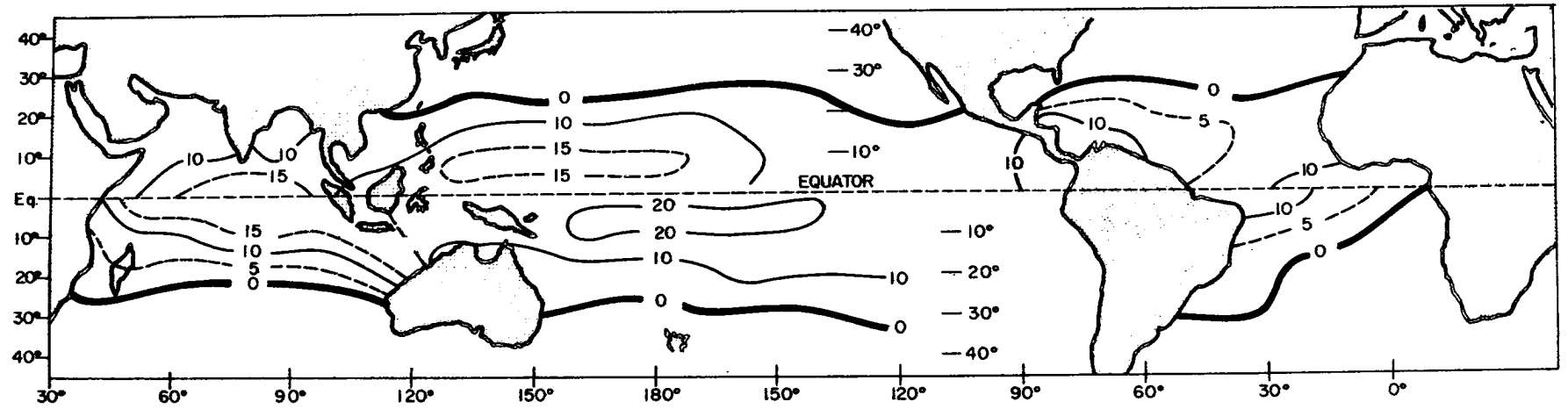

Fig. 22. Potential buoyancy of cumulus. Winter climatology of surface minus 500 mb level equivalent potential temperature difference. Northern Hemisphere is for a January-February average; Southern Hemisphere is for an August-September average.

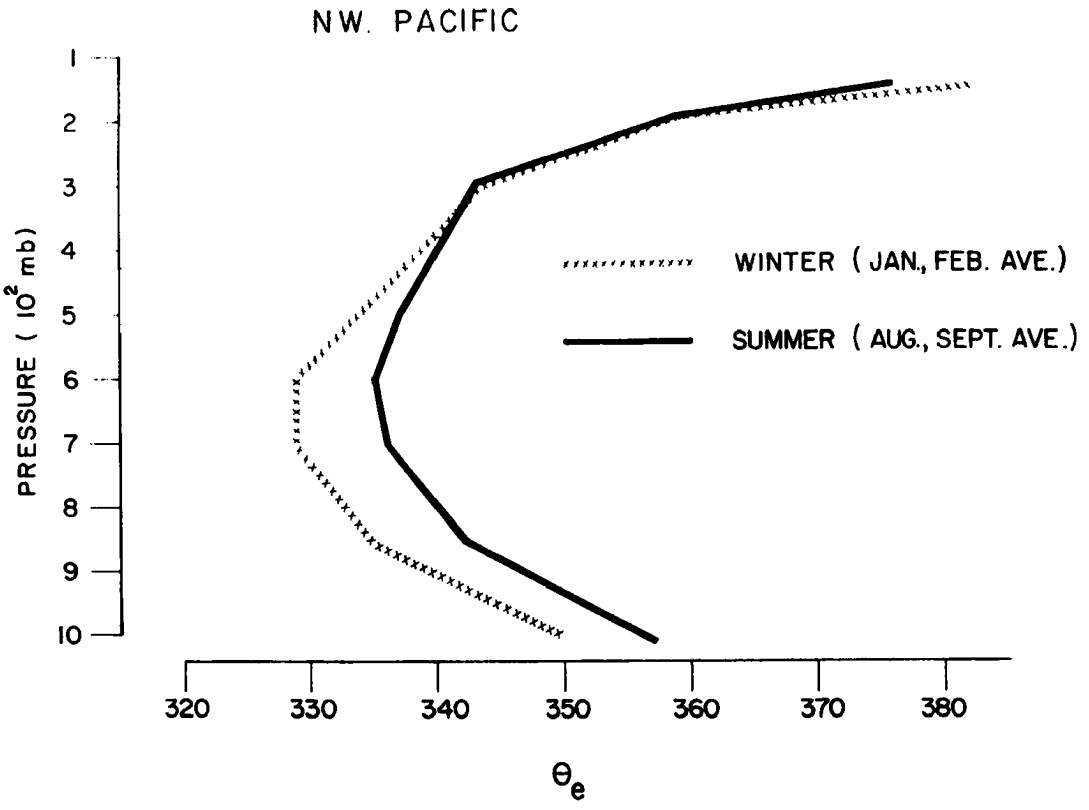

Fig. 27. Variation from summer to winter of the vertical distribution of equivalent potential temperature in the NW Pacific development area.

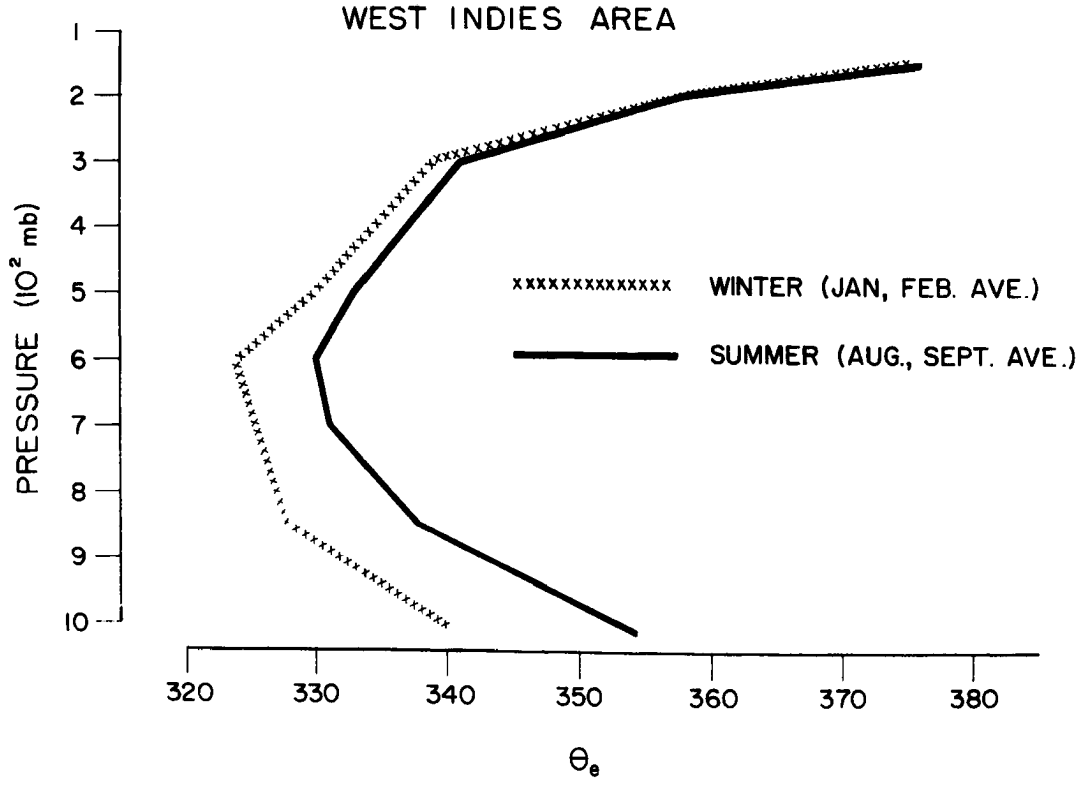

Fig. 28. Variation from summer to winter of the vertical distribution of equivalent potential temperature in the West Indies development area.

At the surface and at 850 mb, θ_e variations from summer to winter result from nearly equal changes of temperature and moisture. At 700 mb and 500 mb, however, changes in θ_e from summer to winter are brought about primarily by variation of moisture. Variation of temperature from summer to winter at these higher levels is typically less than 1°C, while variations of dew point average 4° to 6°C. This occurs from the fact that convection is less frequent in winter than in summer.

Daily variations of potential buoyancy (as defined above) in individual disturbance areas are also observed to be small. A large statistical sample of individual sounding deviations of potential buoyancy shows that the average individual observation variation of this parameter is but 20-35%. Average deviation of this parameter at two or more stations within an individual disturbance shows it to vary from the monthly mean by less than 10-15%.

A change of surface air temperature of 1°C increases the equivalent potential temperature (θ_e) by approximately 5°C. Changes of surface relative humidity of 10% increase θ_e by the same amount. Changes of 1°C and 10% relative humidity at 500 mb result in but 2° and 1° changes of θ_e. Temperature-moisture variations in the surface layers thus have a much larger effect on θ_e changes than variations at 500 mb. In the developing disturbance maximum temperature and moisture increase takes place in the middle levels. Even though increases in temperature and moisture in the middle levels are much larger than in the surface layers, their net effect will alter the potential buoyancy to more stable values by a maximum amount of no more than 20-35%. The average value of the potential buoyancy in the mean summertime tropical atmosphere is 18-20°C. A large statistical sample of this parameter in the tropical disturbance shows it to be in the typical range of 14-17°C.

Although there is a continuous reduction of cumulus potential buoyancy to a more stable value with an ever increasing intensity of tropical disturbance, the percentage reduction of this parameter is not so large. For this reason variations of cumulus potential buoyancy are not considered to be of primary importance in explaining the preferred areas of development. Other physical parameters must be examined before one can understand the strongly preferred areas of disturbance and storm development as portrayed in Figs. 9 and 10.

Climatology of Tropospheric Vertical Wind Shear. Figs. 29 through 32 portray the climatological distribution of tropospheric shear of the horizontal wind between 200 mb and 850 mb for the four months of January, April, August, and October (in knots).[1] Positive values indicate that the 200 mb zonal speed is stronger from the west or weaker from the east than the zonal speed at 850 mb. It is observed that the places of storm formation in January and August show a strong association with regions of climatological minimum or zero zonal tropospheric vertical shear. In the North Indian Ocean tropical storm development occurs primarily in the spring and autumn. Zonal climatological vertical wind shear during April and October also shows this minimum of shear which is present with development in these seasons. In the months of July and August surface westerlies and strong upper-level easterly winds exist over the southern Indian sub-continent; vertical shears are then very large except on the northern fringe of the Bay of Bengal. Disturbance and storm developments do not occur during these months except at the northern edge of the Bay of Bengal.

In the SW Atlantic and central Pacific, where tropical storms do not occur, the observed climatological tropospheric wind shear is large (i. e., 20-40 knots). This is believed to be the major inhibitor to development in these areas. Large vertical wind shears do not allow for area concentration of the tropospheric distributed cumulonimbus condensation. Large shears produce a large ventilation of heat away from the developing disturbance. The condensation heat released by the cumulus to the upper troposphere is advected in a different direction relative to the released heat at lower levels. Concentration of heat through the entire troposphere becomes more difficult.[2]

Fig. 33 portrays a simplified version of the above ventilation concept. Diagram (a) is a plan view of an assumed convergence or "cloud blob" area of east-west width D in which a zonal vertical wind shear

---

[1] Tropospheric wind shear will henceforth be defined as the shear between the levels of 850 and 200 mb.

[2] In the following discussion ventilation will henceforth be equated with tropospheric vertical wind shear.

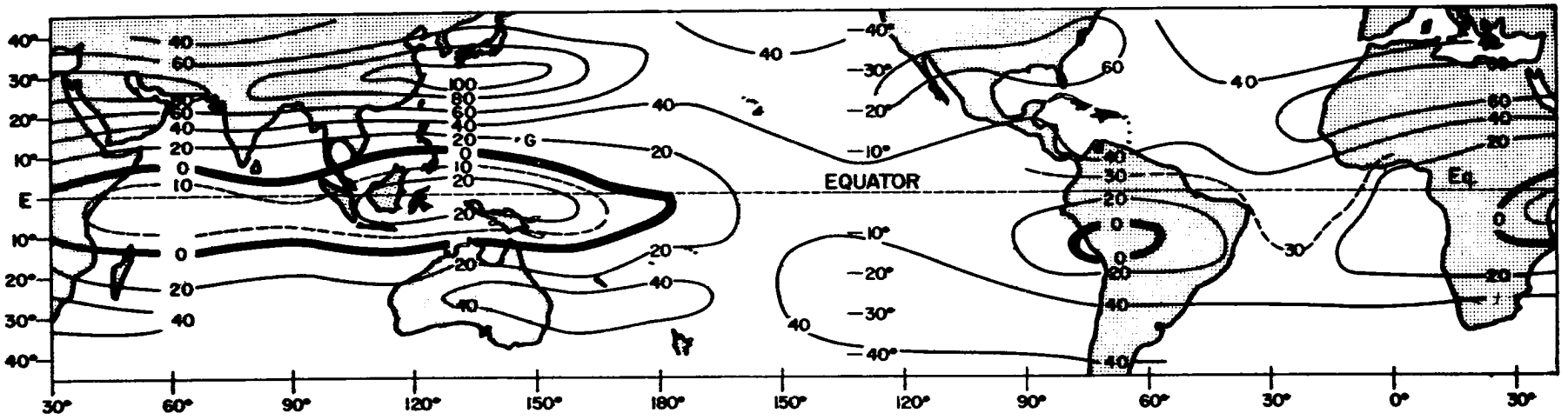

Fig. 29. Climatological average for January of the zonal vertical wind shear between 200 mb and 850 mb. Positive values indicate that the zonal wind at 200 mb is stronger from the west or weaker from the east than the zonal wind at 850 mb. Units are in knots (from U.S. Air Force data tapes, 1963).

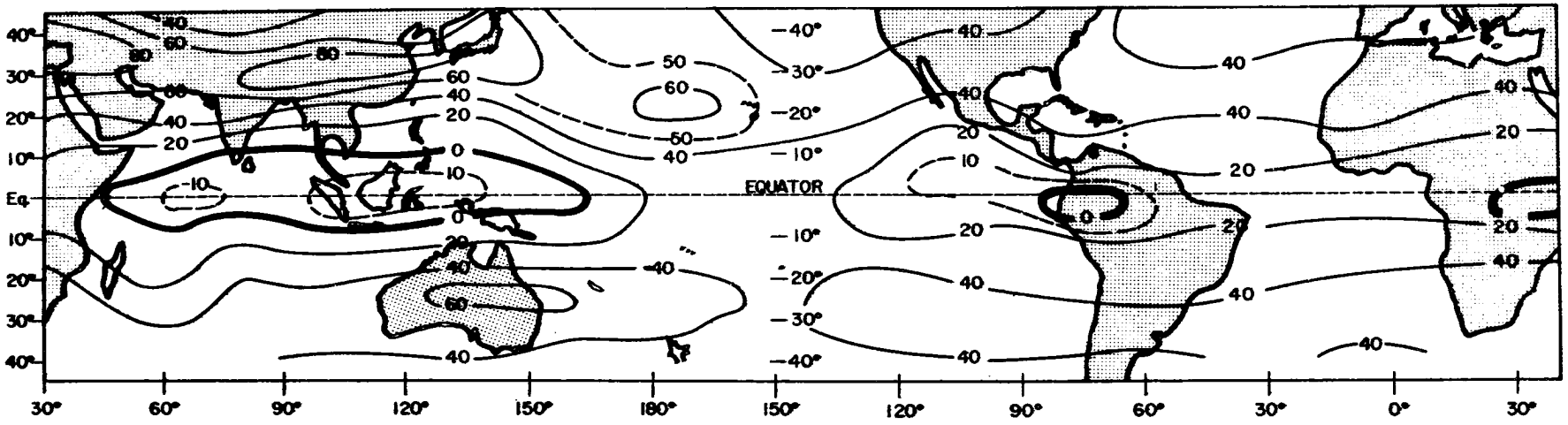

Fig. 30. Climatological average for April of the zonal vertical wind shear between 200 mb and 850 mb. Positive values indicate that the zonal wind at 200 mb is stronger from the west or weaker from the east than the zonal wind at 850 mb. Units are in knots (from U.S. Air Force data tapes, 1963).

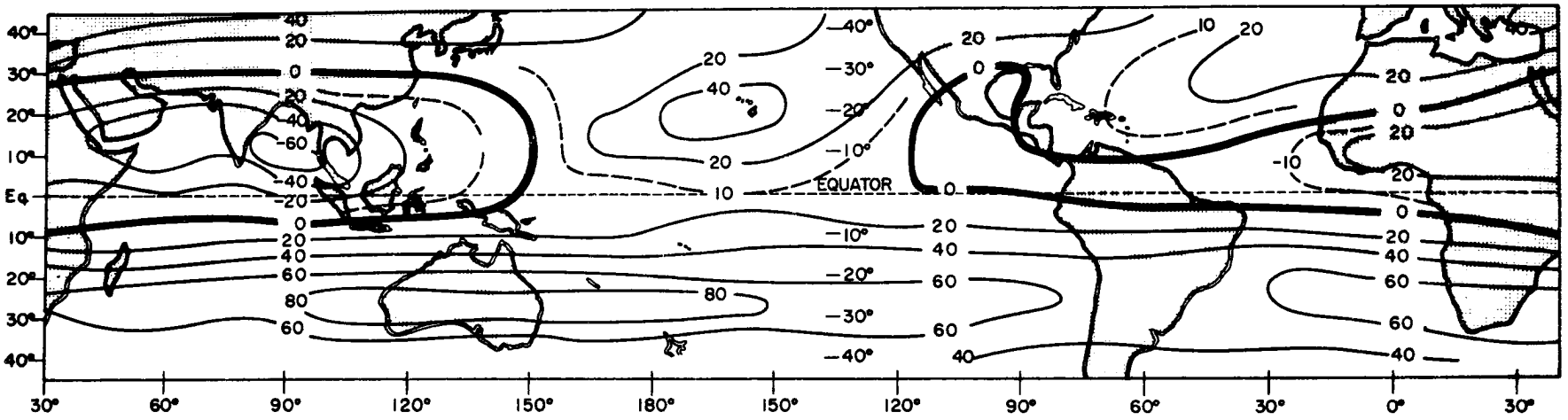

Fig. 31. Climatological average for August of the zonal vertical wind shear between 200 mb and 850 mb. Positive values indicate that the zonal wind at 200 mb is stronger from the west or weaker from the east than the zonal wind at 850 mb. Units are in knots (from U.S. Air Force data tapes, 1963).

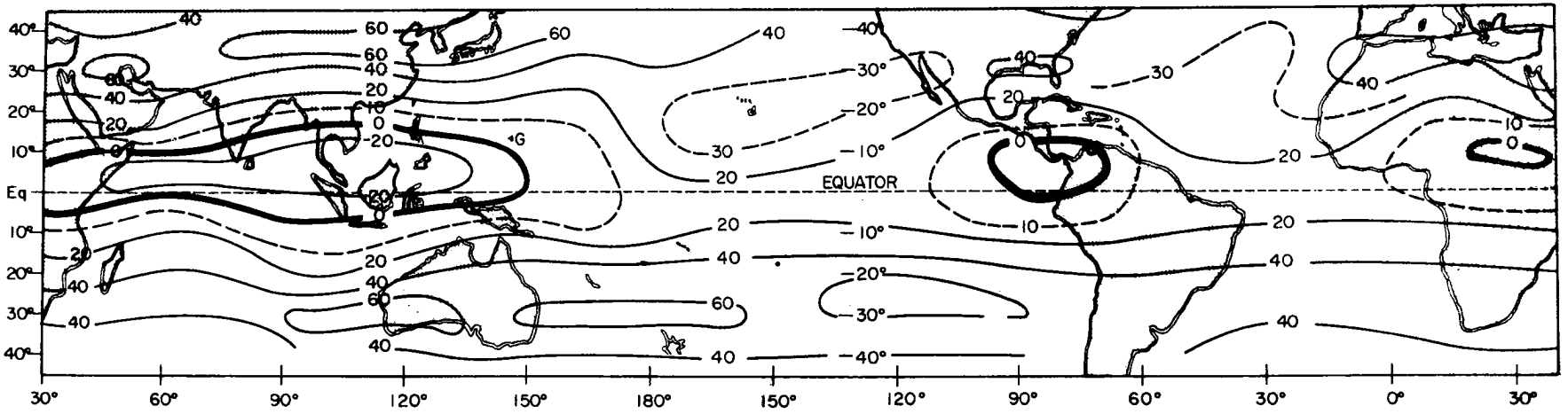

Fig. 32. Climatological average for October of the zonal vertical wind shear between 200 mb and 850 mb. Positive values indicate that the zonal wind at 200 mb is stronger from the west or weaker from the east than the zonal wind at 850 mb. Units are in knots (from U.S. Air Force data tapes, 1963).

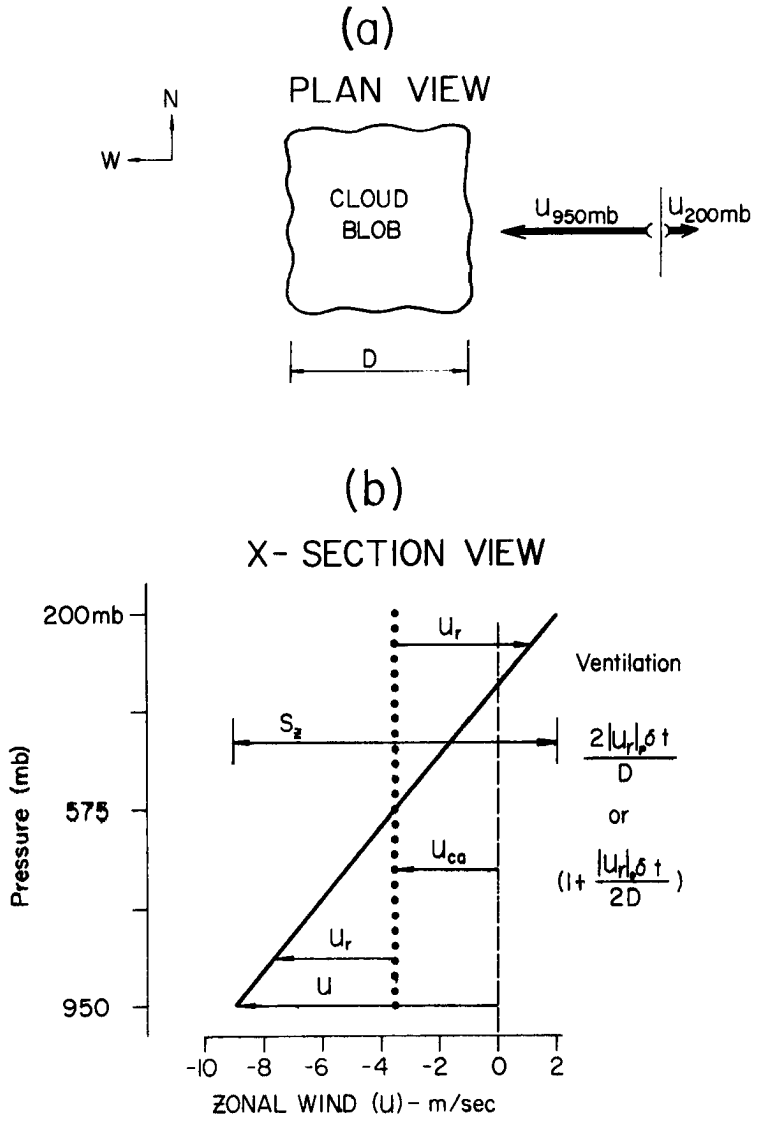

Fig. 33. Diagram (a)--Plan view of schematic convergence area or "cloud blob" of width D. The direction of the zonal wind at the lower and upper levels of the convergence area is at the right.

Diagram (b)--Cross-sectional view of idealized vertical shear (S_z) of zonal wind (u) between 950 and 200 mb. u_{ca} is the assumed zonal velocity of the convergence area or disturbance; u_r the zonal velocity of the wind relative to the convergence area or disturbance; and δt the time interval over which the heating and ventilation are calculated.

is present between 950 and 200 mb. Diagram (b) shows a vertical cross-sectional view of the zonal wind at each pressure height and the vertical shear (S_z) assumed to be linear with pressure between 950 and 200 mb. u is the zonal trade-wind velocity, u_{ca} is the zonal velocity of the convergence area or disturbance. The ventilation factor (V_p) within the convergence area at any level is closely given by

$$V_p = \begin{cases} \dfrac{2\,|u_r|_p\,\delta t}{D} & \text{if } \dfrac{|u_r|\,\delta t}{D} \geq 1, \text{ or} \\ \left(\dfrac{1 + |u_r|_p\,\delta t}{2D}\right) & \text{if } \dfrac{|u_r|\,\delta t}{D} < 1 \end{cases} \tag{1}$$

where

$$|u_r|_p = u - u_{ca}, \text{ or}$$

$$\frac{S_z}{2}\left(\frac{|575 - p|}{375}\right) \text{ for } 200 \text{ mb} \leq p \leq 950 \text{ mb}$$

δt = time interval over which the convergence takes place

The net ventilation for the level between 950 and 200 mb is given by

$$\text{Ven} = \frac{1}{750 \text{ mb}} \int_{200 \text{ mb}}^{950 \text{ mb}} V_p\,\delta p \tag{2}$$

The convergence area is initially assumed to be at the same temperature as the environment.

As discussed in Section 4 and in Fig. 62 (page 57), the magnitude of condensation-produced potential tropospheric heating (H_p)--for conditions of the summertime tropical atmosphere--is directly related to the mass convergence in the lowest 100 mb layer. Vertical motion and condensation produced from convergence above 900 mb does not warm

the troposphere. The potential mean tropospheric heating (H_p) between 950 and 200 mb per unit area is given by

$$H_p = \left(\frac{EL}{750\, c_p} \int_{1000\text{ mb}}^{900\text{ mb}} q\, \nabla\cdot\mathbf{v}\, \frac{\delta p}{g} \right) \delta t$$

where

E[1] = effectiveness of released water vapor condensation in warming the environment. For convergence between the surface and 900 mb for conditions of the mean tropical atmosphere this amounts to roughly 1/8 (see López, 1967).

L = latent heat of condensation

q = specific humidity

$\nabla\cdot\mathbf{v}$ = flow divergence

g = acceleration of gravity

c_p = specific heat of air at constant pressure

and the other symbols are as before.

For simplicity the potential heating is assumed to be equally distributed by the cumulus with pressure from 950 to 200 mb.

The actual tropospheric heating (H_{act}) which can occur from condensation between 950 and 200 mb is reduced by the magnitude of the ventilation factor and is given by the ratio of H_p to Ven. Thus,

$$H_{act} = \frac{H_p}{Ven}$$

---

[1] With the observed vertical gradients of θ_e in the regions where tropical disturbances and storms form, approximately 1/8 of the released condensation from the low-level (surface to 900 mb) water vapor convergence goes into increase of the environmental enthalpy or sensible temperature. The remaining 7/8 of the condensation heat must be given up to expansion and heating of the air mass beyond what would occur with dry adiabatic lapse rate to obtain environmental conditions. Without a vertical gradient of θ_e, none of the released condensation heat could act to warm the troposphere.

TABLE 2

VENTILATION FACTOR

Zonal Vertical Shear (950 to 200 mb) m/sec	D = 500 km δt = 1 day	D = 100 km δt = 1 day
0	1.0	1.0
5	1.1	2.5
10	1.3	4.2
15	1.6	6.4
20	2.0	8.6
30	2.7	12.9
40	3.5	17.3

Table 2 lists values of the ventilation factor for convergent areas equal to 500 km and 100 km and time interval of one day. For other assumed vertical shears and level of condensation heat release, different ventilation factors are obtained.

In addition to the importance of vertical wind shear, ventilation is also greatly affected by the size of the convergence area. For concentration of condensation heating through the troposphere, it is of utmost importance that the size of the convergence area be as large as

possible. (See also Fig. 72 on page 74.) The region of cyclonic wind shear on the equatorward side of the trade winds exhibits such large-scale low-level convergence.

In a detailed study of two cases of development and non-development in the western Caribbean, López (1967) has also noted the importance of small vertical wind shear in development.

Except for the NW Atlantic and NW Pacific, large climatological vertical wind shear is present in all regions poleward of 20° latitude. Only in these regions does disturbance development occur poleward of 20°. Fig. 34 graphically portrays the variation of tropospheric wind shear with latitude in the various development regions. The most frequent area of tropical disturbance and storm development in the NW Pacific possesses the largest area of weak climatological shear. In this region weak vertical shear is observed in a wide latitude belt extending to nearly 30°N. In the North Indian Ocean small vertical wind shears are observed only at latitudes of 20-23° in August and 10-15° in late spring and autumn. In the NW Atlantic climatological wind shear less than 10 knots is present to 33° latitude. Note that in the other development regions small climatological vertical wind shear is not present at such high latitudes.

These regional differences of climatological vertical shear result primarily from differences in upper tropospheric wind rather than in the low-level flow. Trade-wind regimes exist in all oceans. Fig. 35 shows the 200 mb climatological variation of zonal wind with latitude in the development regions in the warmest summer month.

Certainly from the climatological point of view, baroclinic processes cannot be invoked to explain the early stages of tropical storm genesis. The strong statistical association of disturbance and storm development with small vertical wind shear climatology indicates that tropospheric ventilation is probably a crucial developmental feature. Palmén (1956) has previously speculated that small tropospheric vertical wind shear is a necessary requirement for storm eye formation. Ramage (1959) has also hypothesized small tropospheric vertical wind shear to be one of the five necessary initial conditions for disturbance intensification.

Fig. 36 portrays the areas on the poleward side of doldrum Eq. T. where the vertical wind shear between 200 mb and 850 mb is ± 10 knots

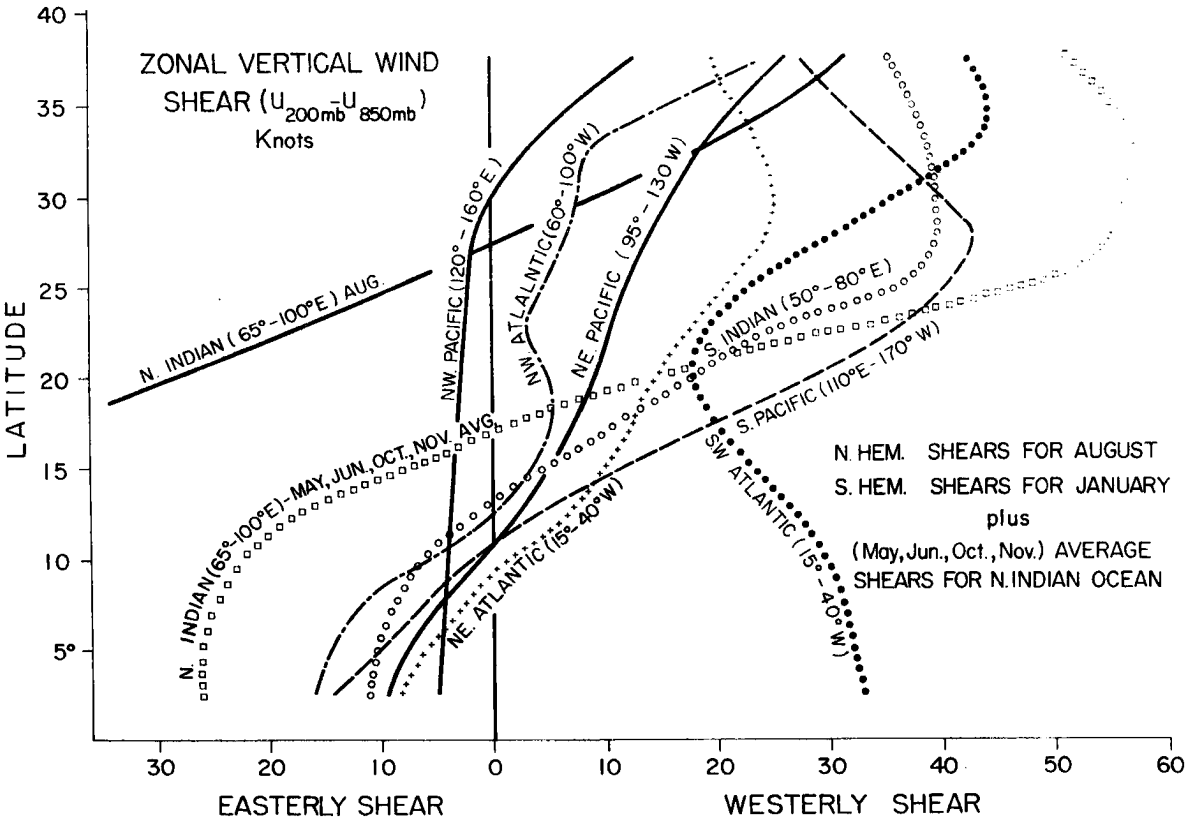

Fig. 34. Latitude distribution of the zonal vertical wind shear between 200 mb and 850 mb in the various development regions and for the SW Atlantic Ocean. Values have been taken off for the warmest summer month plus an average for spring and autumn in the North Indian Ocean.

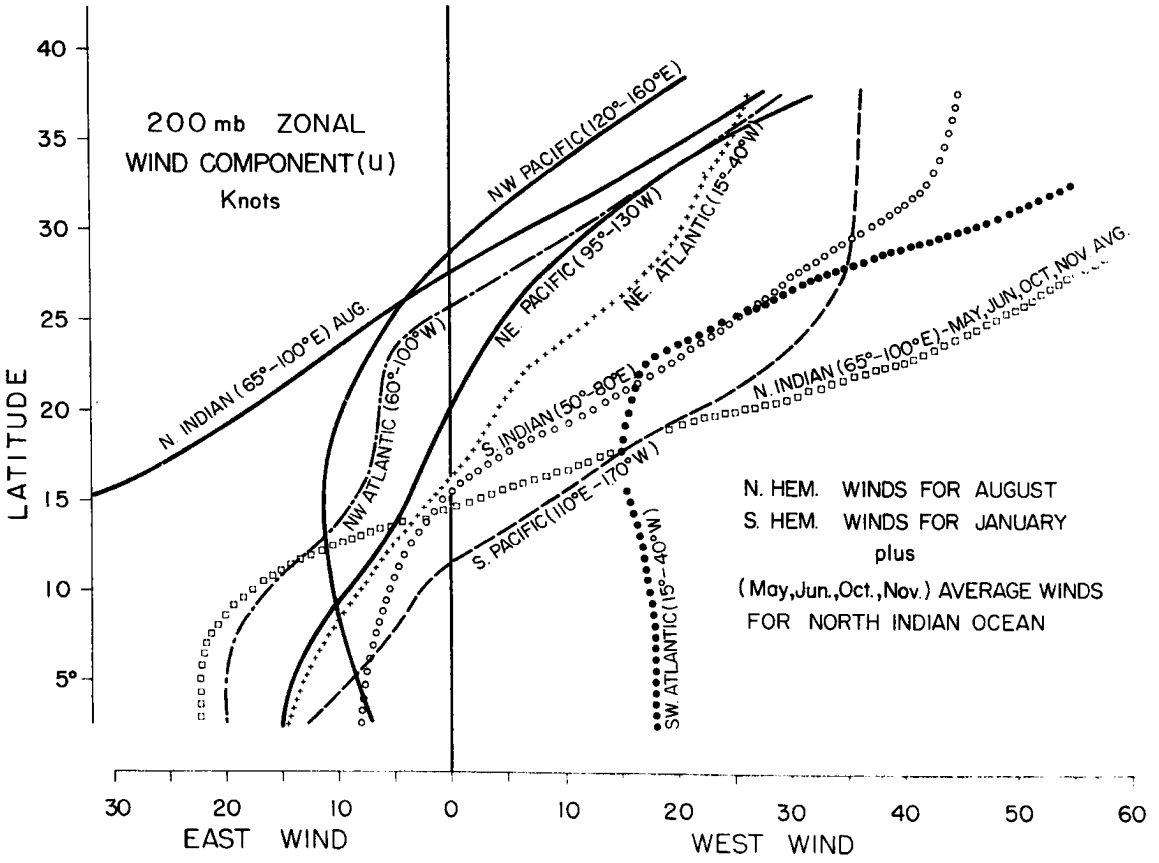

Fig. 35. Latitude distribution of the mean zonal wind at 200 mb in the various development regions during the warmest summer month.

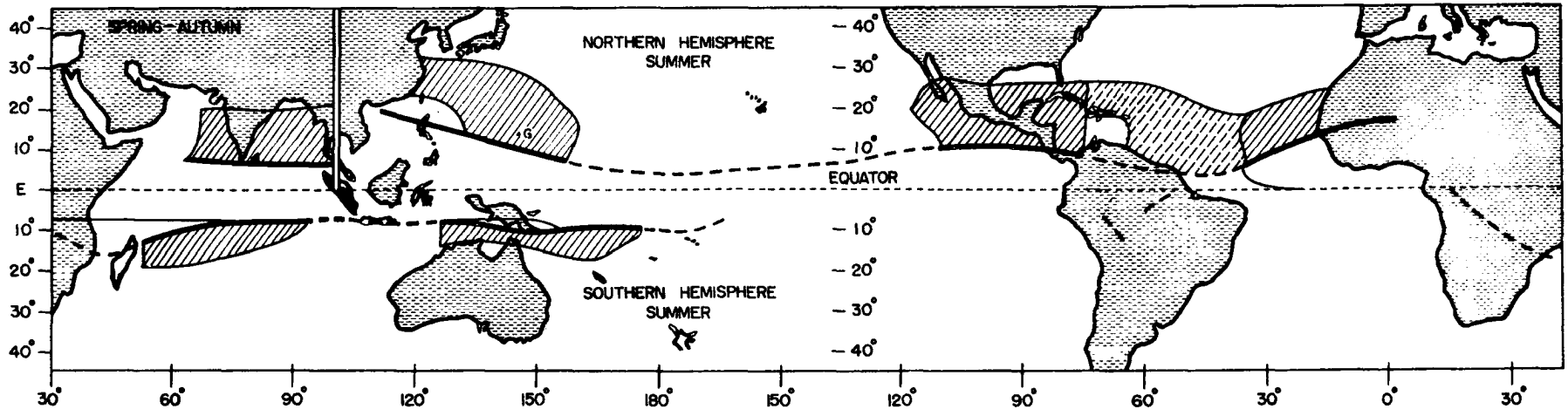

Fig. 36. Solid hashed lines portray the areas on the poleward side of doldrum Equatorial Troughs during August for the Northern Hemisphere and January for the Southern Hemisphere where the vertical wind shear between 200 mb and 850 mb is ± 10 knots or less. Note that the solid shaded areas agree well with the areas of tropical storm development except for the North Atlantic where development can occur in the region of the dashed lines.

or less. Note that the solid shaded areas agree well with the areas of tropical storm development except for the North Atlantic.

Variability from Climatology. The high variability of tropical storms by month and by season is believed to be related to the monthly and seasonal variability of the above-mentioned circulation features from their climatological values. Individual seasonal and monthly environmental features often deviate significantly from climatology. In the three years of 1914, 1925, and 1930 there was a total of but 5 detected tropical storms and hurricanes in the NW Atlantic; while in the three years of 1933, 1949, and 1950 no less than 57 tropical storms were observed. These and other storm frequency variations are believed to be related to monthly and seasonal circulation variations from climatology.

To what extent is the above climatological information representative of individual cases of disturbance and storm development? The next part of this paper discusses the restricted statistics of the individual development cases.

3. STATISTICS OF INDIVIDUAL STORM DEVELOPMENT

In order to determine whether or not individual storm conditions are similar to climatological conditions, a large sample of individual storm data was gathered in the three areas of most densely available upper wind information: (a) NW Pacific; (b) North Indian Ocean; and (c) West Indies. Wind information was gathered and composited in a cylindrical network relative to the center of tropical disturbances that later developed into tropical storms. Sixteen equal azimuthal box-shaped areas 4° latitude wide at three separate radial distances from the center of disturbance are treated. Data from tropical disturbances with sustained wind speeds of 30 knots or less which later developed into tropical storms are presented in the following data sample. In order to increase the data sample, the centers of disturbances first detected with a maximum sustained wind of 20 to 30 knots were moved backward 24 hours or 36 hours in time at the trade-wind velocity. Additional data was composited with respect to these new position centers. The average treated disturbance had three to five time periods of available data. The data sample includes information from 228 individual disturbances which later became tropical storms. Slightly more than one thousand time periods are represented.

Disturbance Intensification Equatorward of 20° Latitude. Figs. 37 to 40 portray information relative to 110 disturbances in the NW Pacific which later became tropical storms. Fig. 37 is a data composite of the zonal wind at 850 mb relative to the disturbance center. Fig. 38 is the same type of composite for the 200 mb level; Figs. 39 and 40 are similar composites of zonal and meridional vertical wind shear.

Easterly zonal winds exist over the disturbance center at 850 mb. These change to westerly zonal winds approximately 2-3° latitude south of the center. At the 200 mb level, easterly winds are present over the disturbance, changing to westerly winds 6-8° north of the center. Thus, the average disturbance in the NW Pacific which later develops into a tropical storm is embedded in an easterly current which extends through the entire troposphere. Minimum or nearly zero vertical wind shear is present over the disturbance center.

Figs. 41-44 and 45-48 portray identical parameters for 54 disturbances in the North Indian Ocean and 26 disturbances in the West Indies region whose centers were located south of 20°N. Nearly identical mean wind conditions exist in these latter disturbances as in the cases of the NW Pacific. Data is also being evaluated on wind conditions surrounding tropical disturbances which later became

tropical storms in the South Pacific. Preliminary results show that the environmental flow features of disturbances in this region are similar to the flow features of the above regions.

Composites of the information of the 190 disturbance cases in the three development regions of the Northern Hemisphere equatorward of 20° are given in Figs. 49-52. The change from easterly shear with height to westerly shear with height while moving poleward across the disturbance center is clearly shown. Fig. 53 is a composite for the three areas of the magnitude of the vector of vertical shear relative to the disturbance center. Small or near zero vertical shear is observed directly over and to the WNW and east of the disturbance center.

Although the above wind composites are an average of a large number of storms, they are representative of individual cases. The average absolute deviation of the zonal and meridional wind at 850 mb from the three region mean was 9 and 6 knots respectively. The average absolute deviation of the zonal and meridional wind at 200 mb was 12 and 11 knots; and 16 and 12 knots were the average absolute deviation of the zonal and meridional vertical wind shears. These deviations are considerably less than the average parameter differences from north to south across the cylindrical grid.

It is therefore concluded that for tropical disturbances that develop into storms equatorward of 20° latitude, there is very small or negligible vertical tropospheric shear. The initiation and intensification of these disturbances within the deep tropics is viewed as primarily a product of the General Circulation flow characteristics. Disturbances develop on the equatorward side of the trade winds at low levels but within a deep easterly current at upper levels. The superposition of the upper-level easterlies over the equatorward fringe of the trades is evident from both the climatological and individual storm cases. Over 87% of the global tropical disturbances begin their initial intensification within these environmental wind conditions. Broad-scale baroclinic processes have no importance for this typical type of disturbance intensification. Fig. 54 is a graph of the initial characteristic zonal wind distribution with height to the north, to the south, and within these intensifying disturbances which later become tropical storms. This is an idealized picture of what the previous observations show.

Disturbance Intensification Poleward of 20° Latitude. For the tropical disturbances which intensify at latitudes poleward of 20°

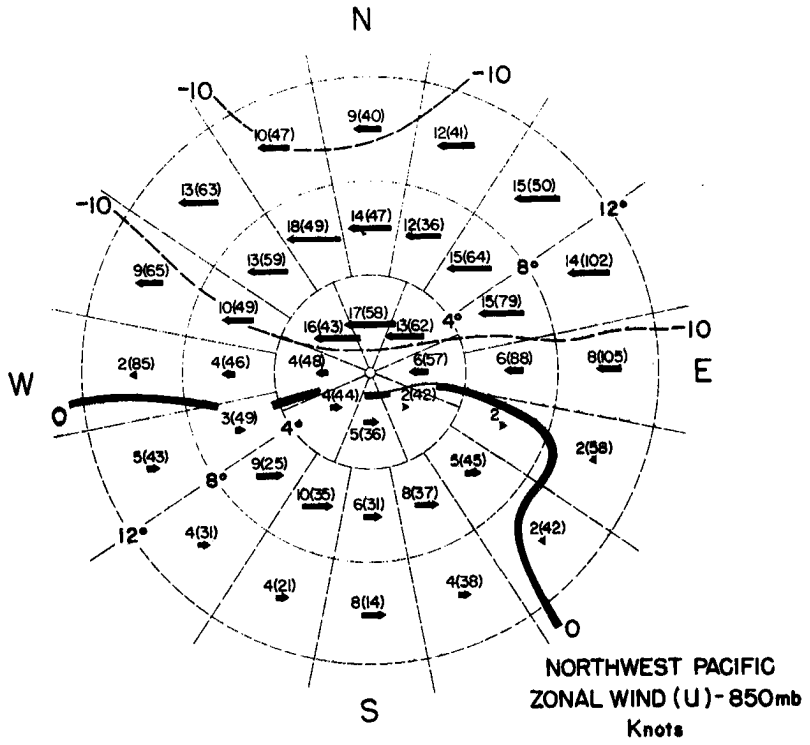

Fig. 37. Composite of average rawin information in each area relative to the center of 110 tropical disturbances which later developed into tropical storms. Length of arrows proportional to wind speed in knots (at left). Values in parentheses are number of wind reports in each area average. Distance from the center is given by the lightly dashed circular lines at 4° latitude increments.

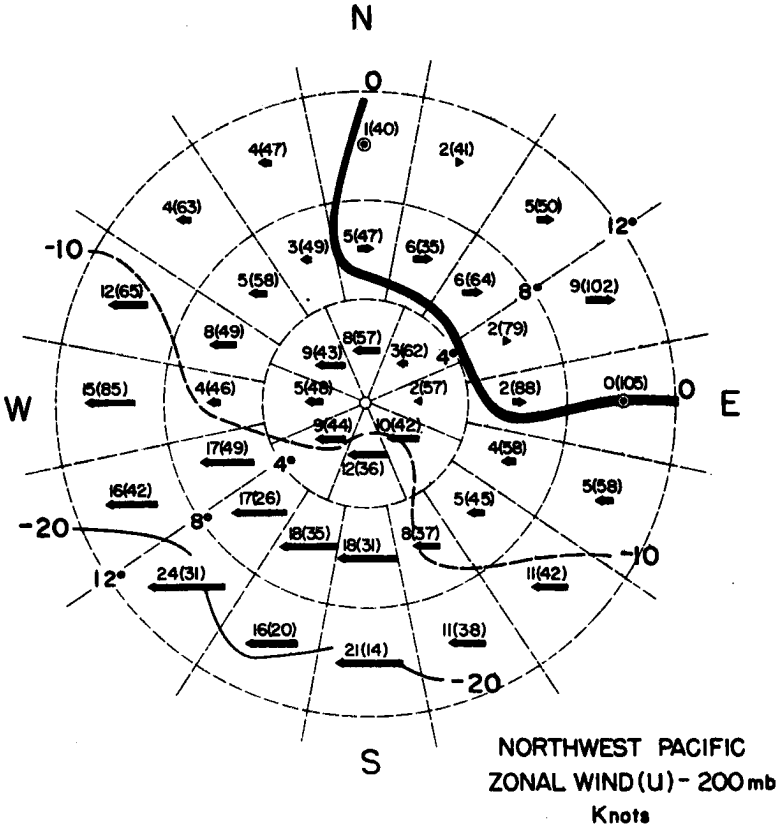

Fig. 38. Composite of average rawin information in each area relative to the center of 110 tropical disturbances which later developed into tropical storms. Length of arrows proportional to wind speed in knots (at left). Values in parentheses are number of wind reports in each area average. Distance from the center is given by the lightly dashed circular lines at 4° latitude increments.

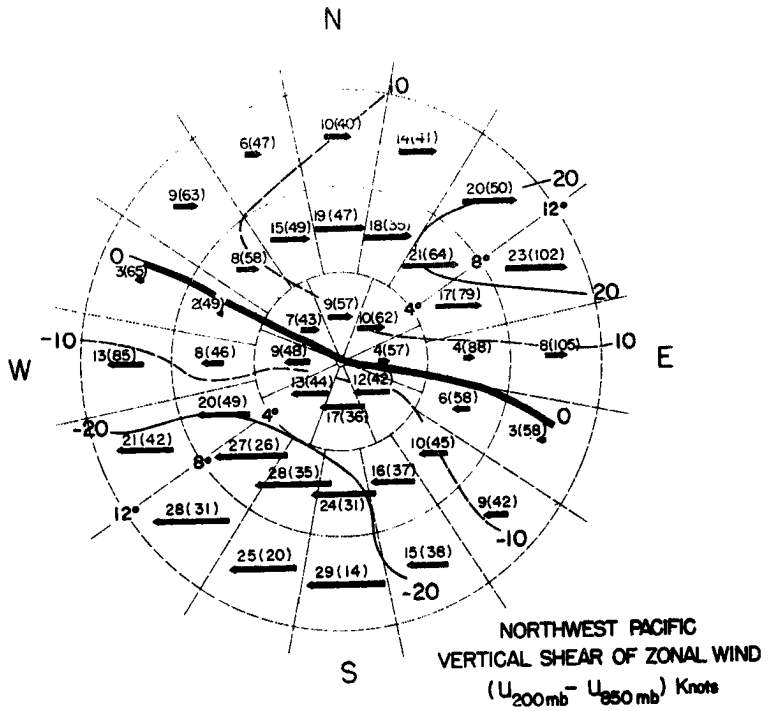

Fig. 39. Composite of average rawin information in each area relative to the center of 110 tropical disturbances which later developed into tropical storms. Length of arrows proportional to wind shear in knots (at left). Values in parentheses are number of wind reports in each area average. Distance from the center is given by the lightly dashed circular lines at 4° latitude increments.

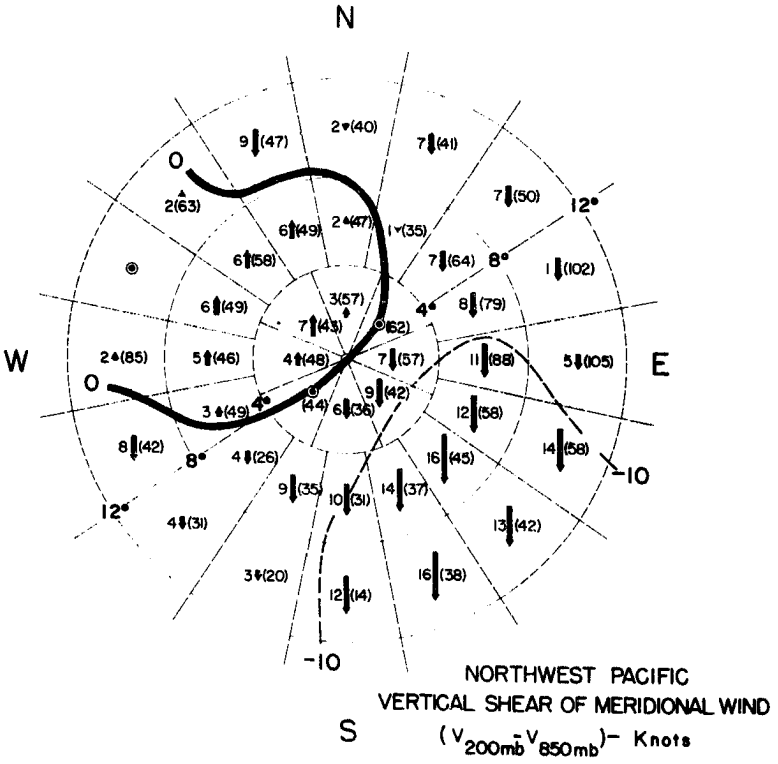

Fig. 40. Composite of average rawin information in each area relative to the center of 110 tropical disturbances which later developed into tropical storms. Length of arrows proportional to wind shear in knots (at left). Values in parentheses are number of wind reports in each area average. Distance from the center is given by the lightly dashed circular lines at 4° latitude increments.

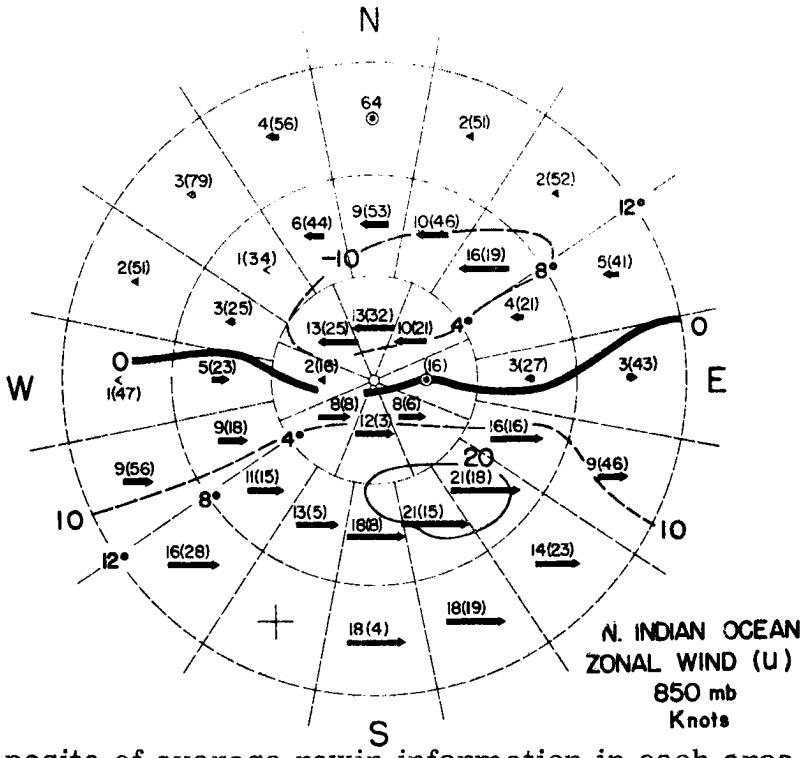

Fig. 41. Composite of average rawin information in each area relative to the center of 54 tropical disturbances which later developed into tropical storms. Length of arrows proportional to wind speed in knots (at left). Values in parentheses are number of wind reports in each area average. Distance from the center is given by the lightly dashed circular lines at 4° latitude increments.

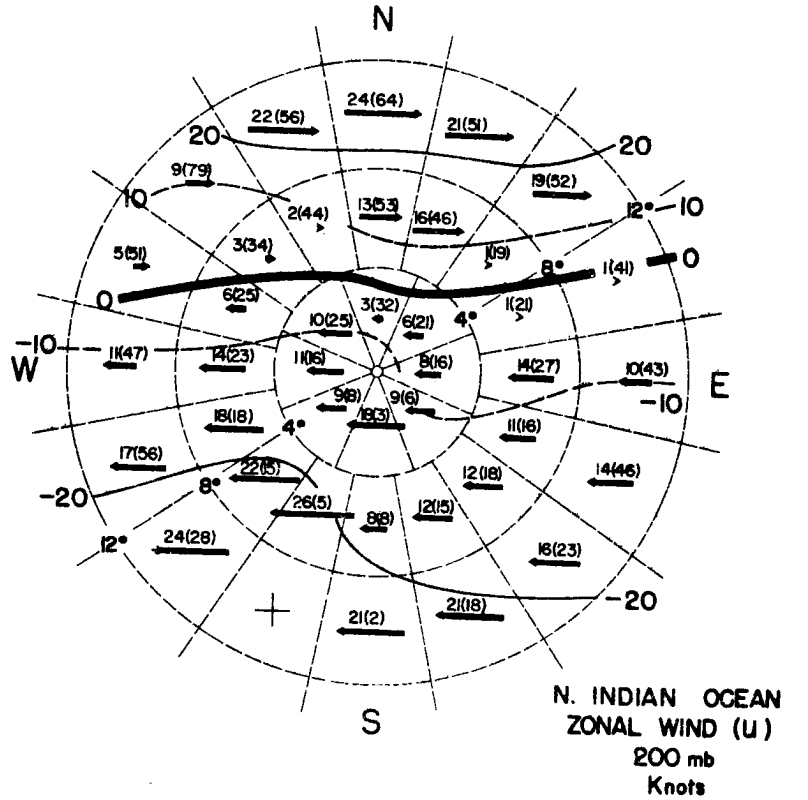

Fig. 42. Composite of average rawin information in each area relative to the center of 54 tropical disturbances which later developed into tropical storms. Length of arrows proportional to wind speed in knots (at left). Values in parentheses are number of wind reports in each area average. Distance from the center is given by the lightly dashed circular lines at 4° latitude increments.

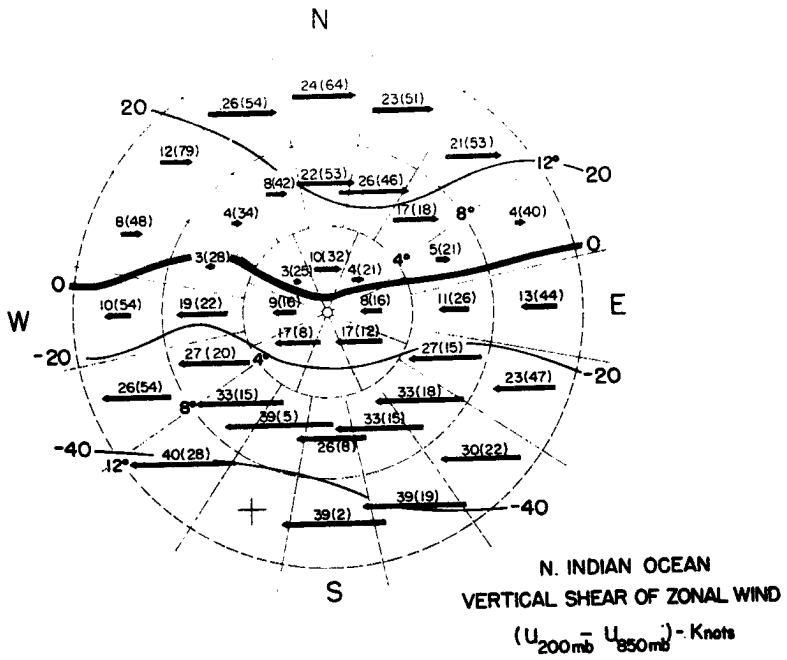

Fig. 43. Composite of average rawin information in each area relative to the center of 54 tropical disturbances which later developed into tropical storms. Length of arrows proportional to wind shear in knots (at left). Values in parentheses are number of wind reports in each area average. Distance from the center is given by the lightly dashed circular lines at 4° latitude increments.

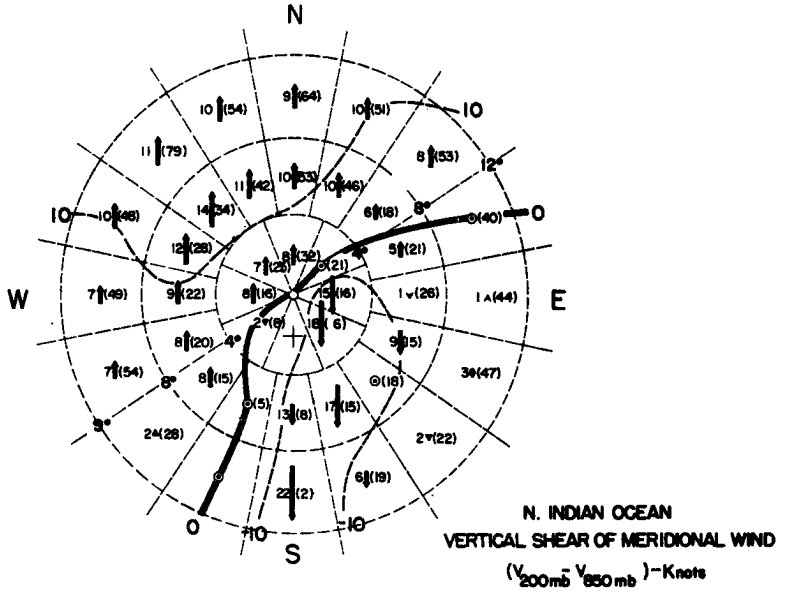

Fig. 44. Composite of average rawin information in each area relative to the center of 54 tropical disturbances which later developed into tropical storms. Length of arrows proportional to wind shear in knots (at left). Values in parentheses are number of wind reports in each area average. Distance from the center is given by the lightly dashed circular lines at 4° latitude increments.

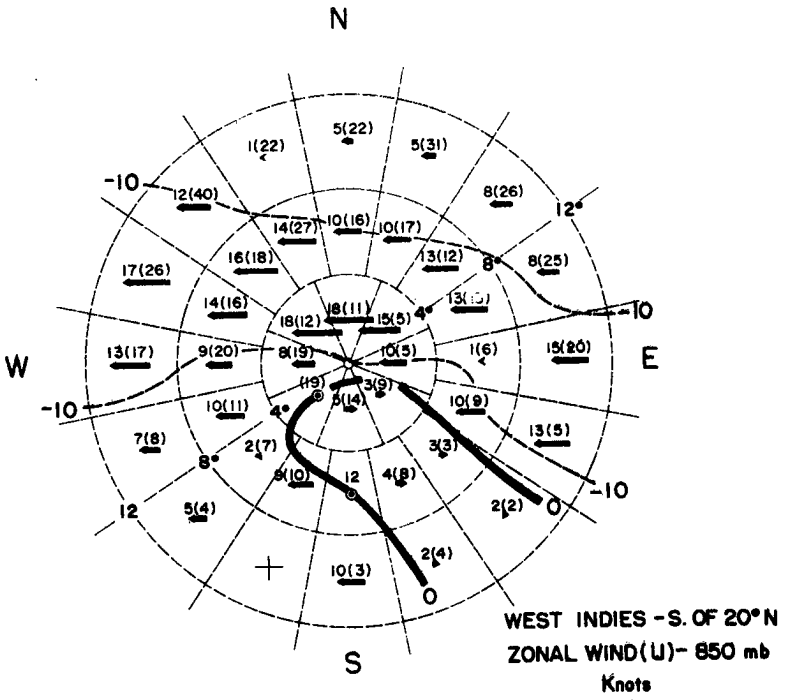

Fig. 45. Composite of average rawin information in each area relative to the center of 26 tropical disturbances which later developed into tropical storms. Length of arrows proportional to wind speed in knots (at left). Values in parentheses are number of wind reports in each area average. Distance from the center is given by the lightly dashed circular lines at 4° latitude increments.

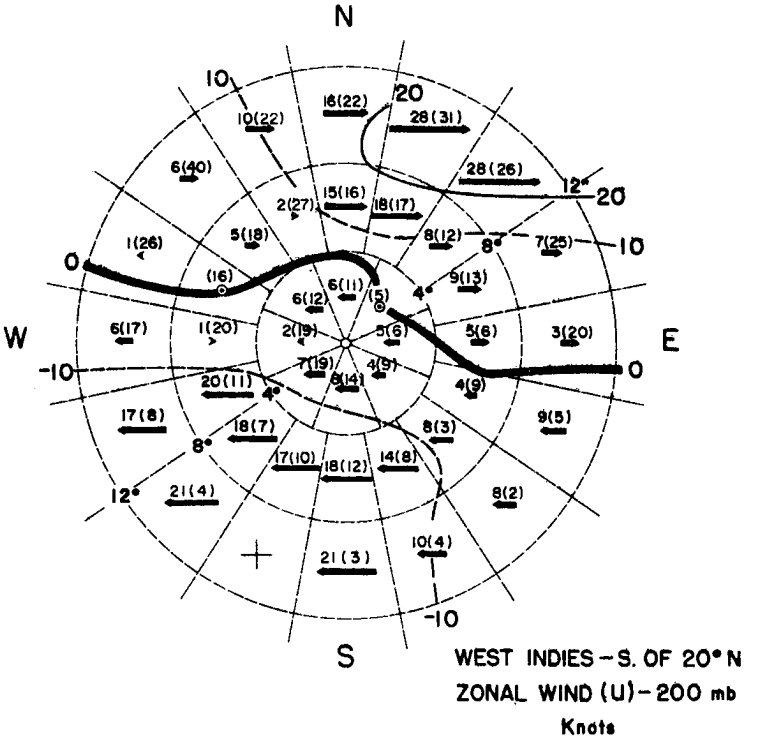

Fig. 46. Composite of average rawin information in each area relative to the center of 26 tropical disturbances which later developed into tropical storms. Length of arrows proportional to wind speed in knots (at left). Values in parentheses are number of wind reports in each area average. Distance from the center is given by the lightly dashed circular lines at 4° latitude increments.

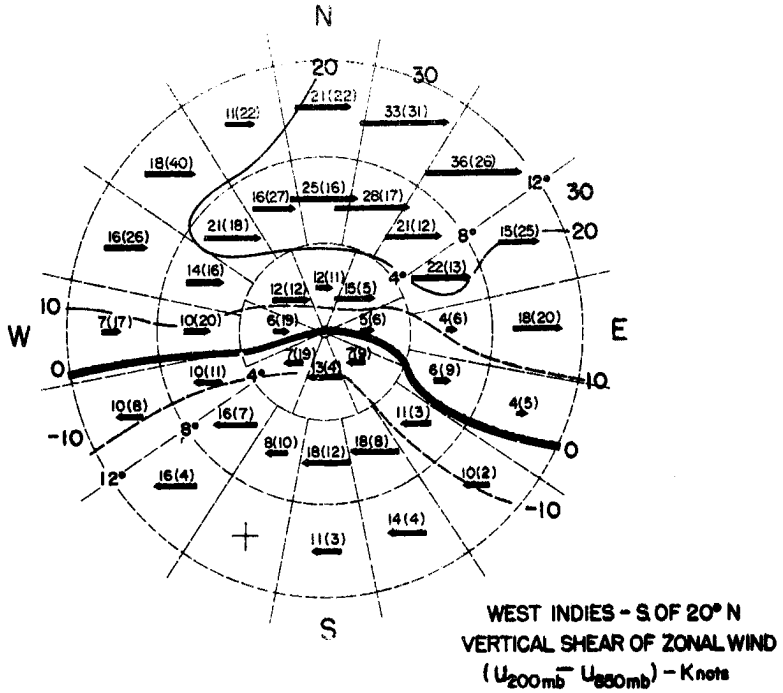

Fig. 47. Composite of average rawin information in each area relative to the center of 26 tropical disturbances which later developed into tropical storms. Length of arrows proportional to wind shear in knots (at left). Values in parentheses are number of wind reports in each area average. Distance from the center is given by the lightly dashed circular lines at 4° latitude increments.

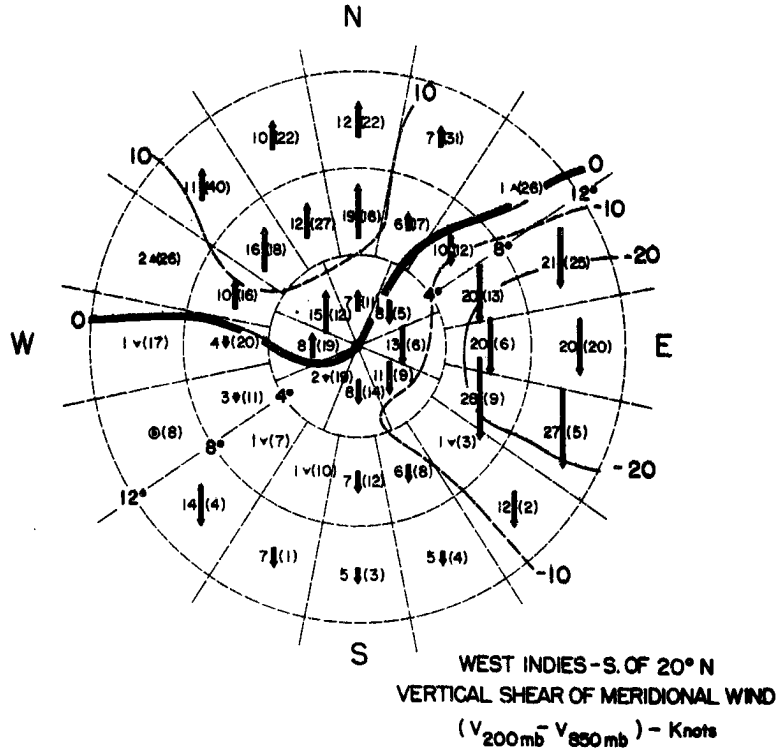

Fig. 48. Composite of average rawin information in each area relative to the center of 26 tropical disturbances which later developed into tropical storms. Length of arrows proportional to wind shear in knots (at left). Values in parentheses are number of wind reports in each area average. Distance from the center is given by the lightly dashed circular lines at 4° latitude increments.

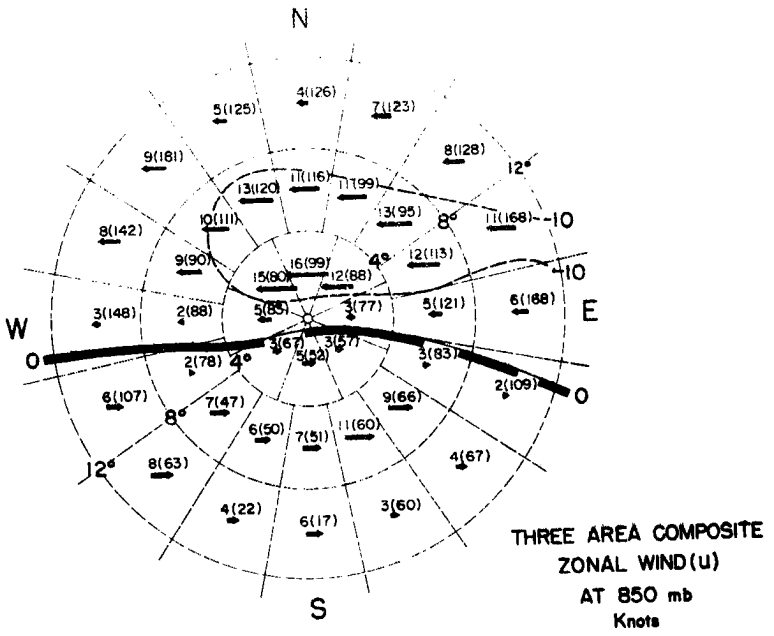

Fig. 49. Composite of average rawin information in each area relative to the center of 190 tropical disturbances which later developed into tropical storms in the three development regions of the Northern Hemisphere where data was available. Length of arrows proportional to wind speed in knots (at left). Values in parentheses are number of wind reports in each area average. Distance from the center is given by the lightly dashed circular lines at 4° latitude increments.

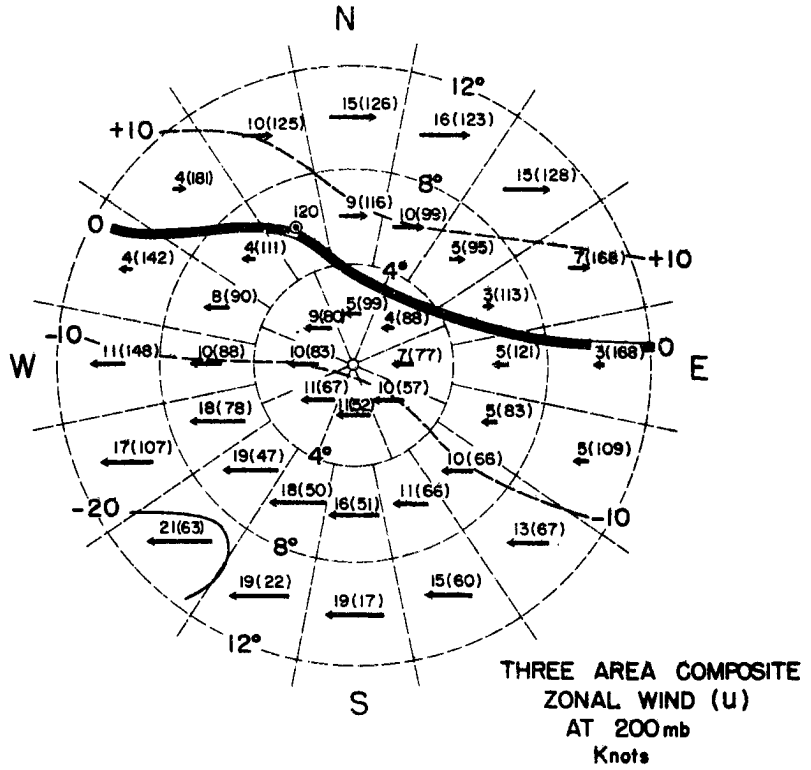

Fig. 50. Composite of average rawin information in each area relative to the center of 190 tropical disturbances which later developed into tropical storms in the three developmental regions of the Northern Hemisphere where data was available. Length of arrows proportional to wind speed in knots (at left). Values in parentheses are number of wind reports in each area average. Distance from the center is given by the lightly dashed circular lines at 4° latitude increments.

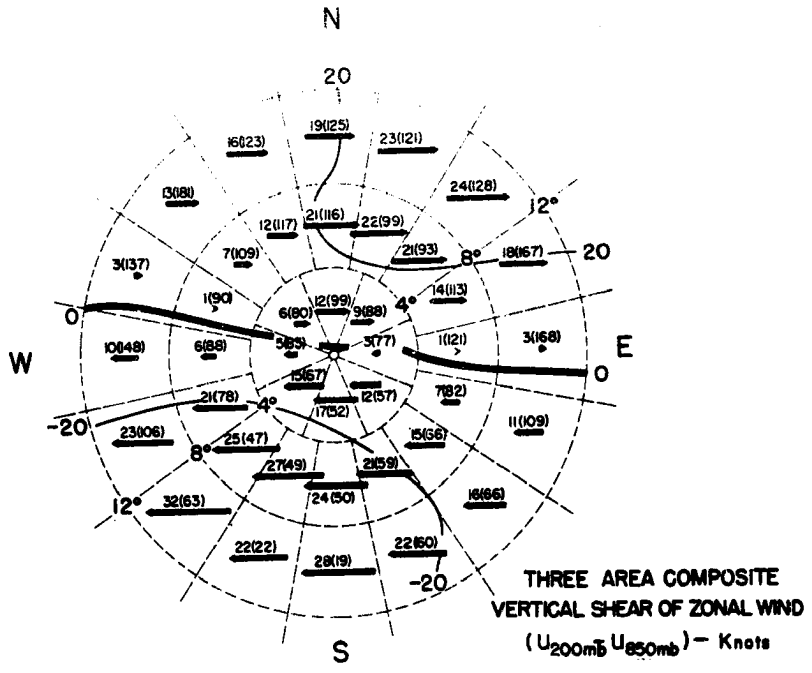

Fig. 51. Composite of average rawin information in each area relative to the center of 190 tropical disturbances which later developed into tropical storms in the three developmental regions of the Northern Hemisphere where data was available. Length of arrows proportional to wind shear in knots (at left). Values in parentheses are number of wind reports in each area average. Distance from the center is given by the lightly dashed circular lines at 4° latitude increments.

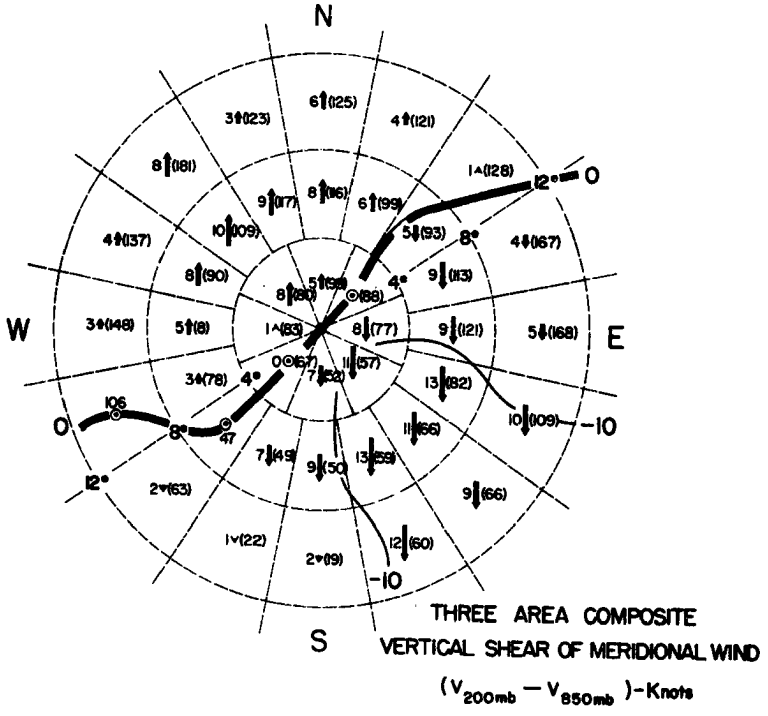

Fig. 52. Composite of average rawin information in each area relative to the center of 190 tropical disturbances which later developed into tropical storms in the three developmental regions of the Northern Hemisphere where data was available. Length of arrows proportional to wind shear in knots (at left). Values in parentheses are number of wind reports in each area average. Distance from the center is given by the lightly dashed circular lines at 4° latitude increments.

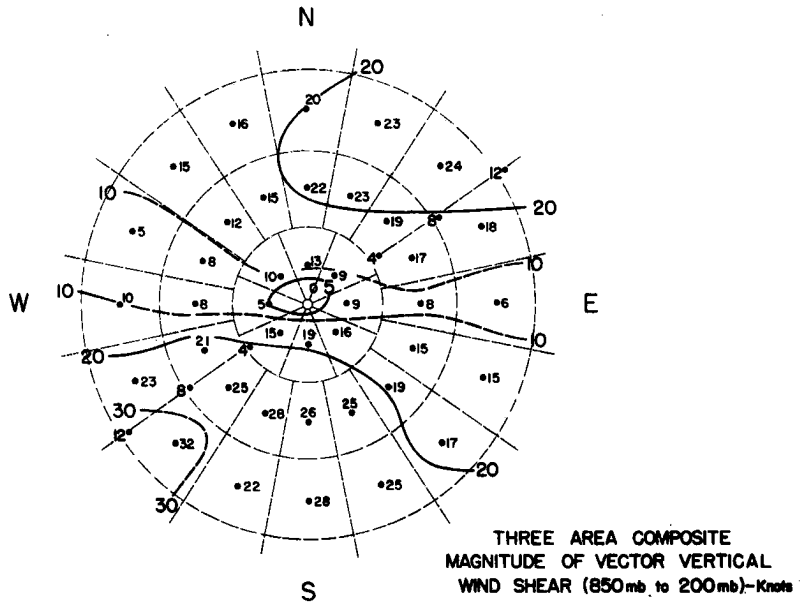

Fig. 53. Composite of average rawin information in each area relative to the center of 190 tropical disturbances which later developed into tropical storms in the three development regions of the Northern Hemisphere where data was available. Wind speeds are portrayed in knots. Distance from the center is given by the lightly dashed circular lines at 4° latitude increments.

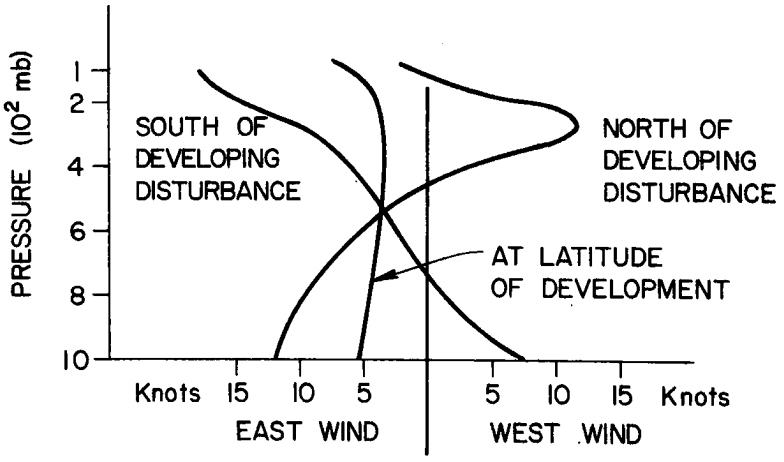

Fig. 54. Schematic vertical distribution of the zonal wind to the north, to the south, and at the center of the typical tropical disturbance which intensifies into a tropical storm equatorward of 20° latitude.

(~15% of global total) in the NW Atlantic and NW Pacific, significantly different broad-scale environmental flow conditions are observed. The Eq. T. does not usually extend poleward of 20°. Intensification in these higher latitudes occurs from disturbances which are deeply embedded in the trade flow with no broad-scale surface westerly winds on their southern fringes. These latter storms result from disturbances which break away from their initial doldrum Eq. T. formation environment and travel in the trade flow to higher latitude locations where environmental conditions are significantly different. These cases should be treated separately. Figs. 55-58 are similar composites of the parameters shown in the previous figures for 38 cases of incipient disturbance intensification in the West Indies - Bahamas - Gulf of Mexico region poleward of 20° latitude.

It is seen that, unlike the cases equatorward of 20°, upper-level westerlies surround the intensifying disturbance. Like the cases equatorward of 20°, however, small or zero tropospheric shear is also observed over a restricted area near the center. The 850 mb westerly winds are not present in a broad area to the south of these developing disturbances. These intensifications result not as a consequence of the much larger-scale General Circulation or climatological features as occurs with the usual type of development in lower latitudes, but occur from a favorable deviation from the local climatological flow. Due to larger tropospheric wind shear, the climatology by itself is slightly unfavorable for intensification. Upper flow is less steady at these higher latitudes and frequency of favorable deviation from the climatology is larger than at lower latitudes. Westerly wind belt influences can penetrate into these sub-tropical latitudes and temporarily establish environmental flow conditions conducive to disturbance intensification. Riehl[1] has often remarked on the probable importance of changes in the westerly wind pattern in association with intensification of tropical disturbances at these higher latitudes. The sequence of flow patterns at lower and upper tropospheric levels associated with a middle-latitude upper trough passing just to the north of an incipient disturbance in the Gulf of Mexico in Figs. 59 and 60 illustrates how the tropospheric vertical wind shear (i.e., ventilation effect) could be greatly reduced over a disturbance as a result of mid-latitude influences. Other things being equal, this decrease in ventilation could lead to intensification. Fig. 61 illustrates the usual upper and lower tropospheric flow patterns associated with the typical dis-

---

[1] Personal communication.

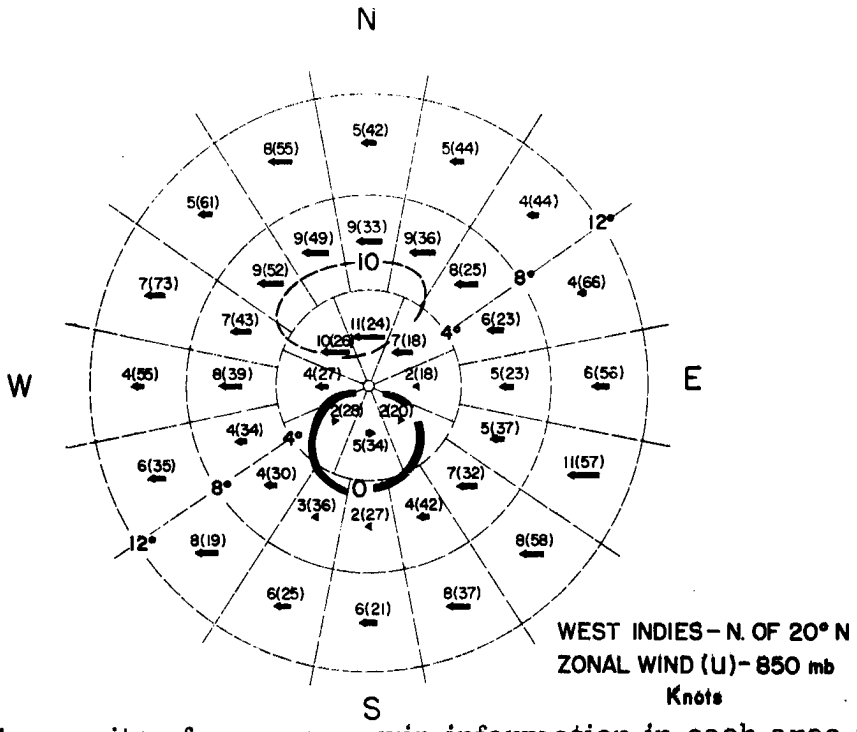

Fig. 55. Composite of average rawin information in each area relative to the center of 38 tropical disturbances which later developed into tropical storms north of 20°. Length of arrows proportional to wind speed in knots (at left). Values in parentheses are number of wind reports in each area average. Distance is given by the lightly dashed circles at 4° latitude increments. Note the difference of environmental flow conditions from those of the typical development equatorward of 20°.

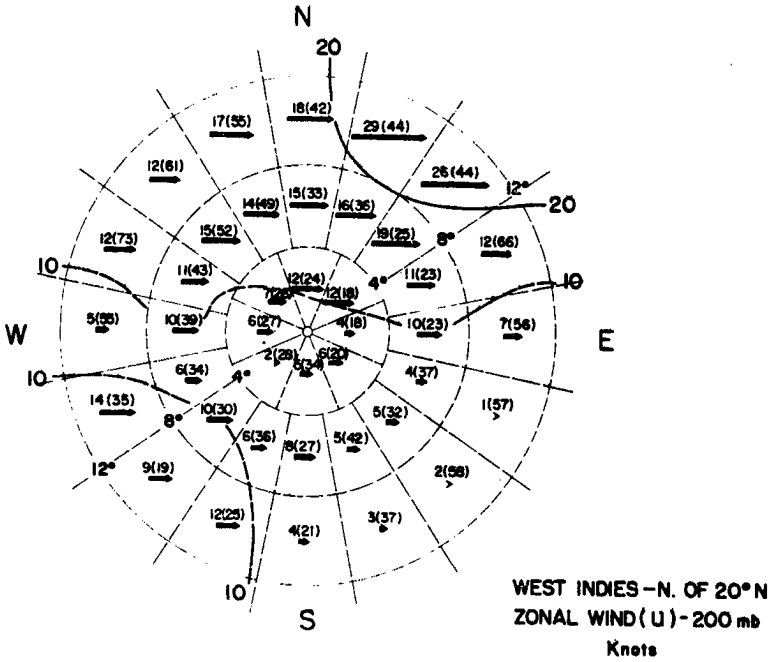

Fig. 56. Composite of average rawin information in each area relative to the center of 38 tropical disturbances which later developed into tropical storms north of 20°. Length of arrows proportional to wind speed in knots (at left). Values in parentheses are number of wind reports in each area average. Distance is given by the lightly dashed circles at 4° latitude increments. Note the difference of environmental flow conditions from those of the typical development equatorward of 20°.

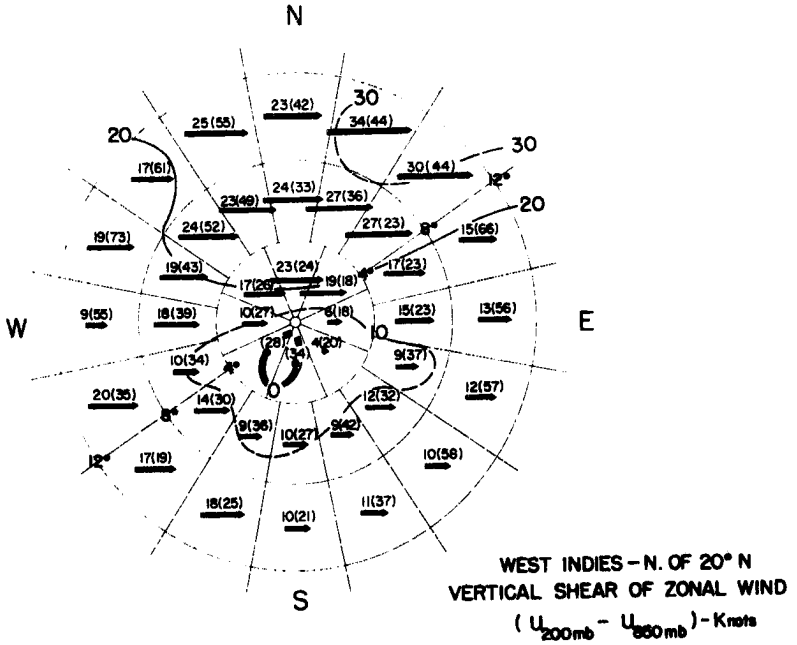

Fig. 57. Composite of average rawin information in each area relative to the center of 38 tropical disturbances which later developed into tropical storms north of 20°. Length of arrows proportional to wind shear in knots (at left). Values in parentheses are number of wind reports in each area average. Distance is given by the lightly dashed circles at 4° latitude increments.

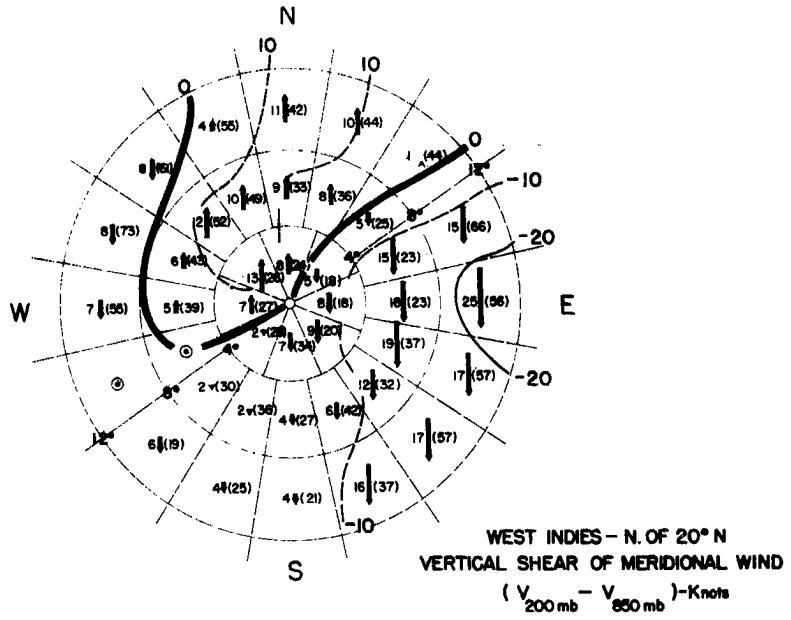

Fig. 58. Composite of average rawin information in each area relative to the center of 38 tropical disturbances which later developed into tropical storms north of 20°. Length of arrows proportional to wind shear in knots (at left). Values in parentheses are number of wind reports in each area average. Distance is given by the lightly dashed circles at 4° latitude increments.

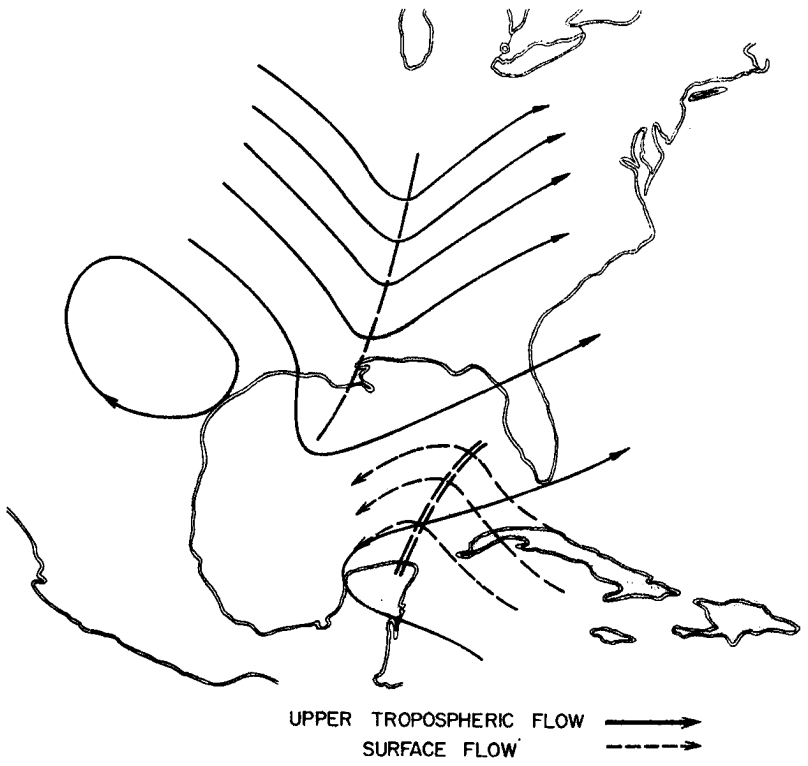

Fig. 59. Portrayal of lower and upper tropospheric flow surrounding a tropical disturbance where the vertical shear above and to the north of the disturbance is large.

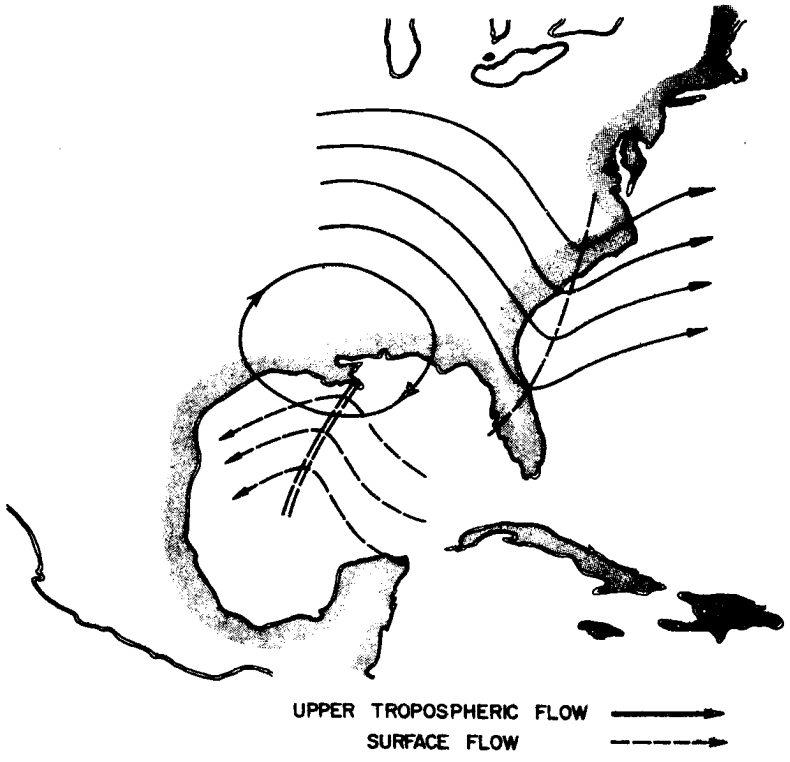

Fig. 60. Portrayal of lower and upper tropospheric flow surrounding a tropical disturbance where the vertical wind shear above the disturbance would be small due to the passage of a westerly wind trough to the north.

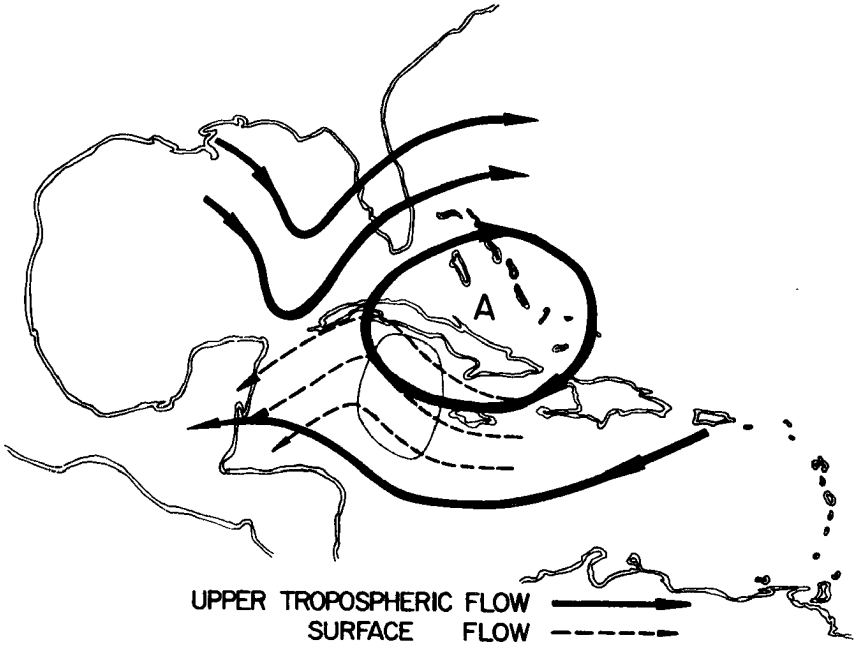

Fig. 61. The usual upper and lower tropospheric flow patterns associated with the typical disturbance intensification in the West Indies. Shaded portion of the drawing portrays the place where cumulus convection is most intense and where the tropospheric vertical wind shear is smallest.

turbance intensification in the Gulf of Mexico and West Indies. Colón and Nightingale (1963) have discussed these characteristic flow patterns. Minimum tropospheric vertical shear results from this superposition of lower and upper tropospheric flow features.

Hybrid Type of Storm. There is another class of hybrid (or cross-breed) type of storm development which occurs in the latitudes between 25° and 35° in the NW Atlantic and occasionally in the NW Pacific, which has intensification characteristics similar to both middle-latitude baroclinic and tropical non-barotropic types of development. Like the tropical storm the strongest winds are often in the lowest levels. These developments can occur with baroclinic conditions and broad-scale flow features quite different from the usual type of tropical development. Typically, these storms do not have intense cumulus convective cores. Their maximum winds are usually located at large distances from their centers. This latter type of storm development makes up a very small percentage (~ 1-2%) of the global total of warm-core formations. Erickson (1967) has discussed one of these hybrid cases. The author makes no attempt to describe the environmental characteristics connected with this third or anomalous class of warm-core formations. Surely they should not be viewed as typical.

Three Types of Disturbance Intensification. Table 3 lists the above described three types of disturbance development. Type A

TABLE 3

TYPES OF DISTURBANCE INTENSIFICATION

Type	Name	Primary Intensification Areas	Percentage of Global Total
A	Tropical	Equatorward of 20° Latitude[1]	~ 83
B	Sub-Tropical	Poleward of 20° in NW Atlantic and NW Pacific	~ 15
C	Hybrid	Poleward of 25° in NW Atlantic and NW Pacific	~ 1-2

[1] Although 87% of the global total of disturbances which later become tropical storms are initially located equatorward of 20°, approximately 5% of these have the major part of their intensification poleward of 20°.

represents the majority of tropical disturbances (~ 83%) which intensify equatorward of 20° latitude. These disturbances intensify as a result of a pre-existing favorable climatological environment. Type B represents the typical sub-tropical development (~ 15% of the global total) which occurs poleward of 20° and not in direct association with the Eq. T. This class of disturbance intensification results from a favorable deviation from a slightly inhibiting climatological environment. These tropical and sub-tropical developments are distinguished by the different initial environmental flow pattern in which they are embedded. The physical requirements of frictionally forced surface convergence and negligible baroclinicity are, however, applicable to both. The third or hybrid class (~ 1-2% of global total) occurs poleward of 25° only in the NW Atlantic and NW Pacific. Development can occur in a baroclinic environment. No attempt is made to explain this latter type.

4. STATISTICAL CHARACTERISTIC OF EKMAN OR FRICTIONAL VEERING OF WIND OVER THE TROPICAL OCEANS

There are a number of important reasons why consideration should be given to the character of the Ekman or frictional veering of wind with height in the sub-cloud layer over the tropical oceans. First, there is the strong association of tropical disturbance and storm development with synoptic-scale surface relative vorticity as seen in Fig. 14. Charney and Eliassen (1949) have drawn attention to the Ekman or frictional veering of wind in the planetary boundary layer as a producer of surface convergence and vertical motion at the top of the layer. Using Ekman theory and the continuity equation, they obtained an expression for the vertical motion at the top of this layer. Thus

$$w_t = \sqrt{\frac{k}{2f}}\, \zeta_{rg} \sin 2\alpha \qquad (5)$$

where

w_t is the vertical motion at the top of the frictional layer,

k is the kinematic eddy viscosity coefficient,

f is the Coriolis parameter,

ζ_{rg} is the average geostrophic relative vorticity through the layer,

α is the angle between the surface wind and the surface isobars.

In the above equation it has also been assumed that there is no curvature of flow, k is constant throughout the friction layer, and geostrophic flow is present at the top of the layer. Secondly, it is observed that over the tropical oceans most cumulus clouds have bases which extend from heights of approximately 600 m ($\sim$950 mb) above the ocean surface. Convergence in the lowest 500-600 m is required for cumulus development. Given the mean summertime vertical distribution of temperature and moisture in the development regions, only vertical motion established by convergence below 900 mb can produce tropospheric warming. Fig. 62 shows that vertical motion to the 200 mb level which is established from convergence above 900 mb produces a net cooling by virtue of the vertical distance the air parcel must travel and cool at the dry adiabatic rate before the condensation level is reached. Moist ascent from the condensation level keeps the par-

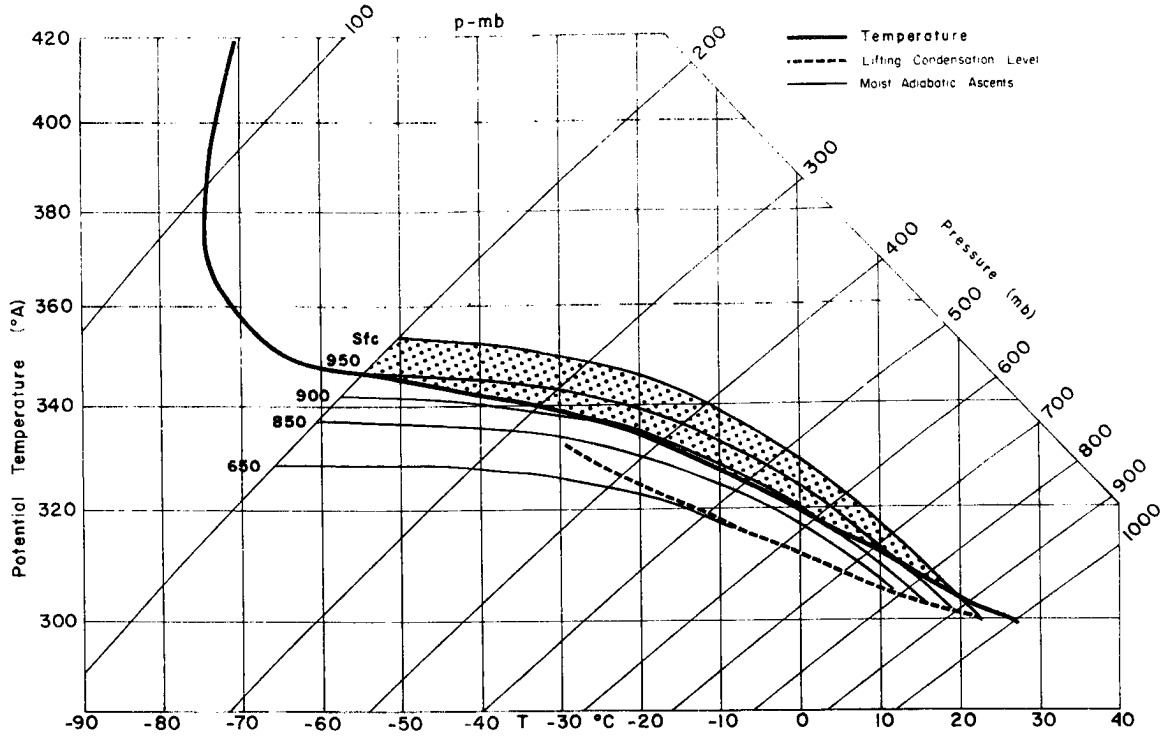

Fig. 62. Tephigram portrayal of the mean summertime tropical radiosonde in regions where tropical storms develop. Numbers in the left center portion of figure represent parcel ascent beginning at the pressure levels indicated. Note that for parcel ascent from levels higher than 900 mb the air parcel remains cooler than its environment.

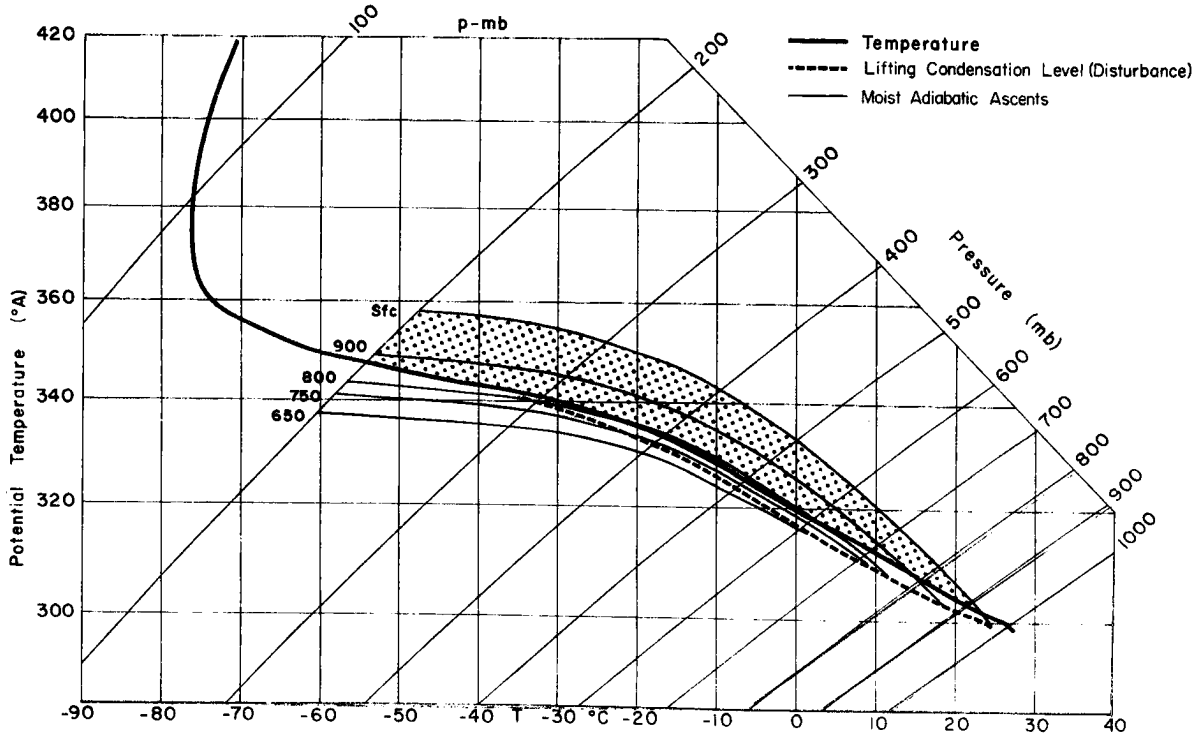

Fig. 63. Same as for Fig. 62 but for average conditions within the rain area of the typical tropical disturbance which later becomes a tropical storm. Only parcel ascent from levels below 850 mb will produce warming.

cel at a temperature cooler than its environment. Fig. 63 portrays similar conditions as in Fig. 62 for the disturbance cases in which tropospheric warming can occur from vertical motion induced by convergence before 850 mb.

For surface pressure in a disturbance to remain lower than the surroundings, the mean tropospheric virtual temperature over the disturbance must remain higher than the surroundings. For a disturbance to maintain its identity or intensify, this higher mean tropospheric temperature must be maintained or increased. Condensation heating to produce this required net tropospheric warming can only be accomplished by vertical motion originating from levels below 900 mb. Because of the importance of cumulus convection in the intensifying disturbance, it is thus of crucial importance to examine the convergence pattern in the lowest 100 mb layer.

Charney and Eliassen (1964a, 1964b) have hypothesized that frictionally forced low-level convergence is an important mechanism for establishment and enhancement of low-level water vapor convergence. Is there, in fact, sufficient frictionally induced veering in the subcloud layers over the tropical oceans (where f is small) to explain initial tropical disturbance generation from this point of view?

In order to explore this question a statistical investigation of the Ekman or frictional wind veering over the tropical oceans was undertaken. This has been made possible by the collection (in the last 8-10 years) of new electronic upper wind measurements from surface ships over the tropical oceans and the storage of this information at the National Weather Records Center in Asheville. Over ten thousand rawin reports were obtained from surface vessels over the tropical oceans from 30°N to 30°S latitude. Wind speeds at all levels had to be 3 m/sec or greater to be considered.[1] The majority of the reports were in the Northern Hemisphere at latitudes between 10° and 30°.

Table 4 portrays the measured statistical averages of wind angle veering between the surface and 1 km and 1 to 2 km for areas in the NW Atlantic and NW Pacific where tropical storms occur. Atoll and small island (Swan, Grand Cayman, San Andrews) veering data from these same regions has also been included in a separate average. The data has been divided into latitude ranges of 10-20°N and 20-30°N. The veering information under A is from surface vessels located at least 1° latitude from any land source. The average observed wind

[1] Ship rawin observations are, in general, not reliable for observed balloon elevation angles greater than 60° or less than 15°, corresponding to wind speed less than 3 m/sec or greater than 19 m/sec for balloon rate of rise of 300 m/sec. Winds above 19 m/sec were seldom observed.

TABLE 4

AVERAGE ANGLE VEERING WITH HEIGHT

Area Location	Surface-1000 m				1000-2000 m			
	No. of Cases (A for Open Sea) (B within 1° Lat. of Land)		Ave. Veering Degrees		No. of Cases		Ave. Veering Degrees	
	A	B	A	B	A	B	A	B
Octant 0 (W of 50°W, 10-20°N)	205	450	9.5	7.9	160	420	1.2	0.0
Octant 0 (W of 50°W) plus Gulf of Mexico (20-30°N)	768	391	12.4	12.7	729	352	3.8	6.0
Island Stations (summer)		1132		14.8		1132		2.8
TOTALS AND AVERAGE	973	1973	11.8	12.8	889	1904	3.3	2.7
Octant 2 (10-20°N)	1441	85	11.5	14.6	1469	82	3.4	3.4
Octant 2 (20-30°N)	701	125	12.0	6.0	601	111	1.9	12.5
Atoll Stations (summer)		1345		10.0		1345		0.1
TOTALS AND AVERAGE	2142	1555	11.7	10.0	2070	1538	3.0	1.2
GRAND TOTAL AND AVERAGE	3115	3528	11.7	11.6	2959	3442	3.1	2.0

veering between the surface and the 1 km level (from the ships at least 1° latitude from land) was approximately 12°. There was little significant difference in turning between latitude belts of 10-20°N and 20-30°N. For ship vessels within 1° of land and for island stations, the average veering angle in the lowest km was 10-13°. Table 4 also presents data on the average veering of wind in the second kilometer layer. In these higher levels the veering of the wind was 2-3°. If it is assumed that a possible thermal wind turning would be the same for both one-kilometer layers, then an average residual frictional veering of 8-9° is to be expected. Fig. 64 graphically portrays this observed wind veering with height through the lowest two-kilometer layer.

The Ekman or frictional veering does, however, exist only in the statistical average. Individual rawin veerings show large deviations from the average. These large individual deviations of veering are thought to be primarily a result of the gust scale (~100-500 m) turbulent mixing in the boundary layer plus observational errors. A balloon rising through different parts of a mechanically produced gust eddy will display different turning information. These small-scale, unsteady features are large in comparison with the individual frictional veering component. The frictional effect can, however, be isolated in a statistical average if the gust scale deviations and instrumental errors occur at random. There is no reason to think that they are systematic.

Considerable observational statistics on frictional veering of wind in the lowest kilometer have been evaluated by Mendenhall (1967) in an attempt to eliminate these small-scale turbulent effects. After isolating and subtracting the influences on veering due to lapse rate and thermal wind differences, he has obtained satisfactory average veering values which agree to an acceptable tolerance with usual computed surface stress values. A later report will more extensively discuss the observational characteristics of planetary boundary layer frictional veering over the tropical oceans.

It is concluded that a significant Ekman or frictionally induced wind veering does, in fact, exist in the sub-cloud layer over the tropical oceans, and, for the reasons previously mentioned, can play a crucial role in establishing the necessary water vapor convergence which is required for disturbance intensification. Fig. 65 portrays quantitative information on convergence and surface pressure fall which would result from sub-cloud layer frictional veering induced by horizontal shear only.

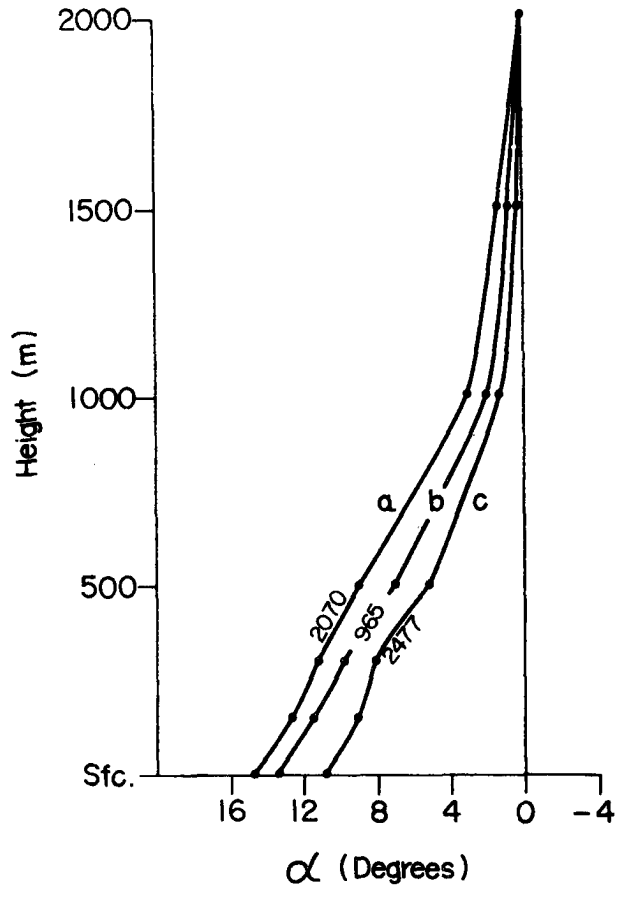

Fig. 64. Graphical portrayal of information of Table 4. Wind angle veering with height in the lowest two km is shown. Wind direction at two km is used as reference. Curve a represents veering of wind with height from surface vessels which were located at least 1° latitude from any land. Curve b represents the frictional veering of wind with height as observed from atoll data in the NW Pacific; curve c as observed from surface vessels located within 1° latitude of land. Note the very small veering of wind with height in the second km layer.

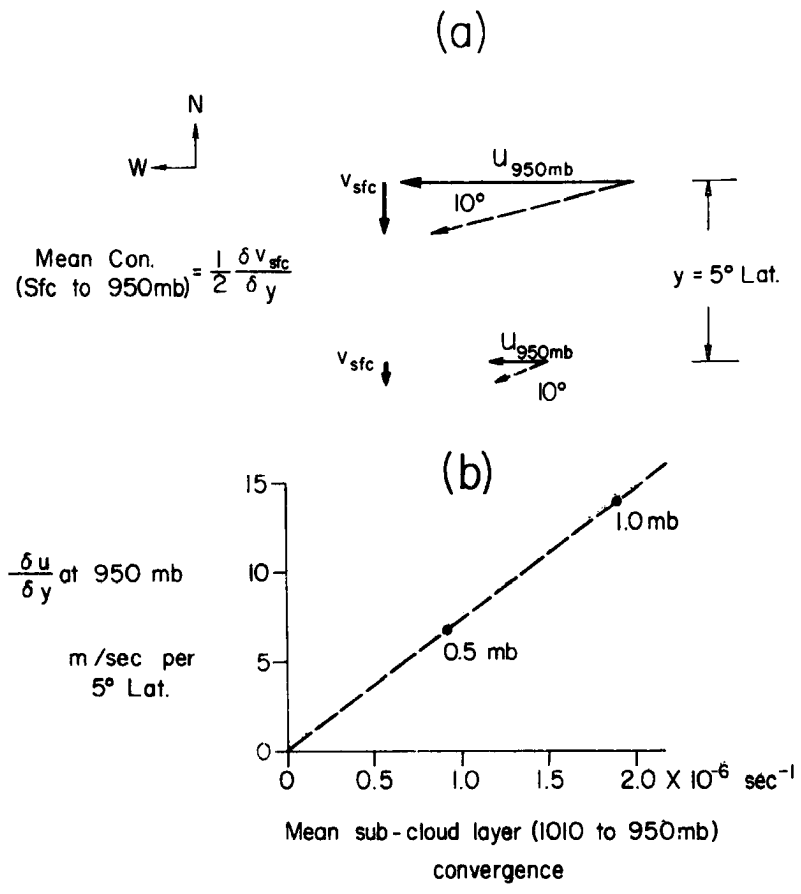

Fig. 65. Diagram (a)--Portrayal of how cyclonic shear in a zonal non-divergent trade-wind current at 950 mb can produce sub-cloud convergence if a frictional veering of 10° were present. v_{sfc} is the meridional surface wind.

Diagram (b)--Magnitude of mean sub-cloud layer convergence vs. strength of cyclonic horizontal wind shear per 5° of latitude for a frictional veering of 10°. Numbers plotted along the sloping curve represent the mean condensation produced surface pressure decrease per 48 hours which would result just from the frictional convergence induced in the sub-cloud layer from the horizontal shearing flow. Mean summertime vertical gradients of θ_e have been assumed. Approximately 1/8 of the released condensation heat in the sub-cloud layer will act directly to increase the mean temperature of the troposphere and lower the surface pressure. The rest of the heat release goes to expansion and warming from the dry-adiabatic lapse rate to environmental conditions.

5. IMPORTANCE OF VERTICAL MOMENTUM TRANSPORT BY THE CUMULUS UP- AND DOWNDRAFTS

In comparison with the middle latitudes, little horizontal temperature gradient is present in the tropical atmosphere. The large temperature gradients observed near the center of tropical storms are produced by concentrated amounts of cumulus condensation even though necessary amounts of sensible and latent heat for cumulus buoyancy are received as a dynamic by-product from the ocean. These strong temperature gradients may exceed wintertime middle-latitude gradients by an order of magnitude.

The enhanced cumulus convection in tropical disturbances acts in two opposing ways. In one sense the condensation heat from the cumulus acts to warm the inner portions of the disturbance and induce vertical shear of the horizontal wind through the thermal wind relationship. In the opposite sense the cumulus act to suppress vertical wind shear by transfer of horizontal momentum within their up- and downdrafts. The operation of this dual or "paradox" role of the cumulus cloud is hypothesized to be of basic importance in the development of the tropical disturbance and in its later intensification.

The previously presented observations show that the tropical disturbance which later develops into a storm starts out with minimum baroclinicity. By the time it has reached tropical storm or hurricane intensity, the weak or zero initial baroclinicity of the lower half of the troposphere has been replaced by baroclinicity of magnitudes exceeding maximum observed middle-latitude values. The vertical wind shear in the lower half of the troposphere of the developing storm has, however, increased by a typical factor of but two to three (Gray, 1967). Fig. 66 portrays the typical tropospheric increase of wind in the inner area of the developing storm and the characteristic associated increase of baroclinicity. $\bar{u}$ is the mean speed of the trade wind or tangential wind of a closed vortex. Note that the vertical wind shear in the lower half of the troposphere increases much less than the baroclinicity. Fig. 67 portrays how cumulonimbus up- and downdrafts acting through a vertical shearing flow can transfer momentum in the vertical and inhibit increase of vertical shear as baroclinicity increases.

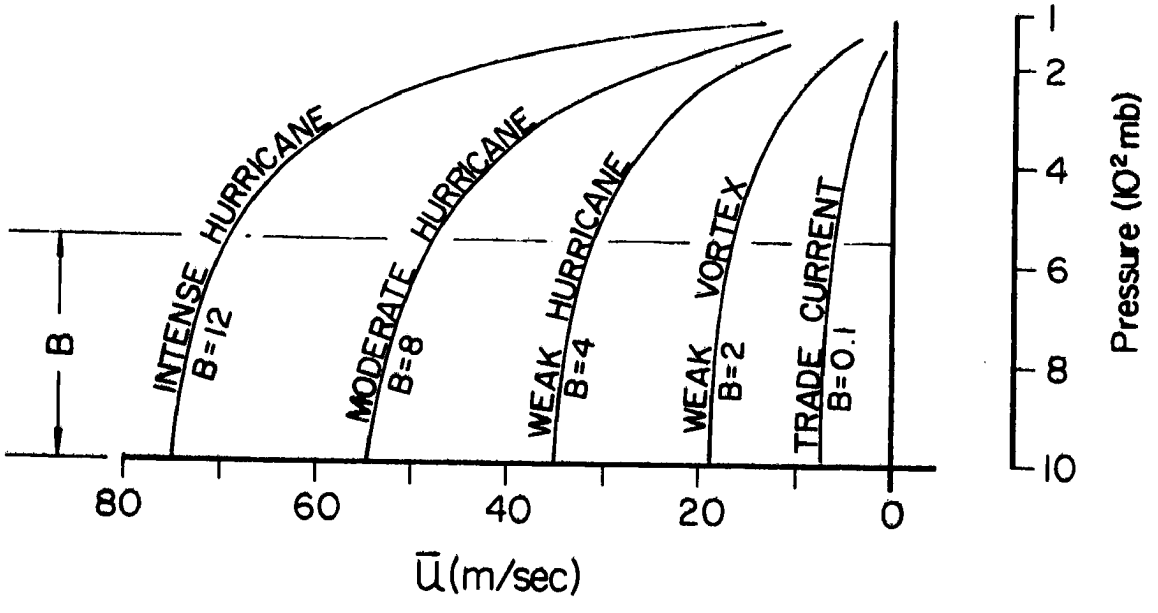

Fig. 66. Typical vertical shear of the horizontal wind existing at 40 km radius in tropical vortices of various intensities and in the usual trade current (radius = ∞) from which storms develop. B is the average magnitude of baroclinicity present (°C/100 km along constant pressure surface)in the lower half of the troposphere (1000-550 mb) under the assumption of cylindrical thermal wind balance. f taken at 15°N. $\bar{u}$ is the mean speed of the trade wind or tangential wind of a closed vortex. B refers to the layer depth over which the baroclinicity is taken.

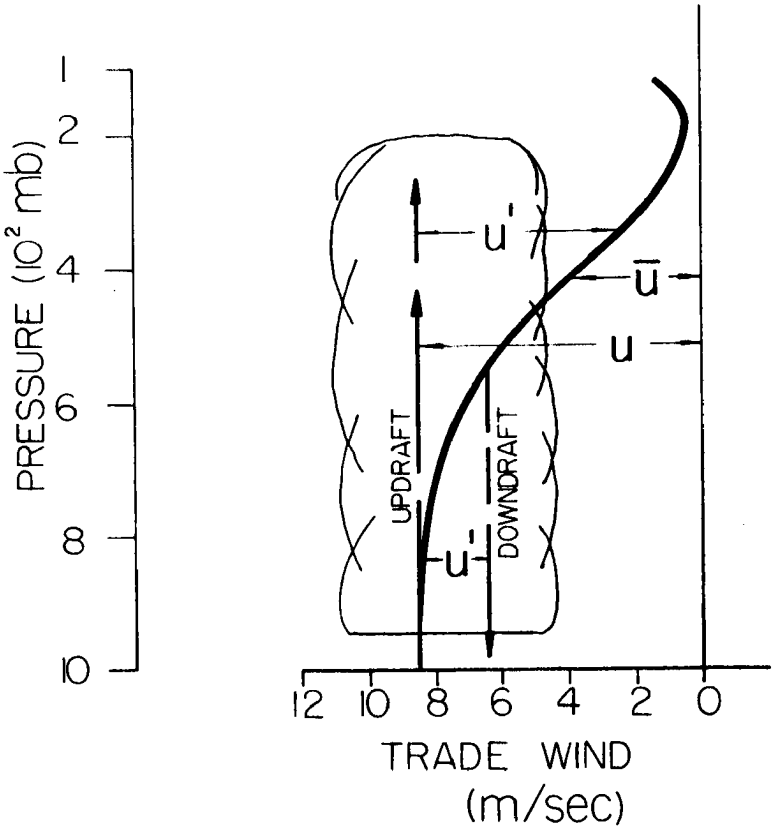

Fig. 67. Portrayal of how the horizontal velocity within the deep cumulus can be different than the velocity of the surrounding cumulus-free area if large vertical shear is present. The trade-wind velocity at any level within the draft (u) may be significantly different (u') than the horizontally average trade-wind velocity ($\bar{u}$) surrounding the cumulus.

If the increase of baroclinicity from the pre-disturbance stage to the developed storm stage went directly to increase the vertical wind shear (as occurs with typical increase of baroclinicity in middle latitudes), then vertical wind shears would have to be much larger than observed. Ventilation effects would become excessive. Heating could not be concentrated. Initial vortex formation could not take place. The mean upward circulation through the disturbance could also inhibit increase of the vertical wind shear. The typical time-scale of intensification and small magnitude of the mean upward motion, however, prevent this from being a major vertical shear inhibiting factor (Gray, op. cit.). It is thus of major importance that the cumulonimbus up- and downdrafts act effectively to inhibit increase of vertical wind shear as the baroclinicity of the disturbance increases. A more precise description follows.

The thermal wind equation in natural coordinates with p as the vertical coordinate may be written as

$$\left(f + \frac{2V}{R}\right)\frac{\partial V}{\partial p} = -\frac{C}{p}\left(\frac{\partial T}{\partial n}\right)_p - \frac{\partial F_n}{\partial p} + \frac{\partial}{\partial p}\left(\frac{dV_n}{dt}\right) \qquad (6)$$

where

f = Coriolis parameter

V = horizontal wind speed

R = radius of trajectory curvature which is assumed to be constant with height

p = pressure

C = gas constant

T = virtual temperature

n = distance along R, positive to the right of the direction of V in the Northern Hemisphere

F_n = horizontal frictional acceleration along R

V_n = wind component along R

$)_p$ = denotes differentiation along the constant pressure surface

$\frac{d}{dt}$ = substantial derivative

In this derivation it is assumed that there is no rotation of the coordinate system with height. The above equation may be more simply written as

$$WS = B + F + A \tag{7}$$

where

$W = (f + \frac{2V}{R})$ = inertial parameter

$S = \frac{\partial V}{\partial p}$ = vertical wind shear parameter

$B = -\frac{C}{p}\frac{\partial T}{\partial n})_p$ = baroclinicity parameter

$F = -\frac{\partial F_n}{\partial p}$ = frictional parameter

$A = \frac{\partial}{\partial p}(\frac{dV_n}{dt})$ = acceleration parameter

This aspect of the intensification process is envisaged to occur in a series of successive infinitesimal growth steps of which one cycle is now described. Frictionally forced surface convergence produces an increase of cumulus activity and baroclinicity. Instantaneous compensating wind, shear, and curvature changes to balance this increased baroclinicity do not immediately occur. Cumulus upper-level frictional accelerations are established by the correlation of cumulus-scale horizontal and vertical wind components as discussed by Gray (1966, 1967). These frictional accelerations inhibit the local and advective accelerations from acting to increase the vertical wind shear. These accelerations then act primarily to increase the mean wind and/or reduce the radius of curvature. In this way vertical wind shears remain small as baroclinicity increases.

Fig. 68 attempts a graphical illustration of the above concept. The cumulus initially act to increase the baroclinicity (B) and establish frictional acceleration (F). A resulting imbalance between the three terms WS, B, and F is established. Local and advective accelerations (A) are activated by this imbalance. These latter accelerations feed back into the inertial coefficient (W) to increase the wind or reduce

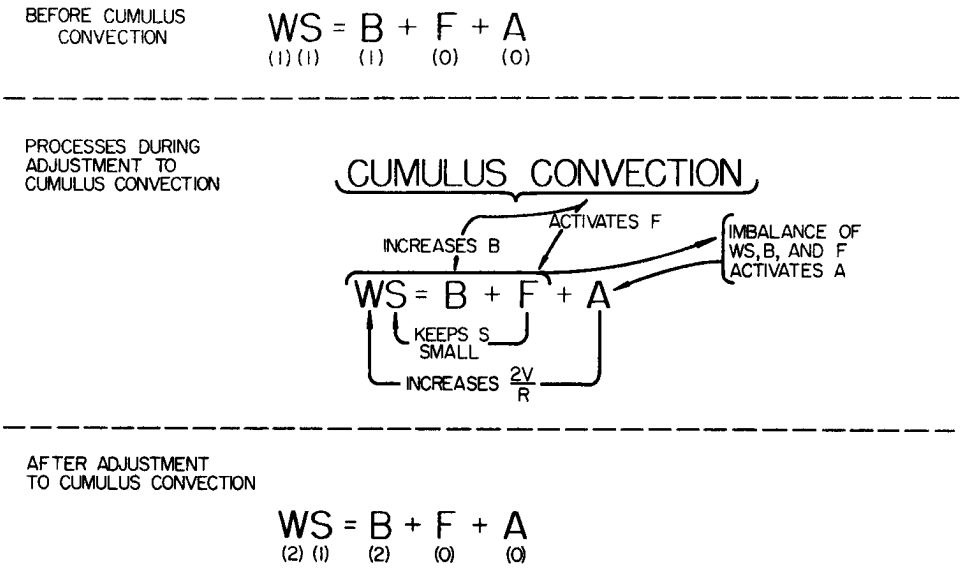

Fig. 68. Description of how B and W can increase as S remains constant.

the curvature while the frictional accelerations act simultaneously to prevent increase of vertical shear (S). In this way the increase of the left-hand term of equation (7) is accomplished primarily by increase of the inertial coefficient rather than the vertical shear. The above example shows that W increases from 1 to 2 while S does not change.

The possible importance of the above processes can be illustrated for an assumed trade wind disturbance with

(1) radius of curvature of 10^3 km

(2) wind shear in the lower two-thirds of the troposphere of 6 m/sec

(3) mean wind of 5 m/sec (8 m/sec at the surface and 2 m/sec at 400 mb)

A 0.1°C/100 km virtual temperature gradient increase with no change of vertical wind shear would require a layer mean wind increase from 5 to ~25 m/sec, or a decrease of the radius of curvature from 1,000

to ~200 km in order that the ratio of $\frac{WS}{B}$ remain constant (f taken at 20° latitude) with no change of S.

The effect of this vertical transport of momentum by the cumulus in inhibiting the increase of vertical wind shear as baroclinicity increases is thus viewed to be of fundamental importance for the initial generation of the disturbance and vortex from zonal trade-wind flow conditions. It is also of major importance in the later stages of intensification. The induced friction of the momentum transport by the cumulus allows for a necessary unbalanced pressure-wind acceleration at various levels during development.

6. IDEALIZED PORTRAYAL OF CONDITIONS ASSOCIATED WITH TROPICAL-TYPE DISTURBANCE INTENSIFICATION

As the majority of the globe's disturbance intensifications ($\sim 83\%$) are of the tropical A type, a hypothesized portrayal of the primary conditions associated with this type of development is now given.

In the cyclonic wind shear regions on the poleward side of the doldrum Eq. T., differential surface stress produces a frictionally forced low-level mass and water vapor convergence. On the equatorward side flow convergence also produces a low-level water vapor convergence as shown in Fig. 69. This water vapor convergence is released primarily into the deep cumulus. Condensation heat is given off. This heating should be considered only as potential heating, for unless it can be concentrated in a smaller meso-scale area it will be ineffectual in developing the required tropospheric warming and surface pressure fall.

The magnitude of the large-scale tropospheric vertical wind shear (or ventilation) is the initial primary factor in determining the extent to which the potential heating can be concentrated. The ratio of surface convergence to tropospheric vertical wind shear or the ratio of potential heating to ventilation will be specified as actual heating. This ratio is the major factor determining disturbance genesis and initial disturbance intensification. Fig. 70 gives an idealized portrayal north and south of an assumed doldrum Eq. T. of the above-mentioned quantities. Note that these quantities lead to very large actual warming in the area just to the poleward side of the Eq. T. On the equatorward side, even though potential heating is larger, actual heating (or potential heating divided by ventilation) is less due to the larger ventilation factor.

If frictionally induced surface convergence (and potential heating) is directly related to the surface relative vorticity as is required from Ekman theory, then the ratio of surface relative vorticity (ζ_r) to tropospheric vertical wind shear $|S_z|$ would be a representative parameter of actual heating. Fig. 71 shows the monthly average of this parameter for August in the Northern Hemisphere and January in the Southern Hemisphere. Note the very high climatological correlation of places of maximum $\frac{\zeta_r}{|S_z|}$ ratio with the location of disturbance genesis

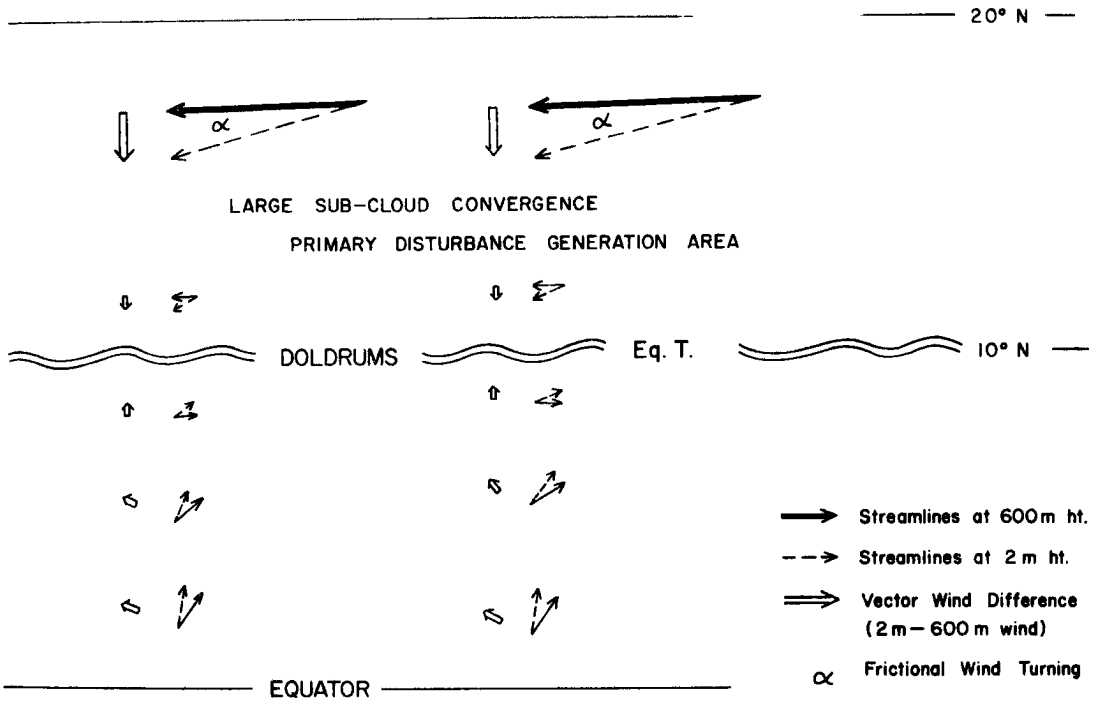

Fig. 69. Idealized portrayal of the difference in wind directions at the surface and at the top of the friction layer relative to a doldrum Equatorial Trough. Note that the wind south of the Equatorial Trough is in general weak and that the sharp cyclonic gradient of trade wind on the poleward side of the Equatorial Trough can lead to substantial low-level convergence by virtue of frictional veering.

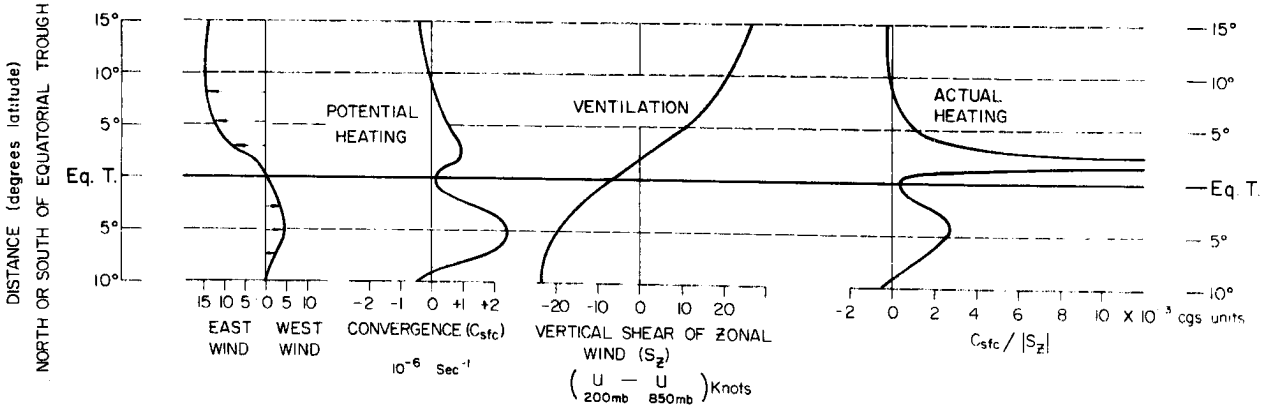

Fig. 70. Idealized portrayal north and south of a doldrum Equatorial Trough of the zonal wind speed (left diagram), surface convergence or potential heating (center left diagram), vertical shear of the zonal wind between 200 and 850 mb or the effect of tropospheric ventilation (right center diagram), and the ratio of surface convergence to vertical shear, or the actual heating which is possible (right diagram). Values of right diagram are in basic cgs units. Note that these conditions would lead to very large actual warming in the area just to the north of the Equatorial Trough.

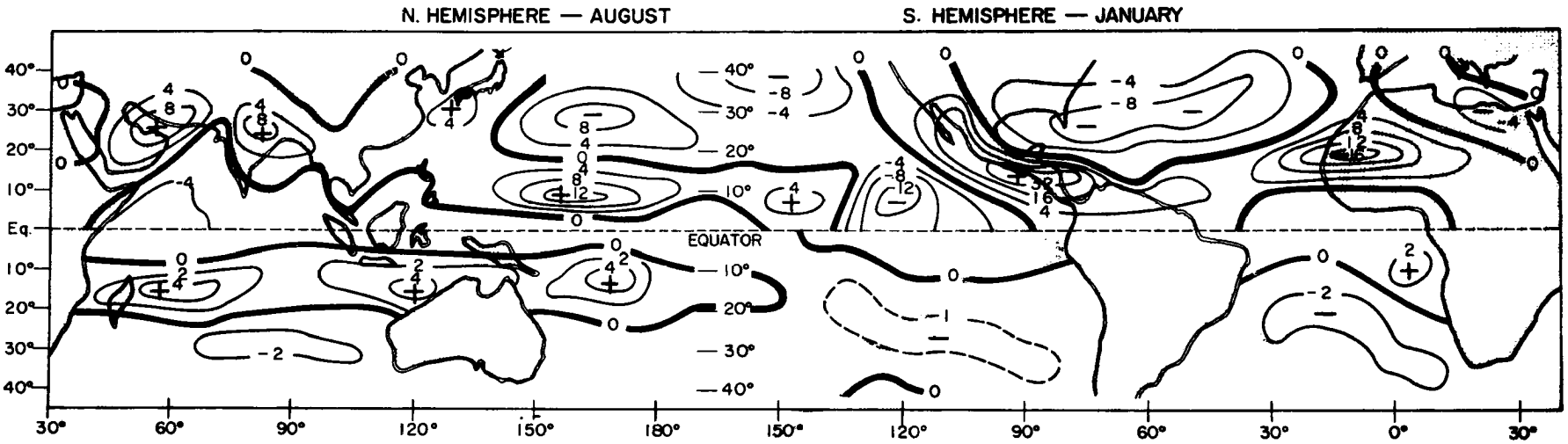

Fig. 71. Mean summer month portrayal of the ratio of $\frac{\zeta_r}{|S_z|}$ (ζ_r is surface relative vorticity, $|S_z|$ is the absolute vertical wind shear between 200 mb and 850 mb). Values are in basic cgs units of 10^{-3}. The total vector shear was used in the calculation of $|S_z|$. The sign of ζ_r determines the sign of $\frac{\zeta_r}{|S_z|}$. Note the very high correlation of places of maximum $\frac{\zeta_r}{|S_z|}$ ratio with location of initial tropical disturbance genesis. These are the primary areas of condensation produced tropospheric heating.

and initial disturbance intensification. Such regions possess the highest combined potential for both tropospheric heating and area concentration of heating. These are the primary regions of condensation-produced tropospheric heating.

The climatology itself, plus the standard deviation from climatology of the required development parameters determine the frequency of favorable development conditions in each region. If the degree of unfavorability of the climatology is much greater than the deviations from climatology, then development does not occur. If the degree of unfavorability of the climatology is less than the individual deviations from it, then development is possible but not frequent. The frequency of development will, of course, be greatest where climatology is most favorable.

Fig. 72 shows how the size of the convergence area is important in determining the degree of ventilation. A large convergence area will have less ventilation for a given vertical wind shear. The larger the convergence area, the more favorable is disturbance genesis and intensification.

Fig. 73 represents an idealized portrayal of the primary requirements for tropical storm development of the typical A type. Six basic requirements are specified. The poleward side of a doldrum Eq. T. is the primary location where it is possible for all six requirements to be satisfied. Even in these locations it is difficult for all requirements to be simultaneously present. For this reason tropical storms are a relatively rare phenomenon.

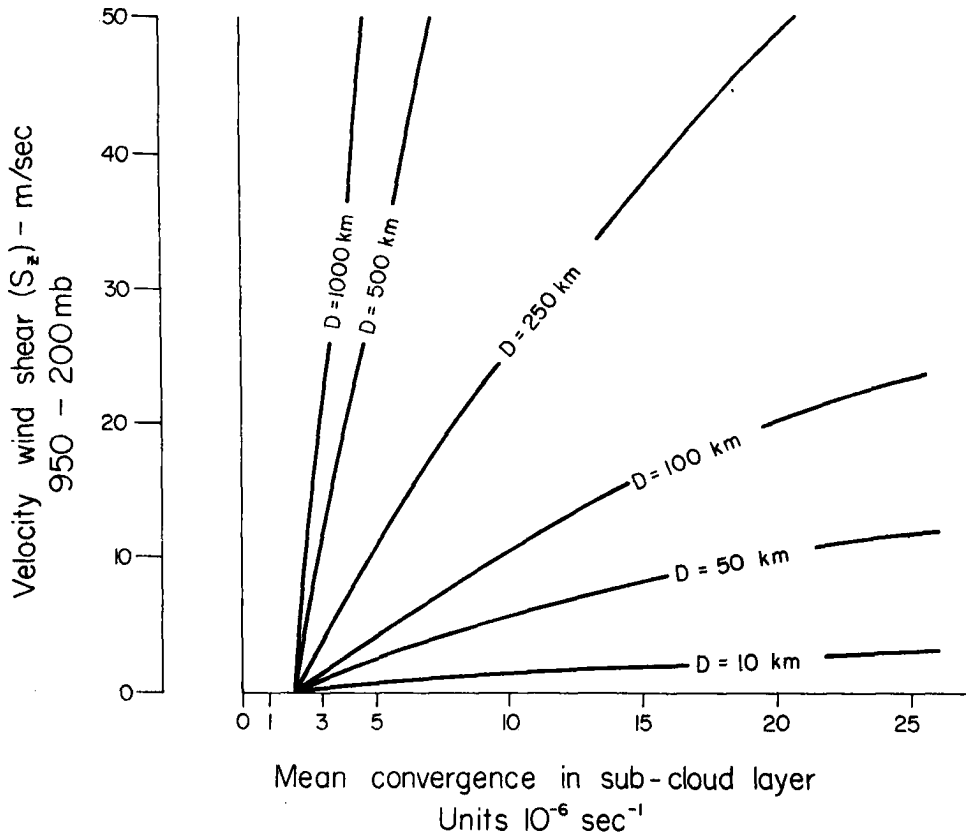

Fig. 72. Portrayal of the relationship between vertical wind shear, size of convergence area, and magnitude of surface convergence in the sub-cloud layer (1010-950 mb) to produce a surface pressure decrease of 1 mb in 48 hours with typical summertime vertical gradient of θ_e. D represents the width of the convergence area. Abscissa-scale represents the intensity of the convergence in the sub-cloud layer. For equal pressure decrease one observes the strong functional dependence of the size of the convergence area to the intensity of required sub-cloud layer convergence. A large convergence area requires much less intensity of surface convergence in order to obtain an equal amount of warming or pressure decrease.

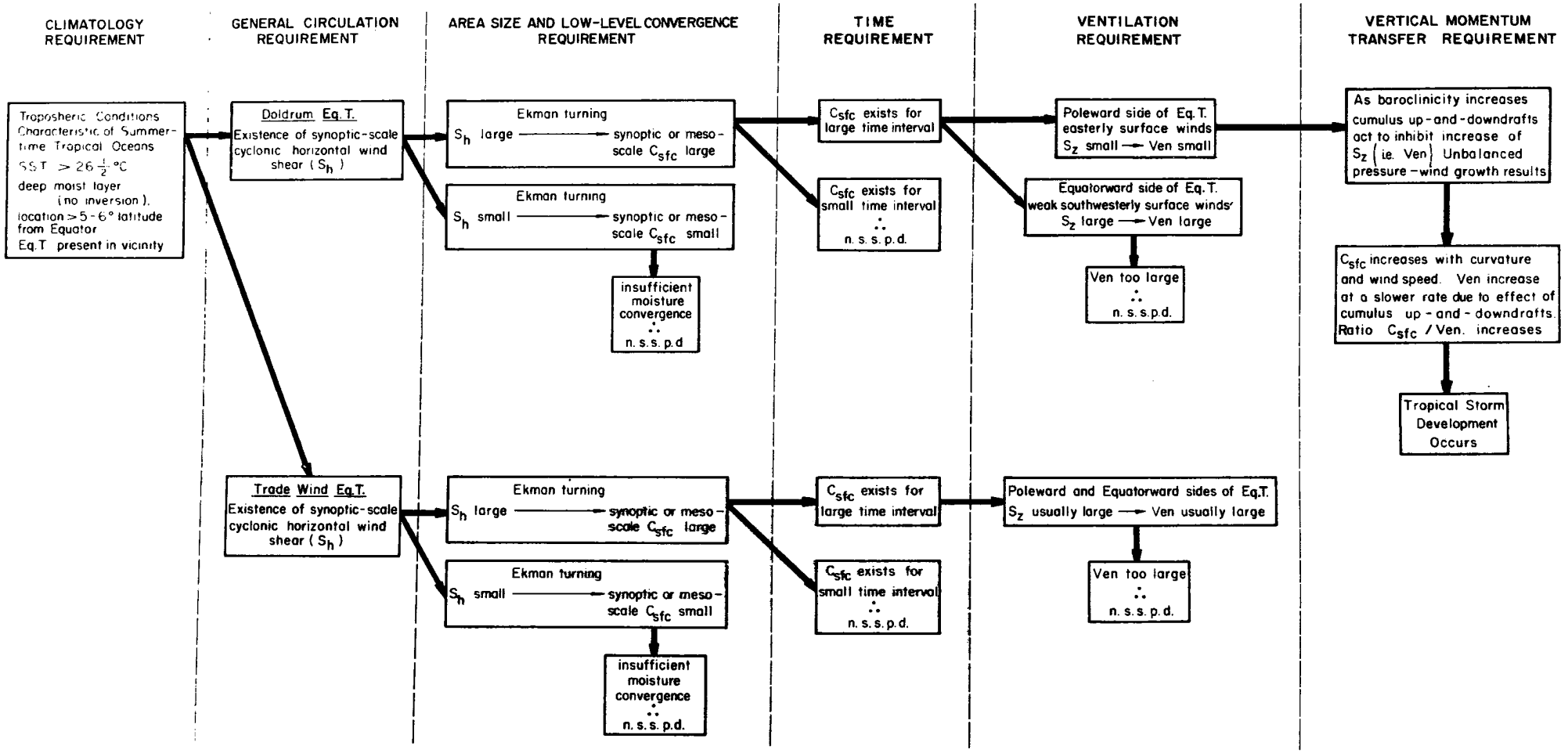

Fig. 73. Idealized portrayal of the primary requirements for tropical storm development of the typical tropical or type A storm; symbols are

→ (inside boxes) = so then ∴ = therefore S_h = horizontal surface wind shear

n.s.s.p.d. = no significant surface pressure drop S_z = tropospheric vertical wind shear Ven = ventilation

7. CHARACTERISTICS OF DEVELOPMENT IN EACH OF THE GENESIS AREAS

Region I. Northeast Pacific. Storms develop in this region from late May through October (Fig. 19). Only the tropical type A intensification occurs. Some disturbances which intensify may have had their initial development in the western Caribbean. No latitude (Fig. 16) or monthly peak of development is observed. Sadler (1963, 1964) and Rosendal (1962--Appendix) have given the best information for this region. This is the only region in which tropical storms do not recurve into the westerlies. Increasingly larger tropospheric vertical shear west of 120°W produces a less favorable environment, which weakens and dissipates the storms before recurvature can occur. Storms which move in a more northerly direction encounter regions of greatly reduced potential buoyancy due to lower sea surface temperature and dissipate.

Region II. Northwest Pacific. Storms in this region can form in all months, but there is a strong concentration in the summer. Most storms are of the A type. The region of maximum intensification is between 130°E and 150°E where minimum climatological tropospheric vertical shear is observed (Fig. 31). Development is strongly controlled by the position of the Eq. T. As shown in Fig. 16 initial disturbances are first observed in the latitude belts of 15-20° in August and 5-10° in winter.

A small percentage (~10-15%) of disturbance intensifications will occur wholly within the trade-wind current at large distances poleward of the Eq. T. These developments are typical sub-tropical or B type. They are referred to as embedded developments by personnel at the U. S. Joint Typhoon Warning Center at Guam. Sadler (1967) has recently presented some cases of this type of development.

Nearly a third of the global tropical storms form in Region II. This is probably due more to the large area of small climatological vertical wind shear (Fig. 31) than to an especially large climatological surface vorticity pattern (Fig. 14). Other regions have as much or more favorable surface relative vorticity. In no other tropical region is there such a large north-south oriented region (as there is at 150°E) of change from easterly to westerly tropospheric shear.

Regions III and IV. North Indian Ocean. In these regions only typical A type development occurs. Developments can occur in all but the three winter months, except in the Arabian Sea where development does not occur in winter or in July and August. The Eq. T. progresses slowly northward from February to April and then quickly swings across the Bay of Bengal in the month of May. Tropical developments move northward with it (compare Fig. 15 with Fig. 16). From September to December the Eq. T. retreats from North India southward to the southern edge of the Bay of Bengal. Development closely follows this southern retreat. Developments occur between 5° and 10°N in early spring and late fall. In the middle of the monsoon, development takes place only at the very northern fringe of the Bay of Bengal from favorable daily combinations of vertical shear values and the Eq. T. fluctuations from their mean monthly positions. Figs. 29-32 show that minimum tropospheric vertical shear regions move in conjunction with the Eq. T. In spring and autumn, when the Eq. T. is located in an east-west position at approximately 10°N latitude, minimum zonal tropospheric vertical shear is also present just to the poleward side. In July and August the climatological position of the Eq. T. is over North India. No developments occur over the Arabian Sea or south Bay of Bengal at this time. A very strong upper tropospheric easterly jet stream is located over South India. Surface flow is from the west. The strong tropospheric ventilation produced by the large vertical shear inhibits storm development despite the fact that large surface convergence and copious convective rainfall is intermittently present during this monsoon period.

The slightly reduced sea surface temperatures over the North Indian Ocean during July and August is not viewed as a major factor in explaining the lack of major intensification during these months.

Region V. South Indian Ocean. Storm developments from this and other Southern Hemisphere regions are all of the type A, tropical type. Only moderate latitude and seasonal frequency peaks are observed in mid-summer. Compare Figs. 15-16 and 18-19. Intensification is restricted to regions equatorward of 20°.

An average of six storms per year attain sustained velocities of 40 mph or greater. Note the very high concentrated area of maximum development frequency northeast of Madagascar of Fig. 1. The furthest poleward penetration of the Eq. T. in the South Indian Ocean occurs

in this region of highest concentration. In the central and eastern South Indian Ocean the Eq. T. is found closer to the equator and development frequency is less.

Regions VI and VII. Area to the Northwest of Australia and South Pacific. These regions have characteristics similar to Regions I and V. All developments are of the A type. On the average two storms per year develop off the NW Australian coast (105-135°E), three per year off the NE Australian coast (135-150°E), and four per year in the South Pacific (150°E to 150°W) for a two regional annual average of nine. (See South Pacific data references.)

Note the climatological differences of Southern Hemisphere vertical wind shear in latitude ranges between 20° and 30° in comparison with vertical shears observed in the NW Pacific and NW Atlantic (Figs. 29-32). These large vertical shears in the Southern Hemisphere act to inhibit intensification poleward of 20°. The low latitude upper tropospheric westerlies also inhibit long easterly trajectories and cause westerly recurvature at lower latitudes in the Southern Hemisphere.

Region VIII. North Atlantic. The North Atlantic is the most complicated development region. All three types of intensification are observed. A near complete absence of development is observed in the eastern half of the Caribbean as first noted by Mitchell (1924). There is a peculiar seasonal shift of development regions. Figs. 74-76 have been taken from Cry (1965) and show that in the early part of the hurricane season (i. e., June) disturbances form in the SW Caribbean and in the Gulf of Mexico. As the season progresses into August developments seldom occur in these areas but take place from disturbances which have formed on or off the west African coast and have moved across the Atlantic into the area to the east of the Antilles or into the Bahamas. By mid-September the Eq. T. off Africa has weakened, vertical wind shears have become greater (Fig. 32), and disturbances no longer develop and move out of that area. In late September and October storms again begin to form from disturbances generated in the western Caribbean. This shifting pattern of development can be explained in terms of the seasonal changes of position and intensity of the Eq. T. and vertical shears.

In late May the Eq. T. moves from its seasonal position in northern Columbia and southern Panama to a position of approximately 10°N. It then lies across the southern Caribbean. From that time on distur-

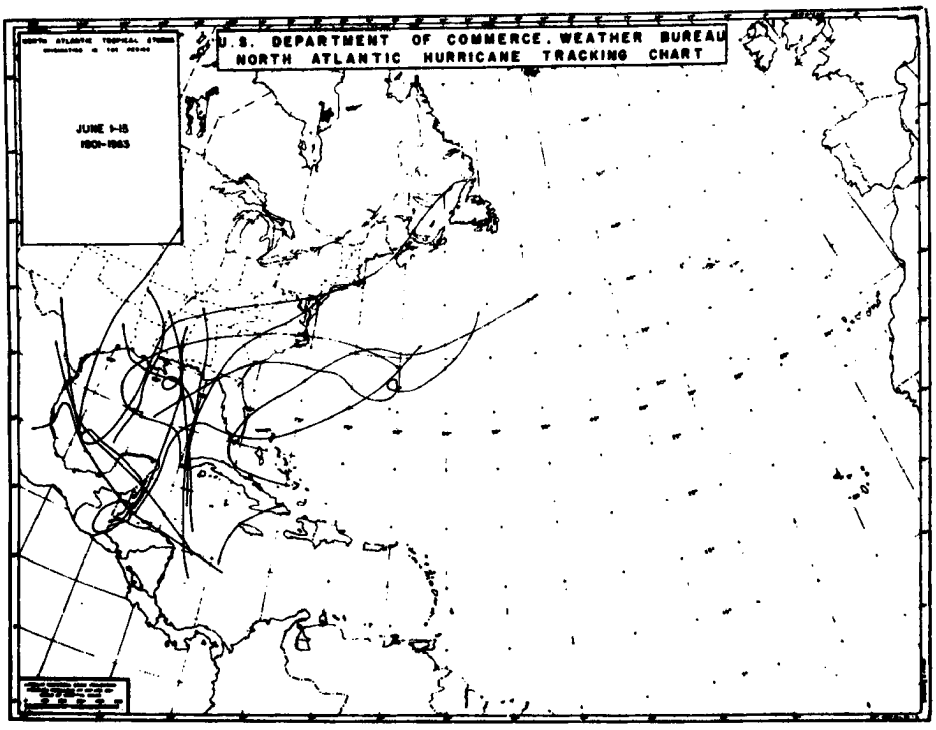

Fig. 74. Climatology of tropical storm tracks in the West Indies for the period of 1-15 June for 63 years (from Cry, 1965). Note that most storm tracks are initiated in the western Caribbean-Gulf of Mexico region.

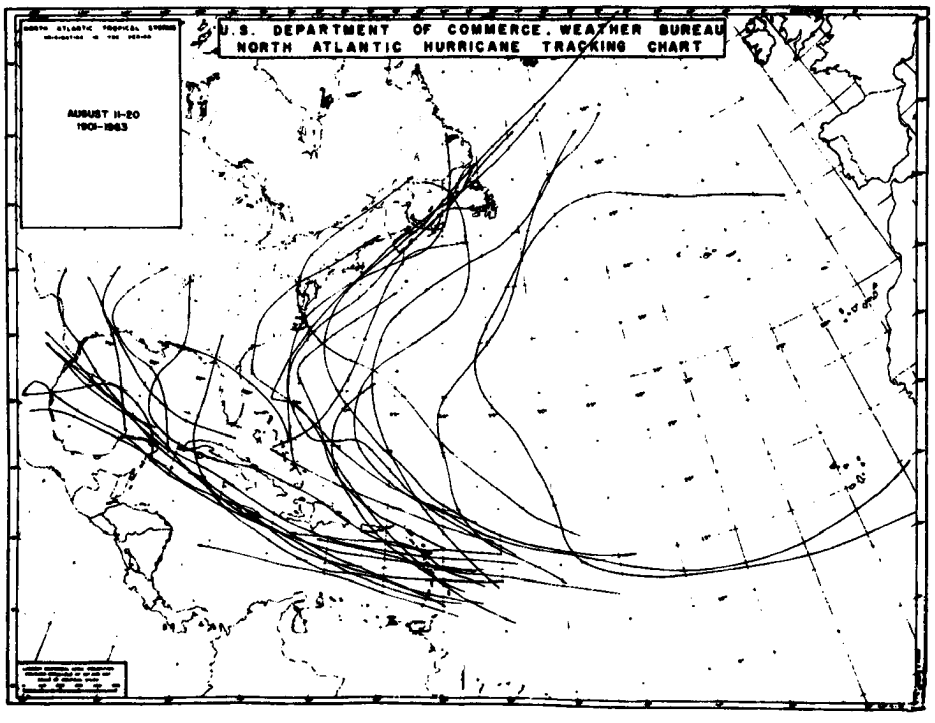

Fig. 75. Climatology of tropical storm tracks in the West Indies for the period of 11-20 August for 63 years (from Cry, 1965). Note the almost exclusive origin of the tracks in the region to the east of the Antilles.

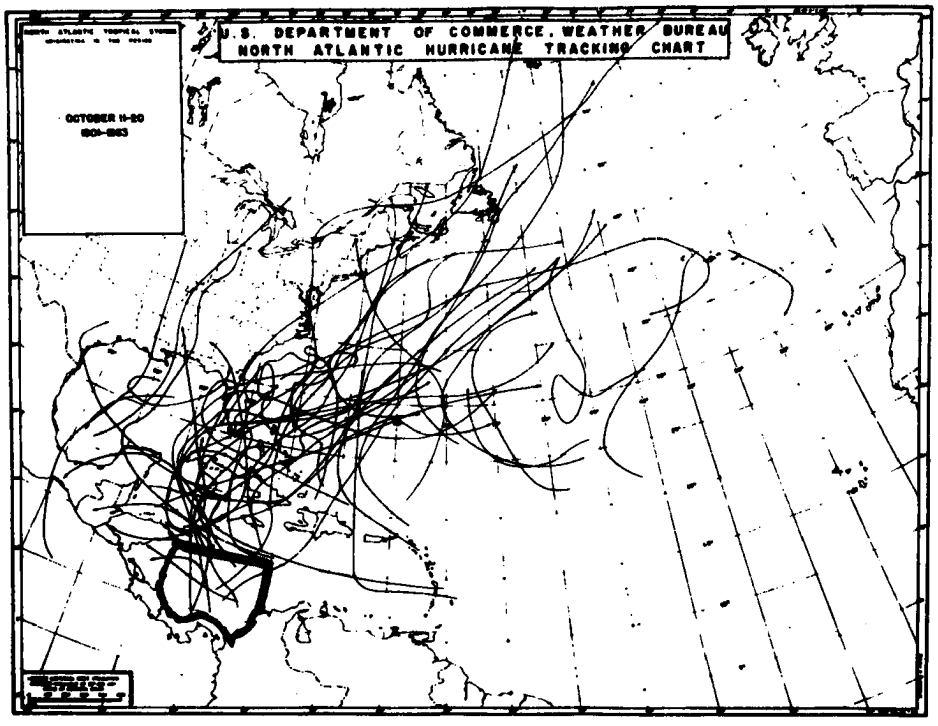

Fig. 76. Climatology of tropical storm tracks in the West Indies for the period of 11-20 October for 63 years (from Cry, 1965). Note the high concentration of track initiation again in the western Caribbean region.

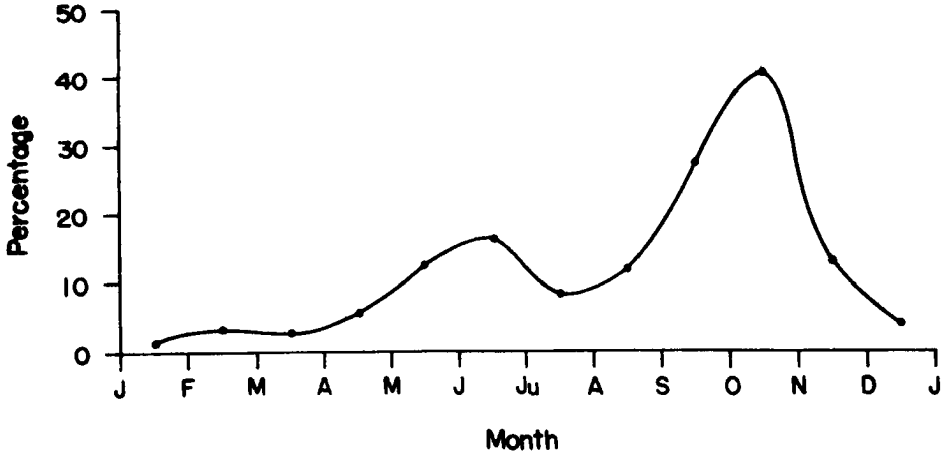

Fig. 77. Portrayal of percentage of ship reports during a 60 year period which reported calm wind or wind direction from the south-through-west in the area 8-15°N and 75-83°W. This area is enclosed within heavy boundary shown in Fig. 76 (from U.S. Navy Oceanographic Atlas of the North Atlantic Ocean, Pub. 700, 1963).

bances are generated in the cyclonic wind shear area on the poleward side of the Eq. T. Some of these disturbances remain and grow in the Caribbean area. Others move into the Gulf of Mexico or the NE Pacific where they later develop. It is at this time that the vertical shears over the western Caribbean and southern Gulf of Mexico are small. In July and August the Eq. T. does not push further poleward as in the other development areas, but retreats somewhat. The surface horizontal shears in the western Caribbean become weaker. At the same time the easterly upper tropospheric winds become weaker or become westerly. Stronger vertical shears are therefore developed. Disturbance development from the western Caribbean is, therefore, inhibited in July and August. Starting in mid-September the surface horizontal shears at the poleward edge of the Eq. T. become stronger and vertical shears become weaker. Again storm development becomes more frequent, reaching maximum intensity in October. After October the Eq. T. weakens, retreats southward, and much stronger westerly vertical shears are established with the result that development ceases. Fig. 77 portrays the monthly percentage of calm or south-through-west component surface winds which are observed in the dark bounded region of the western Caribbean shown in Fig. 76. These conditions would indicate the presence of a doldrum Eq. T. to the north. Note the double maxima of calm or south-to-west winds.

Storms developed from disturbances generated on or off the west African coast usually move long distances across the Atlantic before intensification. Most of the west African generated disturbances dissipate. A small number, however, are able to maintain their identity and later intensify in the more thermally favorable climatological environment of the region to the east of the Antilles or in the Bahamas. The traveling disturbance can break down the unfavorable climatological surface vorticity. Recent satellite and other research has verified this mode of mid-season development as discussed by Aspliden, et al., (1966) and Arnold (1966). Although surface convergence and vertical shear is highly favorable for disturbance genesis on or off the coast of Africa, the weak inversion layer and lower height of the moist layer inhibit storm intensification while allowing for initial disturbance genesis.

In no region other than the North Atlantic do as many disturbances intensify poleward of 20°. In no other region does the initial disturbance travel as far before intensification. For these reasons it is important that American meteorologists do not form any general con-

clusions on global development processes which are derived exclusively from observations in the North Atlantic.

Regions of Southwest Atlantic and North Central Pacific. Tropical storm formation does not occur in these areas, even though sufficient cumulus potential buoyancy is present (Figs. 21 and 22). This is primarily due to the large climatological tropospheric vertical shear present (Figs. 29-31). Even when meso-scale patterns of strong surface convergence are present (i. e., satellite viewed "cloud blob" areas--Fig. 4), storm development cannot proceed because of the large tropospheric ventilation effects which prevent concentration of condensation heating.

8. SUMMARY DISCUSSION

It is remarkable that a meteorological phenomenon of such a large scale as the tropical disturbance and subsequent tropical storm has had such little consensus of opinion as to the general environmental flow features and the dynamical processes associated with its formation. Various meteorologists in the different parts of the world watch for a variety of onset and development criteria. Without firm knowledge of the basic physics they have not known what to look for.

In recent years considerable attention has been given to numerical experiments on the later stages of tropical storm development where a closed vortex is initially assumed. These experiments have in general been run to obtain mathematical experience on parameterization of the cumulus convection and on the associated time rates of growth. The degree of basic insight into the primary development processes which has been gained from these experiments is limited because a pre-existing vortex has been assumed and the dynamics of the individual cumulus have not been considered. Ekman frictional veering by itself requires that all assumed vortices should intensify.

Discussion of processes leading to initiation of the pre-existing disturbance has not been extensive. Semantical differences exist over the definition of the pre-existing disturbance from which storms grow. Riehl and other meteorologists have looked to the pre-existing disturbance as a wave in the trade winds. Other meteorologists have viewed the pre-existing disturbance as something apart from "waves" in the easterlies. A great deal of observational evidence is now at hand to rectify these differences. This paper is but one of a number of observational research studies that are presently possible.

Some of the past methodological difficulties have resulted from beginning attempts to relate the processes of disturbance genesis and intensification to that of other fluids, where the dynamics are already understood. But the atmosphere in which the tropical storm develops is vastly different from the usual idealized fluids assumed or utilized in numerical or laboratory experiments. There are no experimental fluids in which the temperature, density, and pressure have such large percentage changes in the vertical, where such large potential energy (i.e., condensation) is intermittently available and where the vertical transports of heat, moisture, and momentum occur in such

small and isolated areas (i. e., cumulus clouds) in comparison with the broad-scale motion.

Because of the complexity of the cumulus convective atmosphere it may not yet be possible to relate the flow features of the tropical storm to other fluid systems whose dynamics are quantitatively understood. Even though the end results of model experiments may appear similar to the flow features of the real system, with numerous variables a near infinite number of correct solutions is possible. A seemingly realistic answer does not necessarily imply a satisfactory treatment.

At the present state of our knowledge the author feels that the dynamics of development are best viewed as a hydrostatic problem of temperature-pressure-wind adjustment. To have a storm, the mean tropospheric temperature must be increased and concentrated. Development should be considered from the point of view of the physical mechanisms which are responsible for tropospheric concentration of heat. How do the cumulus develop and concentrate tropospheric heating? The question is more involved than just explaining cumulus production because not all concentrations of cumulus produce storms. Some of the heaviest rainfalls over the tropical oceans take place without corresponding development. A mechanism to prevent tropospheric ventilation is also required.

Observations of the developed tropical storm have shown that the strong moisture convergence into the vortex which is needed to produce and maintain the central warming is brought about by low-level convergence and a compensating upper tropospheric ($\sim$ 200 mb) divergence. There is no disagreement among meteorologists over this inflow-outflow pattern of the developed storm. Observations of the circulations developed by deep cumulus convection in the weak disturbance also indicate a similar inflow-outflow pattern.

The crucial aspect of the development problem thus appears to center itself on explaining the physical processes which operate to initially establish this disturbance scale inflow-outflow which is necessary to produce the needed low-level water vapor convergence.

For the surface pressure to fall there must be slightly more net tropospheric mass divergence than convergence. Given the developed storm's inflow-outflow character, plus the concept of the idealized two-level tropospheric model so prevalent in the meteorological litera-

ture in the 1940's and 1950's, it seems natural that meteorologists would look first for an upper tropospheric outflow mechanism which might initiate compensating surface inflow. A number of authors (Sawyer, 1947; Riehl, 1948b, 1950; Alaka, 1958, 1961, 1962; Ramage, 1959) in the last two decades have followed this reasoning and advanced the idea, à priori, that some type of upper tropospheric outflow is initially established over a disturbance which enhances or triggers a lower tropospheric convergence. This outflow was hypothesized to occur as a result of regular flow divergence, by some form of dynamic instability, or by some other unspecified dispersion mechanism. The majority of practicing forecasters today look to upper tropospheric divergence as a precursor to development. Is such an initial upper tropospheric divergence really necessary and does it really take place? Is the observed upper-level divergence only an indicator of existing convergence at a lower level? If an initial upper tropospheric divergence did, in fact, occur would the resulting compensating convergence necessarily take place in the lowest layer? Why would compensation not occur at some other level? In addition, how are upper tropospheric flow patterns established to the point where a dynamically induced outflow can occur? Is development really a random process of favorable statistical superposition of upper and lower tropospheric systems?

The observational information of this paper leads the author to reject the above view of primacy of initial upper tropospheric outflow as an important genesis feature. In accordance with the general ideas of Charney and Eliassen (1949, 1964a, 1964b), the author views development and the resulting upper tropospheric outflow as but a consequence of a lower tropospheric convergence which is frictionally forced. The outflow which occurs in the upper troposphere is mostly determined by what is happening in the sub-cloud boundary layer.

In general, compensation for mass convergence or divergence at any level must always occur at a higher level. This is due to the larger upward or downward bulging of the pressure surfaces at higher than at lower levels. Fig. 78 illustrates the vertical differences in compensating acceleration for assumed impulsive evacuation or addition of mass at an upper and a lower tropospheric level. The lowest level is the least likely level for compensating convergence of an initially produced upper tropospheric divergence.

The disturbance and storm development which the author envisages is one of a series of successive identical infinitesimal growth steps of which one cycle is now described.

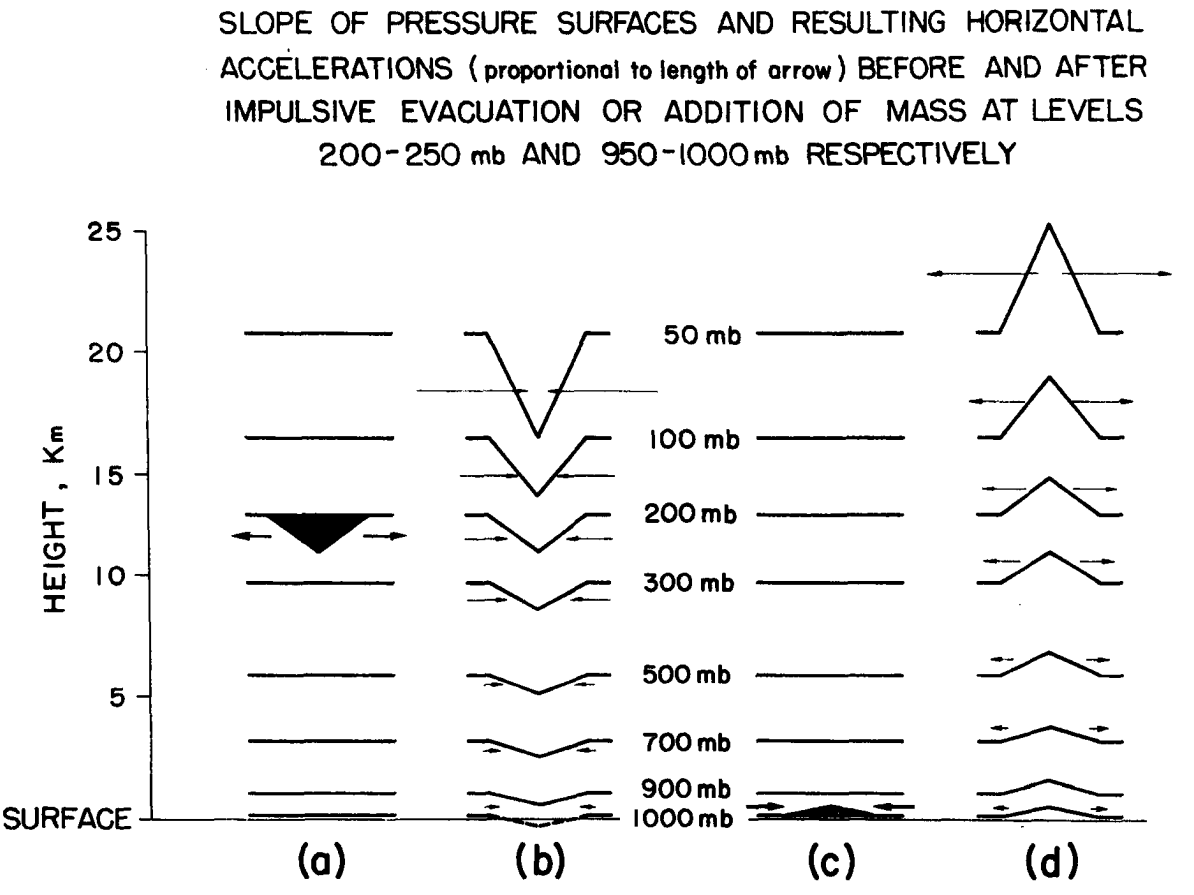

Fig. 78. Portrayal of why author believes upper tropospheric evacuation of mass would not be compensated for by sub-cloud layer convergence. To illustrate point of view an impulsive evacuation of mass has been hypothesized for the 200 to 250 mb layer in column a, and impulsive convergence of mass has been hypothesized for the 950 to 1000 mb layer in column c. Column a shows the pressure surfaces before an impulsive evacuation of 50 mb (or 50 g/cm^2) of mass at the center (shaded area). Column b portrays the resulting slope of the pressure surface after the evacuation of mass has taken place. The thin arrows indicate the resulting acceleration which would be established.

Column c shows the pressure surfaces before an impulsive addition of 50 mb (or 50 g/cm^2) mass at the center of the layer between 950 and 1000 mb (shaded area). Column d represents the resulting slope of the pressure surface after the impulsive addition of mass has occurred. In both cases note that the maximum slope of the pressure surfaces and accelerations occur in the upper levels. For this reason the author does not follow the argument that an upper tropospheric mass evacuation would likely be compensated for in the lowest layer. This is the least likely place of mass compensation.

Meso-scale frictionally driven sub-cloud layer mass and moisture convergence is released into deep cumulus (Fig. 79). The condensation heat from the cumulus is diffused to the surroundings and a small mean tropospheric warming occurs. Thickness between pressure surfaces is increased. This thickness increase plus the excess mass from the surface convergence produces a small bulging up of the pressure surfaces over the convergent areas as seen in an exaggerated manner in column c of Fig. 79. The hydrostatic pressure-height relationship requires that the upward bulging (and consequent height gradients on the constant pressure surfaces) increase with altitude. Large compensating divergent accelerations are immediately developed at upper levels as is shown in column d of Fig. 78. Divergent mass acceleration is stimulated in the upper troposphere at the level where, jointly (1) the deep cumulus updraft velocities are decreasing due to sharp increase of stability and (2) where the compensating outward pressure accelerations are very large. These two effects combine best near 200 mb. This is the primary level of divergent mass compensation.

The stimulated 200 mb divergence then eliminates the upward bulging pressure surfaces at higher levels and causes a small downward bulging (due to the condensation heating) of pressure surfaces. The downward bulging is largest at lower levels. During this inflow-outflow adjustment a small net tropospheric mass divergence has taken place due to the increased thickness between the pressure surfaces resulting from the released condensation. Surface pressure is slightly reduced in the surface convergent area. Without the condensation heating no significant surface pressure decrease would occur, for the mass outflow would have completely compensated for the inflow. The resulting small pressure reduction stimulates a compensating increase of wind circulation within the convergence area. Relative vorticity and frictionally forced, sub-cloud layer convergence are further enhanced. The intensity of inflow-outflow pattern and cumulus convection also increases.

During the above adjustments the hydrostatic temperature-pressure relationship is maintained. As long as

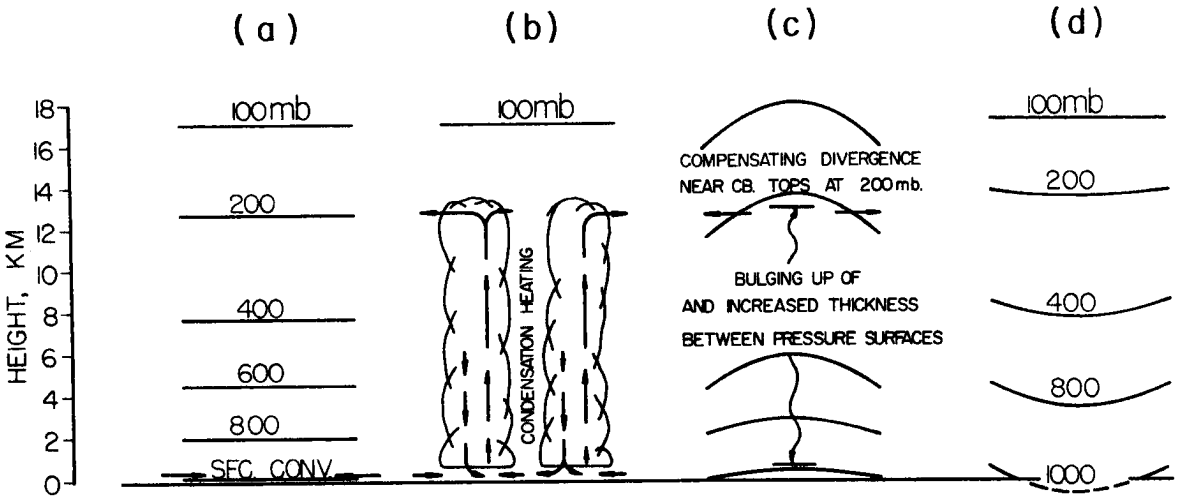

Fig. 79. Schematic exaggerated growth cycle applicable to disturbance genesis or intensification

(a) initial pressure surface distribution at the beginning of convergence

(b) generation of cumulonimbus by surface convergence, release of condensation heating

(c) initial effect of mass convergence and condensation heating to bulge up pressure surfaces--vastly exaggerated

(d) resulting slope of pressure surfaces after compensating upper-level accelerations and outflow have been dissipated. Downward sloping pressure surfaces are due to the increased pressure thickness from condensation heating

surface moisture convergence accompanies the mass convergence there is no apparent contradiction of mass convergence and surface pressure fall. The simultaneous mass and moisture convergence produces an immediate compensating divergence at higher levels.

The above infinitesimal cycle of inflow-outflow, heating, and resulting surface pressure reduction is repeated continuously until substantial surface pressure reduction occurs. The winds increase in response to the increased pressure gradient.

The primary factor in determining whether or not a once established low-level convergence will increase is not whether it exists under a favorable upper troposphere divergence environment, but whether the ventilation of heat away from the convergence area will be too large to prevent tropospheric heating concentration. If tropospheric heating occurs, upper-level outflow will automatically take place. A unique upper-level divergence mechanism is not required.

Due to the low percentage of condensation heat which is available to warm the atmosphere, only a very small number of tropical disturbances are ever able to lower their surface pressures more than a few millibars. If central pressures do lower 5 mb or more below environmental pressures (equivalent to a mean tropospheric virtual temperature increase of 1°C or more), the disturbances are usually "beyond the hump" and continued growth to tropical storm intensity follows. As demonstrated in Figs. 65 and 72, the initial 1°C tropospheric warming is very difficult to obtain with trade-wind surface shearing convergences unless the convergence area is large ($\sim$ 500 km or more), the convergence acts over a long time period ($\sim$ 1-3 days), and the tropospheric ventilation of the released condensation is very small. In that only about 1/8 (Lopez, 1967) of the low-level condensed water vapor is available to warm the troposphere and lower the surface pressure, the crucial importance of initial small vertical wind shear to prevent ventilation of heat away from the system is clearly evident.

This paper has attempted to demonstrate that most tropical disturbance from which storms form is generated from an environment in which a horizontal shearing zonal trade-wind current is present with minimum tropospheric vertical shear. Baroclinic instability is obviously not an initially important genesis mechanism. A shearing barotropic instability is possible, but, due to the requirement of initial large ratio of sub-cloud to cloud level convergence, is not a probable or required mechanism. Charney and Eliassen's (1964b) proposed "conditional instability of the second kind" appears to offer the best physical explanation of initial disturbance genesis.

ACKNOWLEDGEMENTS

To Dr. M. Yanai and Mr. J. Sadler for helpful discussion. The author further acknowledges helpful discussions of tropical meteorology problems with meteorological personnel in Japan, Hawaii, Miami, Guam, Hong Kong, and Poona, India, during visits to these locations in 1965-1966.

The author thanks Mrs. I. Akamatsu and Mr. Y. Nakata of the Meteorological Research Institute, Tokyo, and Mrs. G. Odle of Colorado State University for assistance in the data reduction. Miss Hanae Akari of Colorado State University drafted the figures. Mrs. V. Eloedon of Colorado State University assisted in preparation of the manuscript.

This research has been jointly sponsored by the National Science Foundation under the U. S. - Japan Joint Cooperative Science Program and by the Environmental Science Services Administration.

APPENDIX

Data Sources

General Data References

Crutcher, H. L., 1961: Meridional cross-sections--upper winds over the Northern Hemisphere. Tech. Paper No. 41, U. S. Dept. of Commerce, Superintendent of Documents, U. S. Govt. Printing Office, Washington D. C., 307 pp.

Heastie, H., and P. M. Stephenson, 1960: Upper winds over the world, parts I and II. Geophys. Memoirs, No. 103, Meteor. Office, Air Ministry London, Her Majesty's Stationery Office, 217 pp.

Jenkinson, A. F., 1955: Average vector wind distribution of the upper air in temperate and tropical latitudes. Meteor. Mag., 84, 140-147.

Newnham, Mrs. E. V., 1922: Hurricanes and tropical revolving storms (with introduction on the birth and death of cyclones, by Sir Napier Shaw). Geophys. Memoirs, No. 19, Meteor. Office, Air Ministry London, Her Majesty's Stationery Office, 333 pp.

Royal Alfred Observatory, Mauritius: Annual Reports of Meteorological Department, Port Louis, Mauritius. (Available in U. S. from ESSA Meteorological Library, Washington D. C.)

U. S. Air Force, Air Weather Service Climatological Center, 1963: Monthly data for Northern and Southern Hemisphere. (Electronic climatological data tapes available from the Nat'l Center of Atmos. Res., Boulder, Colo.)

U. S. Navy Marine Climatic Atlas of the World. Components of the 1000 mb winds of the Northern Hemisphere (NAVAIR 50-1C-51) 1 September 1966 (published by direction of Chief of Naval Operations), Superintendent of Documents, U. S. Govt. Printing Office, Washington D. C.

U. S. Navy Marine Climatic Atlas of the World. Selected level temperatures and dew points for the Northern Hemisphere (NAVAIR 50-1C-52) 1 September 1966 (published by direction of Chief of Naval Operations), Superintendent of Documents, U. S. Govt. Printing Office, Washington D. C.

U. S. Weather Bureau, 1953-1966: Monthly climatological data for the world. (Available from U. S. Govt. Printing Office, Washington D. C.)

U. S. Weather Bureau, 1953-1966: Northern Hemisphere daily data tabulations. (Available from U. S. Govt. Printing Office, Washington D. C.)

Van Loon, H., 1967: Personal communication concerning Southern Hemisphere data.

Visher, S. S., 1922: Tropical cyclones in Australia and the South Pacific and Indian Oceans. Mon. Wea. Rev., 50, 288-295.

North Atlantic Data References

Aspliden, C. I., et al., 1966: Satellite study, tropical North Atlantic, 1963, parts I and II. Research Reports, Florida State Univ., 153 and 89 pp.

Cry, G. W., W. H. Haggard, and H. S. White, 1959: North Atlantic cyclones. Tech. Paper No. 36, U. S. Wea. Bur., Dept. of Commerce, 214 pp.

_____, and _____, 1962: North Atlantic tropical cyclone activity, 1901-1960. Mon. Wea. Rev., 90, 341-349.

_____, 1965: Tropical cyclones of the North Atlantic Ocean. Tech. Paper No. 55, U. S. Wea. Bur., U. S. Govt. Printing Office, Washington D. C., 148 pp.

Gentry, R. C., 1963: Historical survey and climatology of hurricanes and tropical storms. Proc's of the Inter-Regional Seminar on Tropical Cyclones, Tokyo, January 1962, Tech. Report No. 21, Japan Meteor. Agency, 17-36.

Haggard, W. H., 1958: The birthplace of North Atlantic tropical storms. Mon. Wea. Rev., 86, 397-404.

Tannehill, I. R., 1938: Hurricanes. Princeton, N. J., Princeton Univ. Press, 45-54.

U. S. Navy Marine Climatic Atlas of the World, Vol. I. North Atlantic Ocean (NAVAIR 50-1C-528) 1 November 1955 (published by direction of Chief of Naval Operations), Superintendent of Documents, U. S. Govt. Printing Office, Washington D. C.

U. S. Navy Oceanographic Atlas of the North Atlantic Ocean, Pub. 700, Section IV, 1963: U. S. Navy Oceanographic Office, Washington D. C., 235 pp.

South Atlantic Data References

U. S. Navy Marine Climatic Atlas of the World, Vol. IV. South Atlantic Ocean (NAVAIR 50-1C-531) 1 September 1958 (published by direction of Chief of Naval Operations), Superintendent of Documents, U. S. Govt. Printing Office, Washington D. C.

Northeast Pacific Data References

Alpert, L., 1945: The intertropical convergence zone of the eastern Pacific region (I). Bull. Am. Meteor. Soc., 26, 426-432.

_____, 1946a: The intertropical convergence zone of the eastern Pacific region (II). Bull. Am. Meteor. Soc., 27, 15-29.

_____, 1946b: The intertropical convergence zone of the eastern Pacific region (III). Bull. Am. Meteor. Soc., 27, 62-66.

Hurd, W. E., 1929: Tropical cyclones of the eastern North Pacific Ocean. Mon. Wea. Rev., 57, 43-49.

Rosendal, H. E., 1962: Eastern North Pacific tropical cyclones, 1947-1961. Mariners Weather Log, 6, 195-201.

Sadler, J., 1964: Tropical cyclones of the eastern North Pacific as revealed by TIROS. J. Appl. Meteor., 3, 347-366.

U. S. Navy Marine Climatic Atlas of the World, Vol. II. North Pacific Ocean (NAVAIR 50-1C-529) 1 July 1958 (published by direction of Chief of Naval Operations), Superintendent of Documents, U. S. Govt. Printing Office, Washington D. C.

Northwest Pacific Data References

Chin, P. C., 1958: Tropical cyclones in the western Pacific and China Sea area from 1884 to 1953. Royal Observ., Hong Kong, Tech. Mem. No. 7, 94 pp.

Climatology Division, 1st Weather Wing, USAF, 1961: Typhoon tracks, 1947-1960. 13 pp.

Fleet Weather Central/Joint Typhoon Warning Center, 1959-1966: Annual Typhoon Reports, Guam, Mariana Islands.

Kakugawa, H. M., and C. W. Adams, 1966: Mean wind profiles 1956-1959 Hawaii and the central Pacific. U. of Hawaii, Inst. of Geophysics Report (HIG-66-13), 175 pp.

LaSeur, N. E., and C. L. Jordan, 1952: A typical weather situation of the typhoon season. Dept. of Meteor., U. of Chicago Research Report, 24 pp.

McCreary, F. E., et al., 1960: Mean monthly upper tropospheric circulations over the tropical Pacific during 1954-1959. Vols. 1-4, Joint Task Force Seven Meteor. Center, JTFMC/TP-19.

Thailand Meteorological Department, 1965: Upper winds over southeast Asia and neighboring areas, Vols. I and II. (Available from Meteor. Dept., Bangkok, Thailand.)

U.S. Navy Marine Climatic Atlas of the World, Vol. II. North Pacific Ocean (NAVAIR 50-1C-529) 1 July 1958 (published by direction of Chief of Naval Operations), Superintendent of Documents, U.S. Govt. Printing Office, Washington D.C.

Visher, S.S., 1925: Tropical cyclones of the Pacific. Bernice P. Bishop Museum Bull. No. 20, Published by the Museum, Honolulu, Hawaii, 163 pp.

Wiedernanders, C.M., Capt., USAF, 1961: Analyses of monthly mean resultant winds for standard pressure levels over the Pacific. U. of Hawaii Scientific Report No. 3, AF 19(604)-7229, March 1961, 83 pp.

South Pacific Data References

Australian Commonwealth Bureau of Meteorology, 1962: Upper wind data. Machine listings, Melbourne, Australia.

Brunt, A.T., and J. Hogan, 1956: The occurrence of tropical cyclones in the Australian region. Proc's of the Tropical Cyclone Symposium, Brisbane, December 1956, 5-18. (Issued by Director of Meteorology, Melbourne, December 1956.)

Gabites, J.F., 1956: A survey of tropical cyclones in the South Pacific. Proc's of the Tropical Cyclone Symposium, Brisbane, December 1956, 19-24. (Issued by Director of Meteorology, Melbourne, December 1956.)

Giovanelli, J.L., 1963: Trajectoires des cyclones tropicaux dans le Pacifique Sud-Ouest. Proc's of the Inter-Regional Seminar on Tropical Cyclones, Tokyo, January 1962, Tech. Report No. 21, Japan Meteor. Agency, 7-16.

Hutchings, J.W., 1953: Tropical cyclones of the Southwest Pacific. New Zealand Geographer, 9, 37-57.

Lamond, M., 1959: Tabulated upper wind data for Australia. Bur. of Meteor., Melbourne, Australia, April 1959.

_____, 1959: Upper winds in the Australia-New Zealand-Fiji area. Bur. of Meteor., Melbourne, Australia, August 1959.

McRae, J. N., 1956: The formation and development of tropical cyclones during the 1955-56 summer in Australia. Proc's of the Tropical Cyclone Symposium, Brisbane, December 1956, 233-262. (Issued by Director of Meteorology, Melbourne, December 1956.)

_____, and J. V. Maher, 1964: Upper wind statistics, Australia. Bur. of Meteor., Melbourne, Australia, 108 pp.

Netherlands Royal Meteorological Institute Report No. 124, 1949: Sea areas around Australia. Staatsdrukkerij-en Vitgeverijbedrijf, The Hague, 79 pp.

U. S. Navy Marine Climatic Atlas of the World, Vol. V. South Pacific Ocean (NAVAIR 50-1C-532) 1 November 1959 (published by direction of Chief of Naval Operations), Superintendent of Documents, U. S. Govt. Printing Office, Washington D. C.

Visher, S. S., 1925: Tropical cyclones of the Pacific. Bernice P. Bishop Museum Bull. No. 20, Published by the Museum, Honolulu, Hawaii, 163 pp.

Indian Ocean Data References

Frost, R., and P. M. Stephenson, 1965: Mean streamlines and isotachs at standard pressure levels over the Indian and West Pacific Oceans and adjacent land areas. Geophys. Memoirs, No. 109, Meteor. Office, Air Ministry London, Her Majesty's Stationery Office, 24 pp.

Indian Daily Upper-Air Meteorological Data Collection, 1953-1965. (Available in U. S. from ESSA Meteorological Library, Washington D. C.)

Indian Journal of Meteorology and Geophysics, 1953-1966: Yearly summaries of tropical storm and depression tracks, Vols. 4-18.

Indian Meteorological Department, 1964: Tracks of storms and depressions in the Bay of Bengal and the Arabian Sea, 1877-1960. 177 pp. (Available from Poona Meteor. Office.)

Koteswaram, P., and C. A. George, 1957: The formation and structure of tropical cyclones in the Indian Sea areas. J. Meteor. Soc. of Japan, 75th Anniversary Vol., 309-322.

_____, 1963b: Origin of tropical storms over the Indian Ocean. Proc's of the Inter-Regional Seminar on Tropical Cyclones, Tokyo, January 1962, Tech. Report No. 21, Japan Meteor. Agency, 69-78.

Naqvi, S. N., 1963: Periodicity of cyclonic storms and depressions in the North Indian Ocean. Proc's of the Inter-Regional Seminar on Tropical Cyclones, Tokyo, January 1962, Tech. Report No. 21, Japan Meteor. Agency, 45-52.

Netherlands Royal Meteorological Institute Report No. 135, 1952: Indian Ocean oceanographic and meteorological data, second edition, text and charts. Staatsdrukkerij-en Vitgeverijbedrijf, The Hague.

Ramon, C. R. V., and C. M. Dixit, 1964: Analysis of monthly mean resultant winds for standard pressure levels over the Indian Ocean and adjoining continental area. Proc's of the Symposium on Tropical Meteorology, Rotorua, New Zealand, 5-13 Nov. 1963, New Zealand Meteorological Service, Wellington, N. Z.

Ray, Choudhuri, S. N., et al., 1959: A climatological study of storms and depressions in the Arabian Sea (resumé). Indian J. of Meteor. Geophys., 10, 283-290.

Sikka, D. R., 1967: Climatological study of tropical storms in the South Indian Ocean. Indian J. of Meteor. Geophys., 18, in press.

U. S. Navy Marine Climatic Atlas of the World, Vol. III. Indian Ocean (NAVAIR 50-1C-530) 1 September 1957 (published by direction of Chief of Naval Operations), Superintendent of Documents, U. S. Govt. Printing Office, Washington D. C.

REFERENCES

Alaka, M. A., 1958: Dynamics of upper air outflow in incipient hurricanes. Geophysica, 6, 133-146.

_____, 1961: The occurrence of anomalous winds and their significance. Mon. Wea. Rev., 89, 482-494.

_____, 1962: On the occurrence of dynamic instability in incipient and developing hurricanes. Mon. Wea. Rev., 90, 49-58.

_____, and D. T. Rubsam, 1964: Some notes on the formation of hurricanes with particular reference to Hurricane Ella, 1962. Proc's of the Symposium on Tropical Meteorology, Rotorua, New Zealand, 5-13 Nov. 1963, New Zealand Meteorological Service, Wellington, N. Z., 641-649.

Arakawa, H., 1952: Mame-Taifu or midget typhoon. Geophys. Mag., 23, 463-474.

_____, 1963: Typhoon climatology as revealed by data of the Japanese Weather Service. Proc's of the Inter-Regional Seminar on Tropical Cyclones, Tokyo, January 1962, Tech. Report No. 21, Japan Meteor. Agency, 31-36.

Arnold, J. E., 1966: Easterly wave activity over Africa and in the Atlantic with a note on the intertropical convergence zone during early July 1961. Satellite and Mesometeorology Res. Proj. Paper No. 65, Dept. of Geophys. Sciences, U. of Chicago, 23 pp.

_____, 1967: The time change of cloud features in hurricane Anna, 1961, from the easterly wave stage to hurricane dissipation. Satellite and Mesometeor. Res. Proj. Paper No. 64, Dept. of Geophys. Sciences, U. of Chicago, 39 pp.

Ballenzweig, E. M., 1956: Seasonal variations in the frequency of North Atlantic tropical cyclones related to the general circulation. Proc's of the Tropical Cyclone Symposium, Brisbane, December 1956, 57-70. (Issued by Director of Meteorology, Melbourne, December 1956.)

Brooks, C. F., 1940: Hubert on the African origin of the hurricane of September 1938. Trans. of Am. Geophys. Union, 1940 vol., Part II, 251-253.

Byers, H., 1959: General Meteorology. New York, McGraw-Hill Book Co., 377-384.

Charney, J. G., and A. Eliassen, 1949: A numerical method for predicting the perturbations of the middle-latitude westerlies. Tellus, 1, 38-54.

_____, 1958: On the formation of tropical depressions. Paper presented at First Tech. Conf. on Hurricanes and Tropical Meteor., Miami, Fla., November 19-22, 1958.

_____, and A. Eliassen, 1964a: On the growth of the hurricane depression, a summary. Geofisica Internacional, 4, 223-230.

_____, and _____, 1964b: On the growth of the hurricane depression. J. of Atmos. Sci., 21, 68-75.

Colón, J. A., 1953: A study of hurricane tracks for forecasting purposes. Mon. Wea. Rev., 81, 53-66.

_____, and W. R. Nightingale, 1963: Development of tropical cyclones in relation to circulation patterns at 200 mb level. Mon. Wea. Rev., 91, 329-336.

Deppermann, C. E., 1947: Notes on the origin and structure of Philippine typhoons. Bull. Am. Meteor. Soc., 28, 399-404.

Dunn, G. E., 1940: Cyclogenesis in the tropical Atlantic. Bull. Am. Meteor. Soc., 21, 215-229.

_____, 1951: Tropical cyclones. Compendium of Meteorology, Am. Meteor. Soc., Boston, Mass., 887-901.

_____, 1956: Areas of hurricane development. Mon. Wea. Rev., 84, 47-51.

_____, and B. I. Miller, 1960: Atlantic Hurricanes. Baton Rouge, La., Louisiana State Univ. Press, 129-136.

Durst, B. A., and R. C. Sutcliffe, 1938: The importance of vertical motion in development of tropical revolving storms. Quart. J. Roy. Meteor. Soc., 64, 75-82.

Ekman, V. W., 1905: On the influence of the earth's rotation on ocean currents. Arkiv Matem. Astr. Fysik, Stockholm, 2(11).

Eliassen, A., 1952: Slow thermally or frictionally controlled meridional circulation in a circular vortex. Astrophys. Norvegica, 5, 19-60.

_____, 1959: On the formation of fronts in the atmosphere. Rossby Memorial Vol., The Atmosphere and the Sea in Motion, New York, Rockefeller Institute Press, 277-287.

Elsberry, R., 1966: On the mechanics and thermodynamics of a low-level wave on the easterlies. Colorado State University, Dept. of Atmospheric Science Research Report No. 101, 31 pp.

Erickson, C. O., 1963: An incipient hurricane near the west African coast. Mon. Wea. Rev., 91, 61-68.

_____, 1967: Some aspects of the development of hurricane Dorothy. Mon. Wea. Rev., 95, 121-130.

Fett, R. W., 1964a: Aspects of hurricane structure: New model considerations suggested by TIROS and Project Mercury observations. Mon. Wea. Rev., 92, 43-60.

_____, 1964b: Some characteristics of the formative stages of typhoon development, a satellite study. Paper presented at Conf. on Phys. and Dyns. of Clouds, Chicago, Ill., March 1964, 32 pp. (Available from Satellite Laboratory, ESSA, Suitland, Md.)

_____, 1966: Upper-level structure of the formative tropical cyclone. Mon. Wea. Rev., 94, 9-18.

Frank, N. L., 1963: Synoptic case study of tropical cyclogenesis utilizing TIROS data. Mon. Wea. Rev., 91, 355-366.

Fritz, S., 1962: Satellite pictures and the origin of hurricane Anna. Mon. Wea. Rev., 90, 507-513.

_____, et al., 1966: Some inferences from satellite pictures of tropical disturbances. Mon. Wea. Rev., 94, 231-236.

Gabites, J. F., 1963a: Historical survey of tropical cyclones. Proc's of the Inter-Regional Seminar on Tropical Cyclones, Tokyo, January 1962, Tech. Report No. 21, Japan Meteor. Agency, 1-6.

_____, 1963b: The origin of tropical cyclones. Proc's of the Inter-Regional Seminar on Tropical Cyclones, Tokyo, January 1962, Tech. Report No. 21, Japan Meteor. Agency, 53-58.

Gaby, D. C., 1964: More on tropical meteorology. Bull. Am. Meteor. Soc., 45, 104.

Gentry, R. C., 1963: Origins of tropical cyclones. Proc's of the Inter-Regional Seminar on Tropical Cyclones, Tokyo, January 1962, Tech. Report No. 21, Japan Meteor. Agency, 59-68.

Gray, W. M., 1962: On the balance of forces and radial accelerations in hurricanes. Quart. J. Roy. Meteor. Soc., 88, 430-458.

_____, 1965: Calculations of cumulus vertical draft velocities in hurricanes from aircraft observations. J. Appl. Meteor., 4 463-474.

_____, 1966: On the scales of motion and internal stress characteristics of the hurricane. J. Atmos. Sci., 23, 278-288.

_____, 1967: The mutual variation of wind, shear, and baroclinicity in the cumulus convective atmosphere of the hurricane. Mon. Wea. Rev., 95, 55-73.

Haggard, W. H., 1965: Climatological-synoptic patterns associated with North Atlantic tropical cyclogenesis. Third Tech. Conf. on Hurricanes and Tropical Meteorology, Mexico City, Geofisica Internacional, 5, 97-113.

Hubert, L. G., 1955: A case study of hurricane formation. J. of Meteor., 12, 486-492.

Ito, H., 1963: Aspects of typhoon development. Proc's of the Inter-Regional Seminar on Tropical Cyclones, Tokyo, January 1962, Tech. Report No. 21, Japan Meteor. Agency, 103-119.

LaSeur, N. E., 1962: On the role of convection in hurricanes. Proc's of the Second Tech. Conf. on Hurricanes, Miami, Fla., 1961, Nat. Hurr. Res. Proj. Report No. 50, 323-334. (Available from U. S. Weather Bureau, Miami, Fla.)

Landers, H., 1963: On the formation and development of tropical cyclones. J. of Appl. Meteor., 2, 206-218.

López, R. E., 1967: A case study of hurricane development. M. S. Thesis, Colorado State University.

Malkus, J. S., 1960: Recent developments in studies of penetrative convection and an application to hurricane cumulonimbus towers. Cumulus Dynamics, C. E. Anderson, New York, Pergamon Press, 211 pp.

Mendenhall, B., 1967: Statistical study of the frictional veering of wind in the planetary boundary layer. M. S. Thesis, Colorado State University.

Merritt, E. S., 1964: Easterly waves and perturbations, a reappraisal. J. of Appl. Meteor., 3, 367-382.

Mitchell, C. L., 1924: West Indian hurricanes and other tropical cyclones of the North Atlantic Ocean. Mon. Wea. Rev., Supp. No. 24, 47 pp.

Namias, J., 1958: Forms of the general circulation as related to hurricane genesis and path. Proc's of 3rd Tech. Conf. on Hurricanes, Miami Beach, Fla., A2-1 to A2-7.

Ogura, Y., 1964: Frictionally controlled, thermally driven circulations in a circular vortex with application to tropical storms. J. Atmos. Sci., 21, 610-621.

Otani, T., 1953: Converging line of the northeast trade wind and converging belt of the tropical air current. Geophys. Mag., 25, 1-122.

Palmén, E., 1948: On the formation and structure of tropical cyclones. Geophysica, 3, 26-28.

_____, 1956: A review of knowledge on the formation and development of tropical cyclones. Proc's of the Tropical Cyclone Symposium, Brisbane, December 1956, 213-231. (Issued by Director of Meteorology, Melbourne, December 1956.)

Palmer, C. E., 1952: Tropical meteorology. Quart. J. Roy. Meteor. Soc., 78, 126-164.

Pike, A. C., 1966: The atmospheric boundary layer beneath gradient wind. Dissertation, University of Cambridge, England.

Portig, W. H., 1964: Atmospheric conditions immediately prior to the formation of a tropical revolving storm. Proc's of the Third Tech. Conf. on Hurricanes and Tropical Meteor., Mexico City, Geofisica Internacional, 4, 241-246.

Ramage, C. S., 1959: Hurricane development. J. of Meteor., 16, 227-237.

Riehl, H., 1945: Waves in the easterlies and the polar front in the tropics. Dept. of Meteor., U. of Chicago Misc. Report 17, 79 pp.

_____, 1948a: On the formation of West Atlantic hurricanes. Dept. of Meteor., U. of Chicago, Misc. Report No. 24, Part 1, 1-67.

_____, 1948b: On the formation of typhoons. J. of Meteor., 5 247-264.

_____, 1950: A model of hurricane formation. J. Appl. Phys., 21, 917-925.

_____, and N. M. Burgner, 1950: Further studies of the movement and formation of hurricanes and their forecasting. Bull. Am. Meteor. Soc., 31, 244-253.

_____, 1951: Aerology of tropical storms. Compendium of Meteorology, Am. Meteor. Soc., Boston, Mass., 902-913.

_____, 1954: Tropical Meteorology. New York, McGraw-Hill Book Company, 323-339.

_____, 1956: Intensification of tropical cyclones Atlantic and Pacific areas. Project AROWA, Fourth Research Report, Task 12, 28 pp. (Available from Naval Air Station, Norfolk, Va.)

_____, and J. S. Malkus, 1958: On the heat balance in the Equatorial Trough zone. Geophysica, 6, 503-538.

_____, and R. C. Gentry, 1958: Structure of tropical storm Frieda, 1957. A preliminary report, Nat. Hurr. Res. Proj. Report No. 17, 16 pp.

_____, et al., 1962: Hurricane formation in the Gulf of Mexico. Third Tech. Report, Prepared for the American Petroleum Inst., Panel on Hurricanes, 27 pp. (Available from Dept. of Atmos. Sci., Colo. State Univ., Fort Collins, Colo.)

Sadler, J., 1963: TIROS observations of the summer circulation and weather patterns of the eastern North Pacific. U. of Hawaii Scientific Report No. 5, 47 pp.

_____, 1964: Tropical cyclones of the eastern North Pacific as revealed by TIROS. J. of Appl. Meteor., 3, 347-366.

_____, 1965: Personal communication.

_____, 1966: The easterly wave--the biggest hoax in tropical meteorology. Seminar presented at the Nat'l Center for Atmos. Res., Boulder, Colo., August 1966.

_____, 1967: The tropical upper tropospheric trough as a secondary source of typhoons and a primary source of trade-wind disturbances. Hawaii Inst. of Geophys. Proj. Report, 44 pp.

Sawyer, J. S., 1947: Notes on the theory of tropical cyclones. Quart. J. Roy. Meteor. Soc., 73, 101-126.

_____, 1949: The significance of dynamic instability in atmospheric motion. Quart. J. Roy. Meteor. Soc., 75, 364-375.

Sen, S. N., 1959: Influence of upper-level troughs and ridges on the formation of post-monsoon cyclones in the Bay of Bengal. Indian J. of Meteor. Geophys., 10, 7-24.

Shiroma, M., and J. C. Sadler, 1965: TIROS observations of typhoon formation. Hawaii Inst. of Geophys. Report No. 65-3 and AFCRL Report No. 65-24.

Spar, J., 1964: A survey of hurricane development. Geofisica Internacional, 4, 169-178.

Tanabe, S., 1963: Low latitude analysis at the formative stage of typhoons in 1962. Kenkyu Jiho (in Japanese), 15, 405-418.

Yanai, M., 1961a: A detailed analysis of typhoon formation. J. Meteor. Soc. Japan, 39, 187-214.

_____, 1961b: Dynamical aspects of typhoon formation. J. Meteor. Soc. Japan, 39, 282-309.

_____, 1963: A preliminary survey of large-scale disturbances over the tropical Pacific area. Conf. on Tropical Meteorology, Mexico City, Geofisica Internacional, 3, 73-84.

_____, 1964: Formation of tropical cyclones. Rev. of Geophys., 2, 367-414.

_____, and T. Nitta, 1967: Computations of vertical motion and vorticity budget. Report of the Geophys. Inst., Tokyo Univ., 56 pp.

Zipser, E. J., 1964: On the thermal structure of developing tropical cyclones. Nat'l Hurr. Res. Proj. Report No. 67, 23 pp. (Available from U. S. Wea. Bur., Miami, Fla.)

Shiroma, M., and J. C. Sadler, 1965: TIROS observations of typhoon formation. Hawaii Inst. of Geophys. Report No. 65-3 and AFCRL Report No. 65-24.

Spar, J., 1964: A survey of hurricane development. Geofisica Internacional, 4, 169-178.

Tanabe, S., 1963: Low latitude analysis at the formative stage of typhoons in 1962. Kenkyu Jiho (in Japanese), 15, 405-418.

Yanai, M., 1961a: A detailed analysis of typhoon formation. J. Meteor. Soc. Japan, 39, 187-214.

_____, 1961b: Dynamical aspects of typhoon formation. J. Meteor. Soc. Japan, 39, 282-309.

_____, 1963: A preliminary survey of large-scale disturbances over the tropical Pacific area. Conf. on Tropical Meteorology, Mexico City, Geofisica Internacional, 3, 73-84.

_____, 1964: Formation of tropical cyclones. Rev. of Geophys., 2, 367-414.

_____, and T. Nitta, 1967: Computations of vertical motion and vorticity budget. Report of the Geophys. Inst., Tokyo Univ., 56 pp.

Zipser, E. J., 1964: On the thermal structure of developing tropical cyclones. Nat'l Hurr. Res. Proj. Report No. 67, 23 pp. (Available from U. S. Wea. Bur., Miami, Fla.)

Shiroma, M., and J. C. Sadler, 1965: TIROS observations of typhoon formation. Hawaii Inst. of Geophys. Report No. 65-3 and AFCRL Report No. 65-24.

Spar, J., 1964: A survey of hurricane development. Geofisica Internacional, 4, 169-178.

Tanabe, S., 1963: Low latitude analysis at the formative stage of typhoons in 1962. Kenkyu Jiho (in Japanese), 15, 405-418.

Yanai, M., 1961a: A detailed analysis of typhoon formation. J. Meteor. Soc. Japan, 39, 187-214.

_____, 1961b: Dynamical aspects of typhoon formation. J. Meteor. Soc. Japan, 39, 282-309.

_____, 1963: A preliminary survey of large-scale disturbances over the tropical Pacific area. Conf. on Tropical Meteorology, Mexico City, Geofisica Internacional, 3, 73-84.

_____, 1964: Formation of tropical cyclones. Rev. of Geophys., 2, 367-414.

_____, and T. Nitta, 1967: Computations of vertical motion and vorticity budget. Report of the Geophys. Inst., Tokyo Univ., 56 pp.

Zipser, E. J., 1964: On the thermal structure of developing tropical cyclones. Nat'l Hurr. Res. Proj. Report No. 67, 23 pp. (Available from U. S. Wea. Bur., Miami, Fla.)